

Declaration

I declare that “Synthesis and Applications of Aminated Biopolymers” is my own work and to the best of my knowledge has never been reported or submitted for any degree or examination in any university. All sources of information used are cited, acknowledged and completely referenced at the end of each chapter.

Signed by candidate

Thaakirah Phillips

20/07/2024

Acknowledgements

All praise be to Allah (swt) for blessing me with the ability and resilience to complete this degree. I would also like to show appreciation to the following people:

My supervisor, Professor Anwar Jardine, for helping me grow into the scientist I am. Thank you Prof AJ for your endless patience and support throughout the project. Besides sharing your brilliance in organic chemistry and research with me, you have also shown me what it is to be a leader with kindness and empathy.

The analytical staff of UCT, especially Dr Dalielah Jappie and Dr Cesarina Edmonds-Smith for help with HPLC. The technical staff in the undergraduate labs for kindly providing me with resources or equipment when needed. The Hunter research group, with special thanks to Dr Fanuel, for the organic chemistry advice and letting me freely raid their chemical inventory. Amina and Evans from H3D for kindly running my samples. Tawfeeq for conducting cytotoxicity studies.

Dr Marwaan Rylands for his insightful feedback on my thesis and for running my NMR samples.

My work besties, Maryam and Lulu, for the love and support. You both made this journey a lot more bearable. My chemistry friends for the laughs and help in the lab.

My best friend Nazihah for being my emotional support person, partner in campus food quests and for distracting me from my thesis ever so often.

Sasol-NRF and NRF for the financial support.

Lastly, a heartfelt thank you to my family for everything they do for me that made pursuing my dreams a lot easier. Thank you for all the love and kindness that you grace me with.

Abstract

Cellulose and chitin have a significant role in the biorefinery where biomass is converted into value-added products. Native cellulose and chitin are known to be insoluble in most common organic and aqueous solvents and are therefore physically and chemically modified with different functionalities to improve solubility to enable further application and modulate bioactivity. The introduction of amino groups into biopolymers is one method to improve solubility in water and enhance other properties such as bioactivity. The solubility of polymers in water is advantageous and enables opportunities for applications in many industries. A simple, green and sustainable synthetic method was sought as an improvement to prior methods using hazardous reagents and producing immense amounts of waste. Innovative synthetic methods were developed for the synthesis of amino- and diamino celluloses. A sustainable, economically viable process for biopolymer amination was sought *via* substitution of C-6 tosyl esters or *via* reductive amination of biopolymer aldehyde derivatives. To this end, C-6 amino cellulose was synthesised by a novel synthetic pathway in which cellulose is firstly tosylated using a surfactant-mediated solvent system to yield DMSO-soluble cellulose tosylates. Subsequently the C-6 partially tosylated cellulose was subjected to a Swern-like oxidation to yield the required C-6 aldehyde functionality primed for reductive amination. The same oxidation-reductive amination strategy was attempted on chitin or chitosan. The established periodate oxidation of cellulose provided dialdehyde cellulose (DAC) ready for reductive amination.

The synthesised diamino and amino celluloses were DMSO-soluble and were tested for cytotoxicity against brain cancer cell lines. Cytotoxicity studies showed that the aminated celluloses did not display any inherent anticancer activity, however, it would be suitable for drug conjugation and delivery.

Previous studies have showed the successful use of recyclable 6-deoxy-6-amino chitosan as an aqueous-soluble solid support for platinum group metal catalysts. This motivated the use of an amination strategy for the immobilisation of pyridoxal and pyridoxal 5'-phosphate (PLP) for application in non-enzymatic deamination of L-phenylalanine to phenylpyruvate. An ionic complex between PLP and Q188 was formed and successfully utilised to convert L-phenylalanine into phenylpyruvate, however, the polymer complex showed a decline in activity over time possibly due to the leaching of PLP. Therefore, immobilisation of PLP *via* covalent

bonding was explored, however, the pyridoxal immobilised biopolymers synthesised were insoluble in water and could not be used in simulating non-enzymatic deamination reactions.

Abbreviations and Symbols

AMINO CELL	amino cellulose
AGU	anhydroglucose unit
Ar	aromatic
BSF	Black Soldier fly
CELL	cellulose
C-6 OXID CELL	C-6 oxidised C-6 tosyl cellulose
CNC	cellulose nanocrystals
CMC	carboxymethyl chitosan
CMC-PL	pyridoxal immobilised on carboxymethyl chitosan
COP	collagen peptides
CrI	crystallinity index
CuAAc	copper-catalyzed azide-alkyne cycloaddition
DAC	dialdehyde cellulose
DDA	degree of deacetylation
DCI	deuterated hydrochloric acid
D ₂ O	deuterated water
DO	degree of oxidation
DIAM CELL	diamino cellulose
DI	deionised water
DS	degree of substitution
DMS	dimethyl sulfide
Da	dalton
d	doublet
dd	doublet of doublets
IMMOB PL TS CELL	immobilised pyridoxal on tosyl cellulose
LMW	low molecular weight
m	multiplet
MCC	microcrystalline cellulose
NAc	<i>N</i> -acetyl

NSCS	<i>N</i> -succinyl chitosan
ppm	parts per million
PLP-DEs	PLP-dependent enzymes
PLA	phenyllactic acid
PL	pyridoxal
PLP	pyridoxal 5'-phosphate
Q188	3-trimethylammonium-2-hydroxypropyl- <i>N</i> - chitosan
r.t.	room temperature
s	singlet
S _N 2	bimolecular substitution reaction
SLS	sodium lauryl sulfate
TEMPO	(2,2,6,6-tetramethylpiperidin-1-yl)oxyl oxidation
TsCl	tosyl chloride
TMS	tetramethylsilane
TS CELL	tosyl cellulose
t	triplet

Table of Contents

Declaration.....	ii
Acknowledgements.....	iii
Abbreviations and Symbols.....	vi
Chapter 1: Introduction.....	1
Biopolymer modifications and selected applications thereof.....	1
1.1 Background.....	1
1.2 Solubility of cellulose, chitin and chitosan.....	4
1.3 Characterisation.....	7
1.4 Derivatisation of cellulose and chitosan.....	8
1.5 Synthesis of aminated biopolymers.....	22
1.6 Aims and objectives.....	23
1.6.1 Aims.....	23
1.6.2 Objectives.....	23
1.7 References.....	25
Chapter 2: Oxidation of Biopolymers.....	29
2.1 Literature review.....	29
2.2 Results and discussion.....	38
2.2.1 Synthesis of dialdehyde cellulose (DAC).....	38
2.2.2 Selective C-6 oxidation of cellulose.....	41
2.2.3 Selective C-6 oxidation of chitosan.....	54
2.3 Conclusion.....	61
2.4 References.....	62
Chapter 3: Amination of Cellulose and a Study of its Properties.....	65
3.1 Literature review.....	65
3.2 Results and discussion.....	70
3.2.1 Synthesis of diaminocellulose.....	70
3.2.2 Synthesis of aminocellulose.....	80
3.3 Summary of the reductive amination of cellulose derivatives.....	88
3.4 Applications of aminated biopolymers.....	89
3.5 Conclusion.....	93
3.6 References.....	94
Chapter 4: Immobilisation of Pyridoxal on Aminated Biopolymer Solid Supports for Biomimetic Applications.....	93
4.1 Literature Review.....	93

4.2 Results and Discussion	100
4.2.1 Background on the ionic immobilisation of pyridoxal phosphate	100
4.2.2 Synthesis of an ionic PLP complex	103
4.2.3 Application of non-enzymatic PLP-mediated conversion of amino acids to α -keto acids	107
4.2.4 Background on covalent immobilisation of pyridoxal.....	109
4.2.5 Synthesis of immobilised pyridoxal on cellulose <i>via</i> direct substitution.....	110
4.2.6 Synthesis of immobilised pyridoxal on carboxy methylchitosan <i>via</i> esterification	114
4.3 Conclusion	116
4.4 References.....	117
Chapter 5: Conclusions and Future Outlook.....	119
5.1 Overall summary and conclusions	119
5.2 Future outlook.....	120
5.3 References.....	122
Chapter 6: Experimental Procedures	123
6.1 General procedures	123
6.2 Experimental.....	126
6.2.1 Synthesis of cellulose and chitosan polymer modifications	126
6.2.2 Synthesis of immobilised pyridoxal on biopolymer solid supports.....	134
6.2.3 Cytotoxicity studies of aminated celluloses.....	137
6.2.4 Non-enzymatic PLP – mediated conversion of amino acids to α -keto acids ^{10, 11} .	137
6.3 References.....	139
<i>Appendix</i>	140

Chapter 1: Introduction

Biopolymer modifications and selected applications thereof

1.1 Background

There has been an increased interest in the valorisation of biomass in recent years to offset dependence on non-renewable fossil resources which is rapidly increasing due to the demand for energy, commodity chemicals and materials. Consequently, along with a rapid population growth, this puts more pressure on the global climate crisis and sustainability challenges.^{1, 2} Biomass refers to renewable organic material derived from plant and animal matter, which has the potential to serve as a renewable and environmentally friendly source of sustainable materials, depending on its growth, harvesting and processing methods.^{3, 4} Agricultural and marine sources are two major contributors to the global amount of biomass with approximately 140 billion metric tons of biomass produced annually by agriculture and 100 M mt by the oceans.^{5, 6} The conversion of biomass into value-added products such as materials, fuel, energy and chemicals is an active area of research using biomass sources such as food waste, wood and wood processing waste, agricultural crops and waste materials, biogenic materials in municipal solid waste, as well as animal manure and human sewage.^{3, 4} The ideal source of biomass is one that does not compete with food or feed.⁷ Hall *et al.* discusses the global challenge of ‘food vs fuel’, highlighting that both food and fuel are key constraints in development and must be locally and sustainably available. Moreover, a pivotal question is ‘how can the existing ample food supply be equitably distributed?’.⁸

The feedstocks explored as potential sources of alternative materials include those derived from food waste sectors, forestry and agriculture, such as cellulose, chitin, corn stover, pectin, starch, straw, vegetable oils, waxes, wood, and zein.⁹ The waste hierarchy and biomass value pyramid are given in **Figure 1.1**.^{10, 11} Most of these materials come from agricultural waste, however, the disadvantage of terrestrial biorefineries is that it is limited by food production and competition, since water and land are required.¹² Aquatic biorefineries do not require the use of land, and do not interfere in food production, hence is a more suitable alternative than terrestrial biorefineries.^{7, 12, 13} Aquatic biomass contains a higher amount of organic content than terrestrial biomass, which furthers the suitability for its use.^{12, 14} On the other hand, aquaculture and fishing may have both positive and negative impacts on aquatic ecosystems.

Overfishing leads to the loss of biodiversity as it depletes fish populations which affect marine ecosystems. Destructive fishing methods like trawling causes habitat destruction and aquaculture infrastructure could also cause habitat loss.¹⁵ However, positive consequences of sustainable aquaculture practices include the conservation of biodiversity and restoration of marine ecosystems as discussed in a review by Overton *et al.*¹⁶

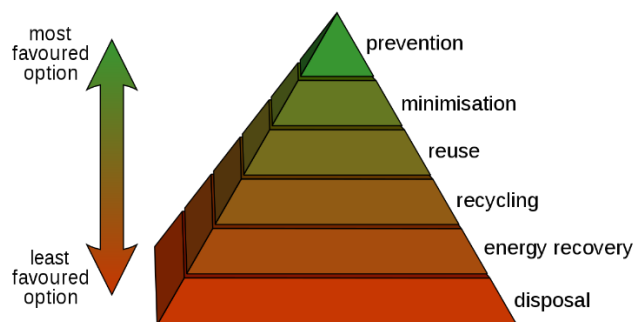


Figure 1.1 (a) The waste hierarchy.

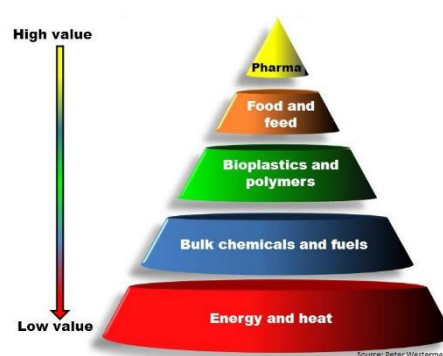


Figure 1.1 (b) The biomass value pyramid.^{10, 11}

Cellulose was discovered by the French chemist Anselme Payen in 1838 when he observed a substance that was not starch but behaved similarly to starch in that it could be separated into its basic units of glucose. This new substance was termed ‘cellulose’ because it was obtained from the cell walls of plants.¹⁷⁻²⁰ The main sources of cellulose are wood pulp and cotton fibres. Cellulose (**Figure 1.2**) is the most abundant natural biopolymer on Earth and consists of a linear chain of D-glucopyranose residues connected by β -(1 \rightarrow 4)-glycosidic units. Recent reviews by Aziz *et al.* and Etale *et al.* highlight the sources, modifications and applications of cellulose.^{21, 22}

The backbone of cellulose consists of hydroxyl groups which contributes to its significant biocompatibility as well as broadens the possibilities of chemical modifications. Therefore, applications of cellulose derivatives are an active area of research in drug development, nanoparticles, food and cosmetics. Its applications as a functional material are limited due to cellulose’s insolubility in water and organic solvents.

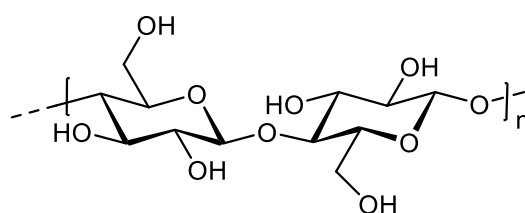


Figure 1.2. Structure of cellulose.¹⁷

The second most abundant biopolymer, chitin, is the major material obtained from marine and terrestrial biomass.¹² Chitin is poly[β -(1 \rightarrow 4)-2-acetamido-2-deoxy-D-glucopyranose] and is structurally similar to cellulose except that the C-2 hydroxyl group of cellulose is replaced by an acetamido group in chitin (**Figure 1.3**).²³ Chitin was first isolated from mushrooms by Henri Braconnot in 1811, and in later years various other sources of chitin were discovered such as the exoskeletons of arthropods, namely crustaceans (e.g. lobster, shrimp, crabs), insects (e.g. ants, silkworm, honeybees), fungi, annelids, cephalopods (e.g. squid and octopus) etc. (**Figure 1.4**).^{3, 24, 25, 26} Chitin extracted from the various lifecycles of the black soldier fly (BSF) is the most studied insect source and is expected to grow exponentially in future years.²⁷ Reportedly, an approximate amount of 10^{11} tons of natural chitin is produced annually with a significant amount discarded as commercial waste, such as fungal and seafood waste.²⁶ Therefore, the need arises for the utilisation of chitin and its deacetylated form chitosan to reduce waste and create value-added products.

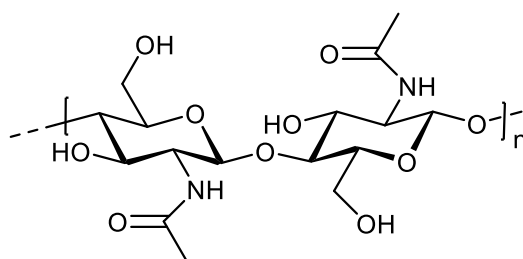


Figure 1.3. Structure of chitin.²³

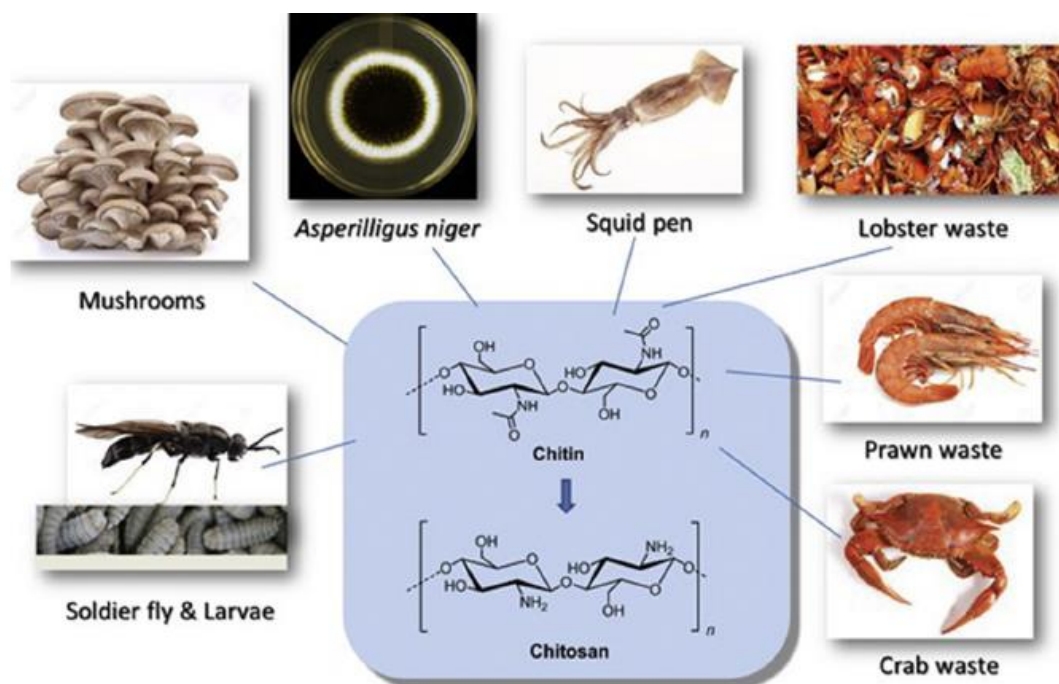


Figure 1.4. Biomass waste supply chain for the preparation of chitin and chitosan.²⁶

1.2 Solubility of cellulose, chitin and chitosan

Cellulose

The use of native biopolymers in applications is limited by their insolubility in most common organic solvents. The insolubility of cellulose is due to its high crystallinity.²⁸ Cellulose's ordered structure is a consequence of a three-dimensional hydrogen-bond network between the hydroxyl groups attached to each polymer chain. For the successful dissolution of cellulose, solvents must be able to compete for the existing intermolecular hydrogen bond interactions to separate the polymer chains from each other (**Figure 1.5**).²⁹ Other important characteristics of a solvent for cellulose are low toxicity and viscosity, recyclability, low melting point as well as high thermal stability as these properties collectively allow for more efficient, safer and sustainable processing of cellulose and are critical for large-scale reactions involving cellulose. Moreover, an efficient solvent for cellulose must be able to reduce its crystallinity.³⁰

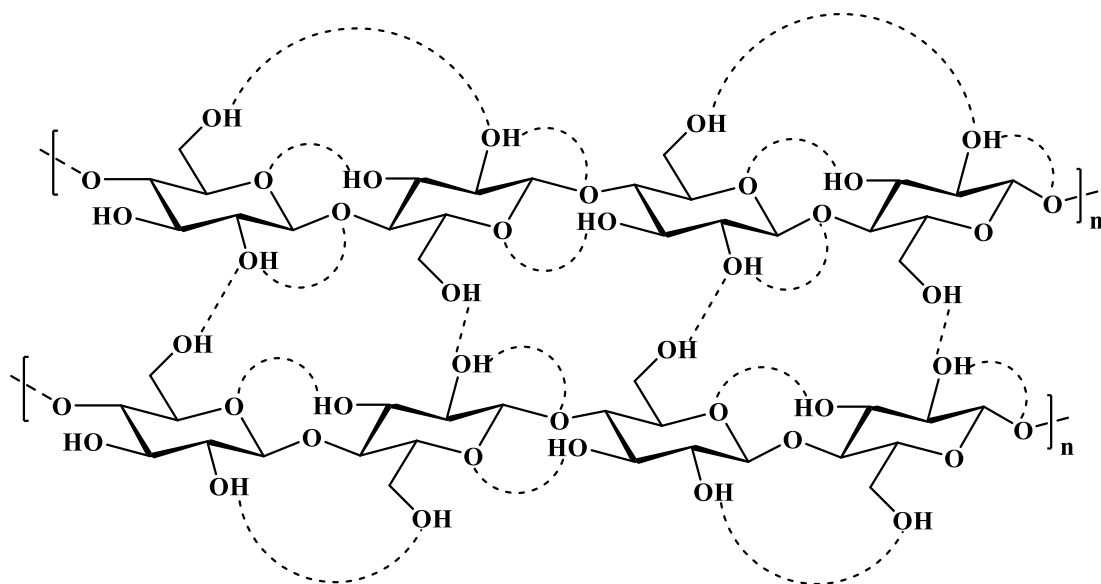


Figure 1.5. Representation of the extensive intra- and intermolecular hydrogen bonding network occurring in cellulose by Visakh *et al.*³¹

A study by Pinkert *et al.* highlights the use of three non-derivatising solvent systems for cellulose: *N,N*-dimethylacetamide + lithium chloride (DMAc + LiCl), dimethylsulfoxide + tetrabutylammonium fluoride (DMSO + TBAF), and *N*-methylmorpholine-*N*-oxide (NMMO) (Table 1.1 summarises solvents in which cellulose is soluble in, without derivatising the polymer).³⁰

Table 1.1: Table showing solvents in which polymers are soluble in	
Polymer	Solvents in which polymer is soluble
cellulose	<ul style="list-style-type: none"> • DMAc + LiCl • NMMO • DMSO + TBAF • Ionic liquids: 1,3-dialkylimidazolium, 1,3-dialkylpyridinium, acetate, formate, dialkylphosphate, thiocyanate, chloride, bromide
chitin	<ul style="list-style-type: none"> • TCA • DCA
chitosan	<ul style="list-style-type: none"> • 1 % AcOH • 1 % HCl • 1 % nitric acid • formic acid • lactic acid

These solvents represent different structural types of cellulose solvent that function without the breakage of any chemical bonds.³⁰ NMMO is the most successful traditional solvent for cellulose due to its properties of low toxicity, biodegradability, and the rate of its recovery in large scale systems is greater than 99 %. However, the use of NMMO has limitations of possible side reactions in the Lyocell process (commercial fiber processing).³² Therefore, the use of ionic liquids has been explored as an alternative solvent for cellulose. A review by Pinkert *et al.* discusses the literature reports on the use of ionic liquids to dissolve cellulose.²⁸ Ionic liquids consist of an organic cation and an inorganic anion (**Table 1.1**). Ionic liquids which contain pyridinium, imidazolium cations and OAc⁻, HCOO⁻, (MeO)₂ PO₂⁻, Cl⁻ anions have demonstrated the ability to dissolve cellulose.³³ Cyrene is a green solvent that is obtained from cellulose-derived biomass *via* a two-step process and has favourable properties of biocompatibility, non-toxicity and non-mutagenicity. Cyrene is commonly used in the development of sustainable chemical transformations and for biomaterials production, however, is unable to dissolve native cellulose and chitosan.³⁴

Chitin and chitosan

Chitin is insoluble in most common organic solvents due to extensive intra- and intermolecular hydrogen bonding between polymer chains, whereas chitosan is soluble in dilute acidic solutions with pH less than 6.³⁵ This is attributed to the primary amino groups with a pKa value of 6.3 in chitosan which alters its charge and properties.³⁶ At acidic pH, these amines are protonated and hence positively charged which make chitosan a water-soluble cationic polyelectrolyte. At basic pH, chitosan exists as a free base and the polymer loses its associated charge leading to insolubility (**Table 1.1** shows the common solvents in which chitin and chitosan are readily soluble in).³⁵ Chitosan can dissolve in organic acids such as acetic, lactic and formic acids due to chitosan forming quaternary ammonium salts at low pH.^{37,38} The most commonly used solvent is 1 % acetic acid at a pH of 4. Chitosan has also demonstrated solubility in 1 % hydrochloric acid and dilute nitric acid.^{37,39} Chitin is soluble in strong polar protic solvents such as trichloroacetic acid (TCA) and dichloroacetic acid (DCA).^{40,41} There is a need for sustainable solvents for the dissolution of biopolymers that has not yet been met at an industrial-scale. There are many reports on the use of ionic liquids and deep eutectic solvents as alternative solvent systems to dissolve biopolymers as discussed in a review by Prasad *et al.*⁴² These alternative solvent systems have favourable characteristics such as recyclability, thermal stability and low vapour pressure, however, have limited use in industry due to high cost, poor recyclability and waste disposal issues.⁴²

1.3 Characterisation

The source of biopolymer influences its properties. It is therefore important to evaluate all aspects of the polymer using spectroscopic and analytical techniques. A few commonly used analytical techniques are described in **Table 1.2**. For chitin and chitosan, the degree of acetylation (DDA) is an important factor as it affects the solubility and reactivity of the polymer.

Analytical Technique	Description
Size Exclusion Chromatography (SEC)	<ul style="list-style-type: none">• For determination of the average molecular weight number (M_n) and the average molecular weight (M_w).⁴³• The polydispersity index (M_w/M_n) of the polymer is calculated, which gives an indication of the molecular weight range.⁴³
Nuclear Magnetic Resonance (NMR)	<ul style="list-style-type: none">• Used for structural analysis of polymers.• ^1H, ^{13}C and ^{15}N-NMR for polymers in solution.• Solid state ^{13}C NMR for solid samples.
Infrared Spectroscopy (IR)	<ul style="list-style-type: none">• For determination of key functionalities of the polymer.• Can be used for qualitative and quantitative analysis.
Viscometry	<ul style="list-style-type: none">• The viscosity of the polymer can be used to calculate the molecular weight of the polymer using the Mark-Houwink Sakurada (MHS) equation: $[\eta] = K(M_v)^a$ where $[\eta]$ is the intrinsic viscosity, M_v the viscosity-average molecular weight, K and a are constants for a given solute-solvent system.^{43, 44}

Analytical Technique	Description
Thermogravimetric Analysis (TGA) and Differential Scanning Calorimetry (DSC)	<ul style="list-style-type: none"> • Thermal analytical techniques that can describe the change in polymer due to modification.⁴⁵
Elemental Analysis (EA)	<ul style="list-style-type: none"> • For determination of the elemental composition of the polymer from which the DS can be calculated.
X-ray diffraction (PXRD)	<ul style="list-style-type: none"> • For determination of the crystallinity of the polymer. • Can be used to determine the effect of modification on the polymer.^{43, 46}

The aforementioned techniques (**Table 1.2**) are but a few used in the analysis of biopolymers. Other techniques used are scanning electron microscopy (SEM), atomic force microscopy (AFM), UV-Vis spectroscopy, zeta potential, high performance liquid chromatography (HPLC), gas chromatography (GC), and mass spectroscopy amongst others.⁴⁷ Advances in analytical methods leads to more in depth research in the field of biopolymer chemistry. Chemical modifications of biopolymers are guided by the structural parameters of the polymer, hence analytical techniques are important for the design and study of new or improved modification methods.

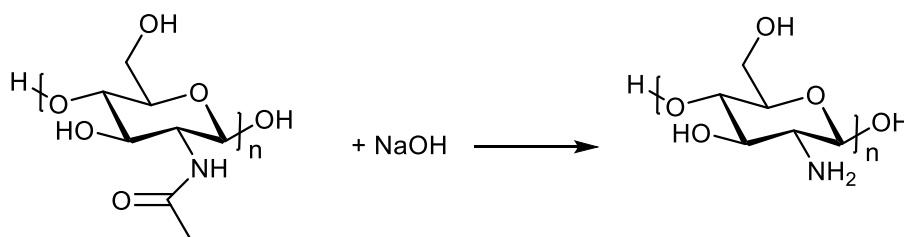
1.4 Derivatisation of cellulose and chitosan

Regioselectivity is important in the derivatisation of biopolymers as a good understanding of the property-structure relationship of biopolymers is dependent on the control of the position of the substituents around the monosaccharide ring and along the polymer chain. Furthermore, the ability to analyse the position of substitution is important in the derivatisation of biopolymers.⁴⁸

The main aims of derivatising biopolymers are to produce functional polymers for smart materials with enhanced or new properties, as well as improve their solubilities.⁴⁹

The poor solubilities of cellulose and chitosan are the key limiting factors in applications thereof. Derivatisation of biopolymers is a common method used to overcome the solubility issue. This is done by attaching hydrophilic or hydrophobic functional groups to the polymer backbone.^{12, 50} The reactive hydroxyl groups of cellulose and chitosan, as well as the amino group at the C-2 position of chitosan, allow for regioselective modification of the polymers.¹²

Mechanochemical and sonochemical derivatisation of cellulose and chitosan have been explored in literature as a means of derivatisation that overcomes the poor solubilities of the biopolymers. The deacetylation of chitin can be performed by means of a solid-state mechanochemical method whereby a mixture of chitin and NaOH in the solid form is mechanically ground in a ball mill. This method is solvent-free and the activation-energy for the deacetylation reaction is provided by the external mechanical force.⁵¹ The solid-state mechanochemical synthesis of chitosan from mud crab (*Scylla serrata*) chitin was reported by Asrahwi *et al.*⁵² This method involved the mechanical mixing of chitin with solid NaOH with varying weight ratios for a fixed period of 30 minutes. This solvent-free process produced chitosan with high degrees of deacetylation; notably a weight ratio of NaOH to chitin of 4:1 produced chitosan with a degree of deacetylation of 93.5 % and a crystallinity of 75.3 %. The proposed reaction mechanism of the mechanochemical deacetylation involves the reaction between the hydroxyl groups on the NaOH particle surfaces and the acetamide groups of chitins (**Scheme 1.1**). This method has advantages relative to conventional methods for the deacetylation of chitin such as requiring less base, being simpler and possibly suppressing depolymerisation of the resulting chitosan. Therefore, this is a suitable method for large-scale industrial applications.⁵²



Scheme 1.1. Deacetylation of chitin using a strong base.⁵²

Poucke *et al.* reported the green and solventless mechanochemical synthesis of water-soluble *N*-sulfonated chitosan.⁵³ This method yielded *N*-sulfopropyl chitosan with DS values up to 78 % in less than two hours; with properties of pH-dependent dissolution behaviour.⁵³ Vallejo-

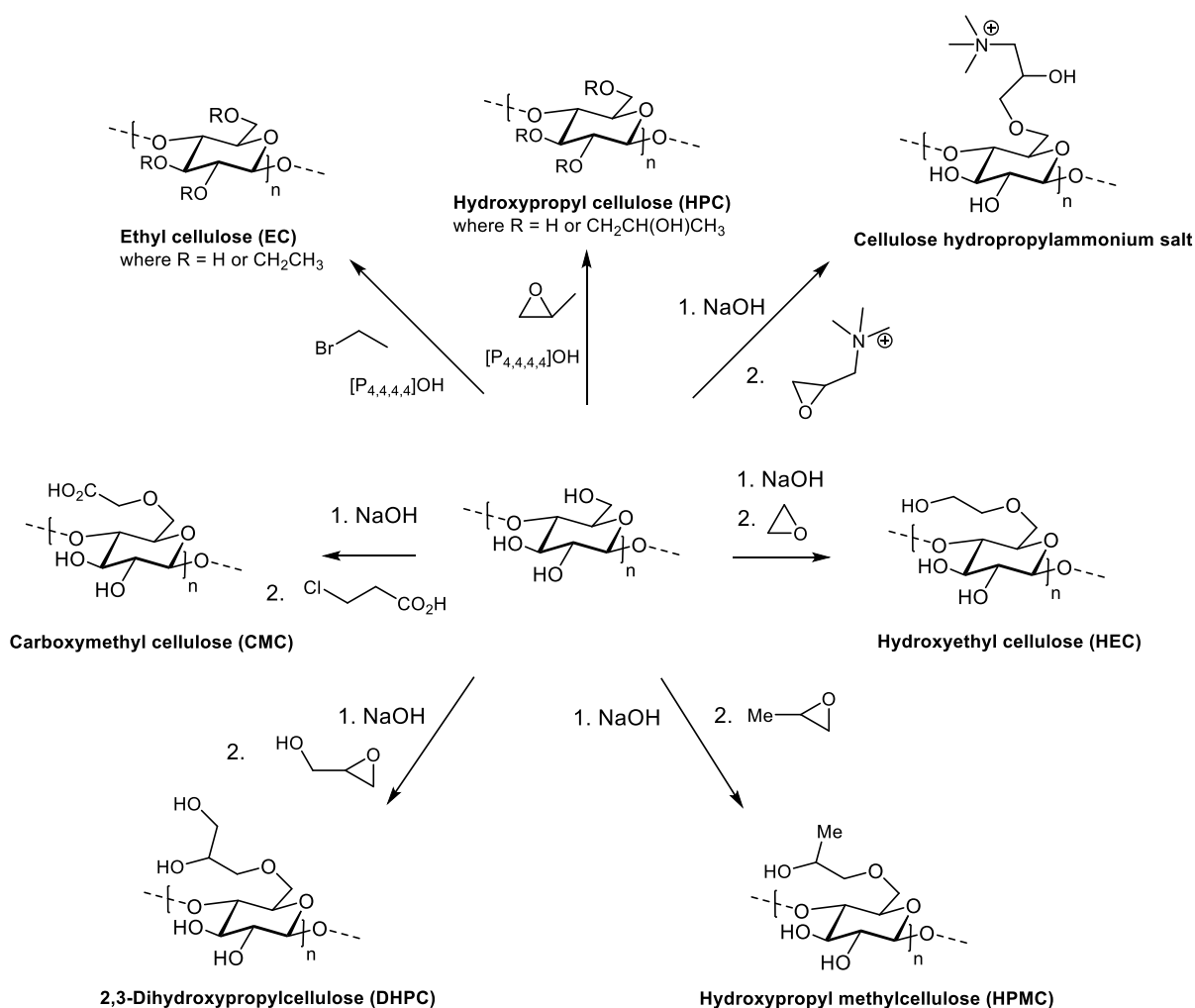
Domínguez *et al.* used high-frequency ultrasound in the deproteinization process for chitin and chitosan production.⁵⁴ The results showed that deproteinization is more efficient with an increase in the sonication time, as confirmed by the low residual nitrogen content in the chitin samples. Furthermore, enhanced properties of the obtained biopolymer such as increased crystallinity was observed when the biopolymer was subjected to higher sonication times. However, the particle sizes of chitin and chitosan products were reduced due to the erosion caused by ultrasound. Higher sonication times produced chitosan products with high degrees of deacetylation, and moderate to low molecular weights. The functionality of chitosan was investigated *via* a ten-day beef preservation study using chitosan films. The red colour of fresh beef was maintained because of the potent antioxidant activity of the prepared chitosan. The chelating property of chitosan allows the chitosan membrane to prevent the oxidation of the beef by the formation of a film that prevents oxygen from entering the beef's cells.⁵⁴

Despite the successful derivatisation of biopolymers by means of mechanochemical and sonochemical reactions to overcome issues of solubility, the challenge of regioselectivity still arises. The following section discusses the main types of reactions that highlight the chemical regioselectivity challenges of cellulose and chitosan: (i) Etherification, (ii) Esterification, (iii) Tosylation (iv) Halogenation, (v) Oxidation, and (vi) Azidation and further derivatisation.

i. Etherification

Cellulose ethers have relatively higher molecular weights because of the replacement of the hydrogen atoms of the hydroxyl groups in the anhydroglucose units of cellulose with alkyl or substituted alkyl groups. Important properties of cellulose ethers such as surface activity, solubility, viscosity and stability against oxidation, hydrolysis, heat and biodegradation are influenced by the chemical structure, molecular weight, degree of substitution and molar substitution, as well as the distribution of substituent groups. The molecular weight of cellulose ether correlates to its viscosity.⁵⁵ Controllable homogeneous etherification of cellulose is challenging to achieve because of the insolubility of cellulose in most organic solvents.^{56, 57} Under certain concentration ranges, aqueous tetra-*n*-butylphosphonium hydroxide [P4444][OH](aq) is known to rapidly dissolve up to 20 wt% of cellulose at 25 °C. You *et al.* reported the successful etherification of cellulose using tetra-*n*-butylphosphonium hydroxide aqueous solution as the reaction medium.⁵⁶ The etherification in this medium was efficient, mild and rapid and produced a series of cellulose ethers with varying substituents and degrees of substitution (DS), and were easily and manageably synthesised.⁵⁶ Ethyl cellulose (EC) (**Scheme 1.2**), the first nonionic cellulose ether in industry, is one of the most popular and well-

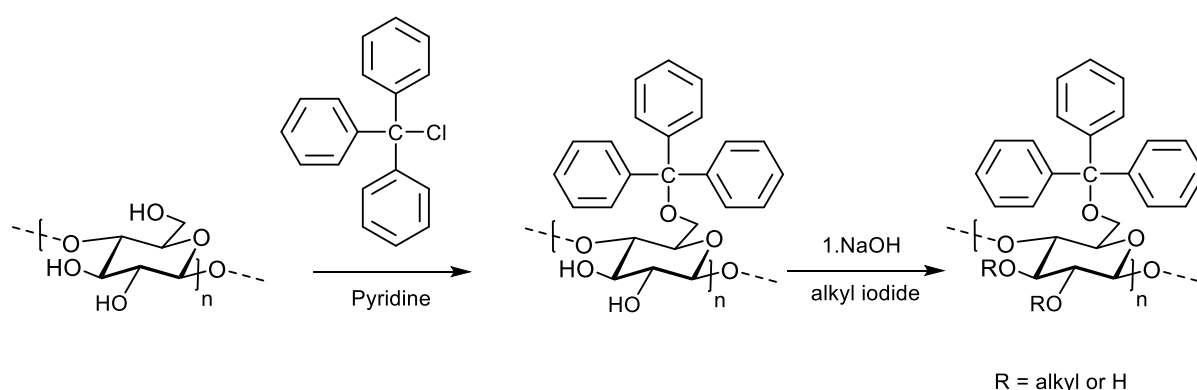
used cellulose derivatives. Commercial EC products have DS of 2.1 to 2.6 and have been used as thermoplastic molding and paint, resin, ink, modifier etc.^{56, 58-61} Hydroxypropyl cellulose (HPC) (**Scheme 1.2**) is also a broadly-used cellulose ether due to its many appealing properties such as thickening effect, gelation, emulsifying effect and gluing property which are useful in applications of pharmaceuticals, building materials and commonly-used chemicals.^{56, 62-65} Cellulose ethers are commonly used as rheology modifiers in personal care products.⁶⁶ **Scheme 1.2** depicts the synthesis of commonly used cellulose ethers in haircare as conditioning quats and rheology modifiers, e.g. cellulose hydropropylammonium salt, hydroxyethyl cellulose (HEC), carboxymethyl cellulose (CMC), hydroxypropyl methylcellulose (HPMC), and 2,3-dihydroxypropylcellulose (DHPC).



Scheme 1.2. Synthetic scheme of commercially important cellulose ethers.

A review by Fox *et al.* highlights the regioselectivity of etherification of cellulose.⁴⁸ There are extensive studies reported in literature regarding the possibilities of utilising the reactivity differences of cellulose hydroxyls for regioselective control. The most important reactivity

differences include the greater acidity of the 2-OH as well as the 6-OH being significantly less sterically hindered. Most researchers exploit the higher reactivity of the 6-OH of cellulose by utilising bulky reagent for etherification reactions.⁴⁸ An example of reaction in which a bulky substituent is used in etherification is the tritylation of cellulose (**Scheme 1.3**). The tritylation of cellulose with trityl chloride (triphenylchloromethane) is an effective protecting group method for the regioselective synthesis of cellulose derivatives. Trityl chloride prefers to react with the 6-OH of cellulose because of steric demands.⁶⁷⁻⁷⁰ Additionally, the trityl group can be removed by acid hydrolysis after derivatisation of the secondary hydroxyl groups (at C-2 and C-3) with acid stable functionalities, such as alkyl ethers, to regenerate the free hydroxyl group at the C-6 position. This allows for the synthesis of a variety of cellulose derivatives where the hydroxyl O-2/3 substituents differ from those at O-6.⁴⁸



Scheme 1.3. Preparation of cellulose ethers via 6-O-trityl cellulose.^{48, 71}

The homogeneous etherification of chitosan and preparation of high strength hydrogel was studied by Ding *et al.*⁷² The authors synthesised a series of chitosan ether derivatives using alkali/urea aqueous solution as the solvent and homogenous reaction medium for the etherification of chitosan. Subsequently, chitosan and quaternized chitosan were dissolved in the acrylic acid monomer aqueous solution, and *in situ* polymerisation resulted in the chitosan/polyacrylic acid and quaternized high strength polyelectrolyte composite hydrogel (PEC). Lastly, PEC was treated with Ag^+ to produce the ultra-high strength of the dual interaction of static electricity and coordination bonds, as well as a physical cross-linked hydrogel (DPC) with properties of high strength and toughness (**Figure 1.6**). The chitosan-

based hydrogel with good mechanical properties has potential for applications in articular cartilage, wound dressings, etc.⁷²

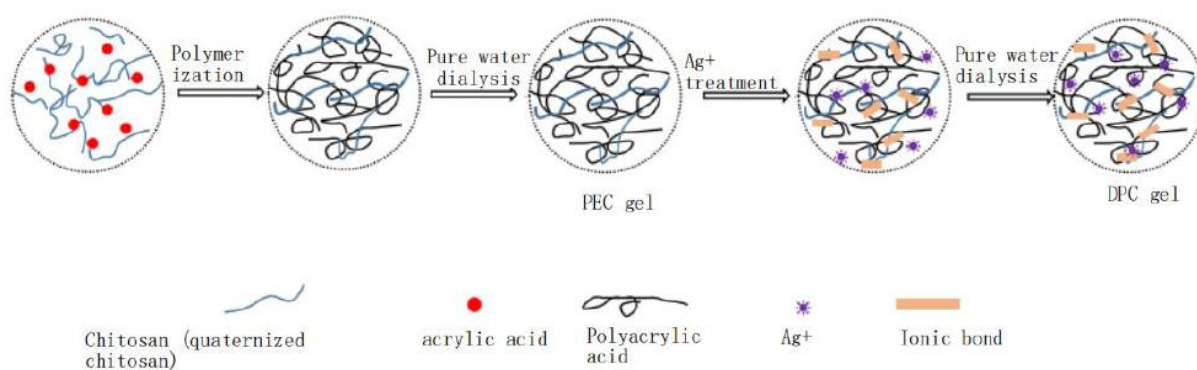


Figure 1.6. Schematic diagram of the preparation of PEC and DPC hydrogels.⁷²

ii. Esterification

The esterification of cellulose can proceed *via* a number of homogenous or heterogenous techniques using either organic acids or inorganic acids or anhydrides in different reaction conditions.⁷³ Cellulose esters are water insoluble and have excellent film forming abilities. Therefore, cellulose esters are used in pharmaceutical controlled release preparations, for example enteric and osmotic coated drug delivery systems.⁵⁵ Cellulose esters are divided into two main groups, namely, organic and inorganic cellulose esters. Organic cellulose esters such as cellulose acetate (CA) (**Figure 1.7**) are mainly used in pharmaceutical industries. CA is one of the most important cellulose esters and is synthesised from a reaction of cellulose with acetic anhydride and acetic acid with sulfuric acid present. CA can be used for an assortment of applications such as the manufacturing of films, fibers and membranes, depending on its processing.⁷⁴ Inorganic cellulose esters such as cellulose nitrate and cellulose sulfate are less commonly used in pharmaceutical industries due to issues of poor solubility and high flammability.⁵⁵

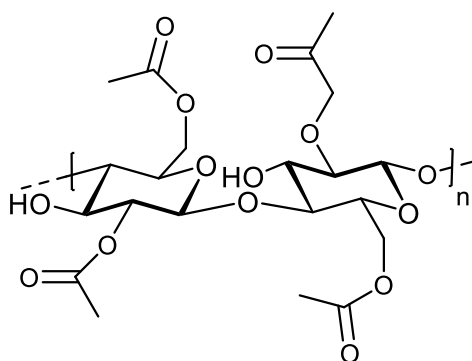
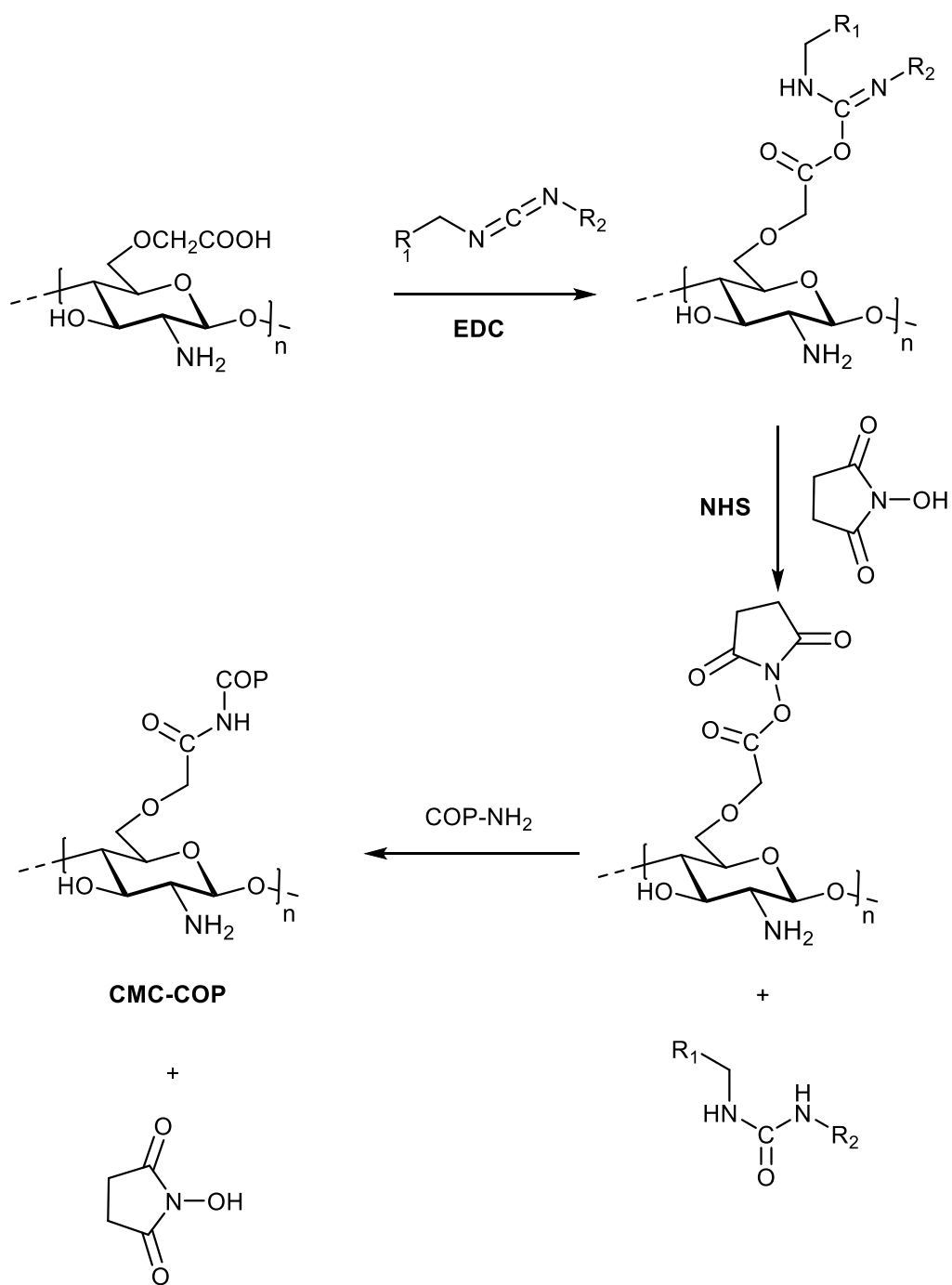


Figure 1.7. Structure of cellulose acetate (CA).⁷⁴

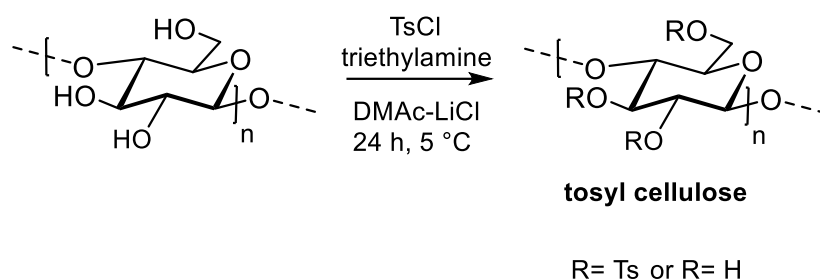
Ester linkages between biopolymers and substituents is a common cross-linking method. Cheng *et al.* grafted sponges of carboxymethyl chitosan (CMC) with collagen peptides (COP) by covalent coupling and freeze-drying for wound healing.⁷⁵ The mechanism for the grafting of CMC with COP is shown in **Scheme 1.4**. The CMC sponges grafted with COP (CMC-COP) were synthesised using 1-(3-dimethylaminopropyl)-3-ethylcarbodiimidehydrochloride (EDC) and *N*-hydroxysuccinimide (NHS) as cross-linkers. *In vitro* studies showed that CMC-COP sponges had significant biological activities such as promotion of cell viability and migration of fibroblast. Experiments of scald wound healing were conducted on rabbits and showed that CMC-COP sponges are effective in applications of burn care.⁷⁵ The esterification is selective at the C-6 position of CMC because EDC primarily reacts with its carboxy groups, therefore there was no need for protection of the C-2 amino group of chitosan.



Scheme 1.4. Mechanism of carboxymethyl chitosan sponges grafted with collagen peptides (CMC-COP).⁷⁵

iii. Tosylation

The tosylation of biopolymers is an attractive strategy to improve solubility and is advantageous for further substitution reactions as the tosyl ester is a good leaving group. Tosyl celluloses need to be structurally uniform and properly soluble for further conversion.^{76, 77} The most common method to achieve uniformly tosylated cellulose is the homogenous tosylation of cellulose dissolved in DMAc-LiCl with *p*-toluenesulfonyl chloride in the presence of a base (usually triethylamine) (**Scheme 1.5**).



Scheme 1.5. Tosylation of cellulose dissolved in DMAc-LiCl.⁷⁸

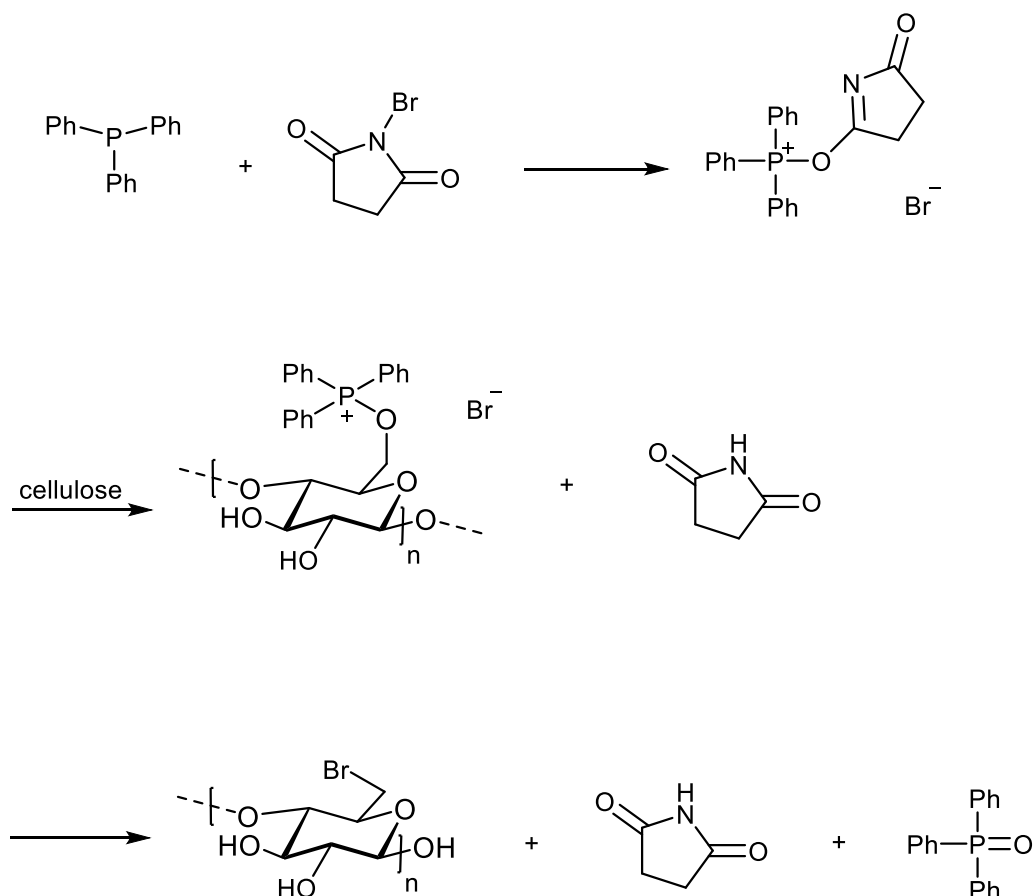
This method produces tosyl cellulose that are soluble in many common organic solvents, depending on the degree of substitution (DS).^{76, 79} However, limitations of this method include extensive time and energy consuming dissolution steps, expensive reagents, and the use of an amine as a base, which might lead to side reactions and by-products that are challenging to remove. More recently, Schmidt *et al.* reported the use of a green NaOH-urea solvent system in the presence of the nonionic surfactant Imbetin for the synthesis of soluble tosyl cellulose in good yield and high purity.⁸⁰ The tosylation of cellulose occurs regioselectively at the C-6 primary hydroxyl group of cellulose because it is the least sterically hindered. However, under certain tosylation conditions, a DS > 1 may occur as a result of substitution at the C-2 and C-3 hydroxyl groups. This method was explored in **Chapter 2**.

There are few reports on the tosylation of chitosan. The free amino groups of chitosan are selectively protected with phthaloyl groups prior to tosylation to obtain *N*-phthaloyl chitosan which is soluble in common organic solvents such as DMSO, DMAc and pyridine. Santoso *et al.* reported the tosylation of *N*-phthaloyl chitosan without drying of solvents and purging of water vapour.⁸¹ *N*-phthaloyl chitosan was tosylated using excess tosyl chloride in the solvent system DMAc-LiCl with triethylamine as catalyst at a temperature less than 10 °C for 12 h to obtain 6-*O*-tosyl-*N*-phthaloyl-chitosan. For comparison, the authors performed the tosylation reaction on *N*-phthaloyl chitosan (phthaloyl protection which was not chemoselective at amine groups only) and found that no product of tosylation could be isolated. Therefore, it was

concluded that tosylation of chitosan is influenced by the selectivity of phthaloyl group protection on chitosan.⁸¹

iv. Bromination

Furuhata *et al.* reported a method for the regioselective halogenation of cellulose at the C-6 position without the formation of an isolated intermediate such a tosyl cellulose (**Scheme 1.6**).⁸² This method involves the dissolution of cellulose in DMAc/lithium bromide, with subsequent addition of triphenylphosphine (Ph₃P) and *N*-bromosuccinimide (NBS). The 6-deoxy-6-bromo cellulose is similar to the 6-*O*-tosylate in that it can behave as a protecting group under certain reaction conditions as well as a good leaving group for substitution at the C-6 position. The advantage of bromination relative to tosylation is that it is completely selective for C-6.^{48, 82} Additionally, a DS of 0.98 has been reported using this method which implies that all primary hydroxyl groups of cellulose have been substituted with bromide.⁸³ However, the disadvantage of regioselective bromination compared with tosylation is that the 6-deoxy-6-bromo cellulose obtained is insoluble in common aqueous and organic solvents, although it can be dissolved again in DMAc/LiBr. Despite this, there are many cellulose derivatives with substituents at C-6 which have been synthesised by nucleophilic substitution with 6-deoxy-6-bromo cellulose under heterogeneous conditions, e.g. L-cysteine, benzenethiol and thiocyanate amongst others.⁴⁸



Scheme 1.6. Mechanism for regioselective bromination of cellulose by Furuhata *et al.*⁸²

v. Oxidation

Selective oxidation of biopolymers is an important chemical modification as the introduction of carbonyl or carboxyl groups into the polymer structure allows for opportunities for further chemical modification such as Schiff base formation and reductive amination amongst others. Oxidation can also improve the aqueous solubility of biopolymers by increasing the hydrophilicity. Improved water solubility of modified chitosan is useful in applications in the biomedical field, as well as in the production of hydrogels and bioadhesives.^{84, 85}

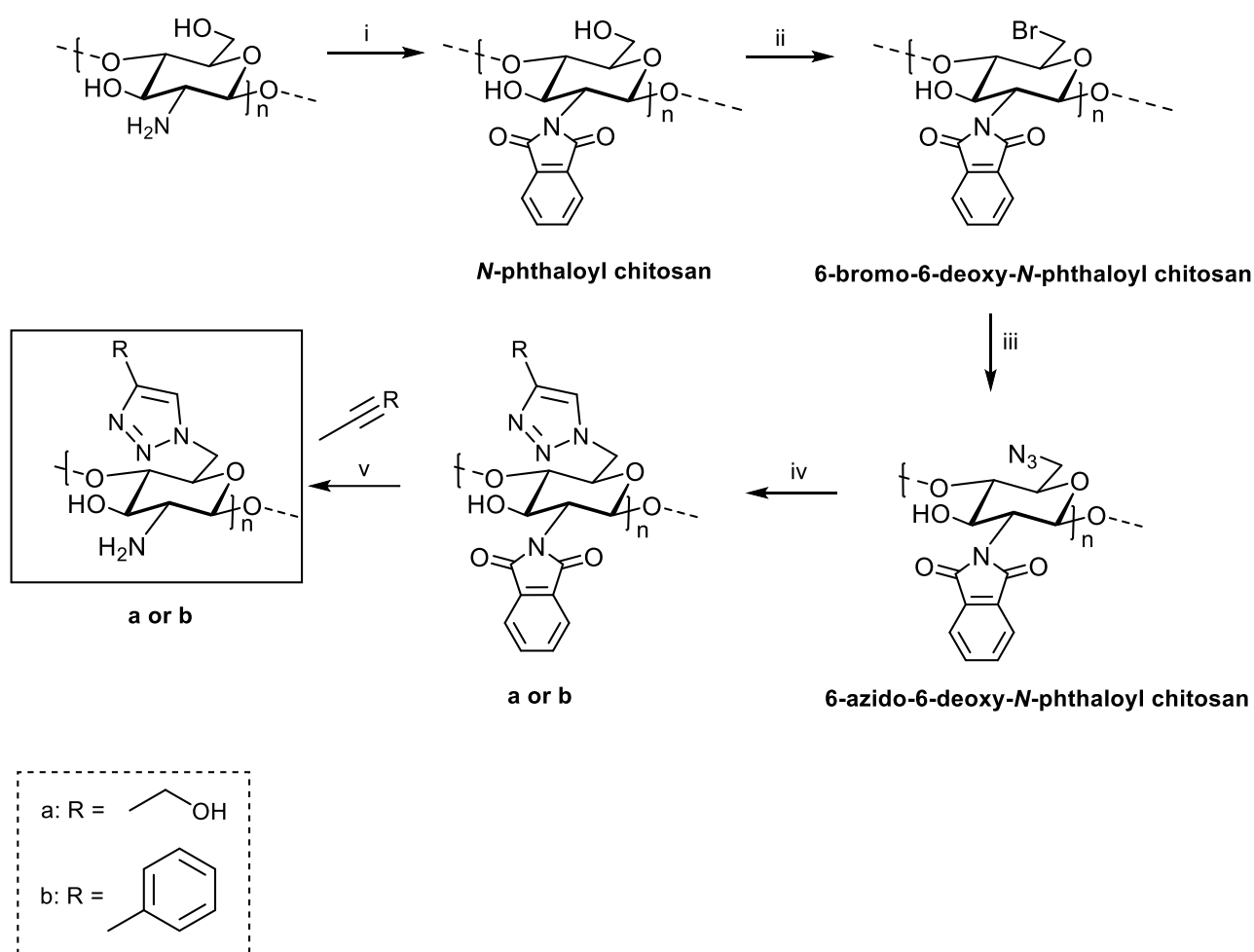
There are two main methods for the selective oxidation of biopolymers: TEMPO-mediated C-6 selective oxidation and periodate-mediated C2-C3 oxidation, which are discussed in **Chapter 2**.

Regioselectivity is a major challenge in the oxidation of biopolymers. The structures of biopolymers are complex and may be irregular, which can result in non-uniform oxidation. An example of this is the hydroxyl groups present at three different positions of cellulose which

all have different reactivity towards oxidation. This makes selective oxidation at one specific position a challenge.⁸⁶ Furthermore, the crystallinity of a biopolymer may also contribute to challenges in regioselectivity. In cellulose, some hydroxyl groups are more easily accessible whereas others may be more densely packed in its crystalline structure.^{84, 86} Other challenges regarding the oxidation of biopolymers include varying chain lengths and DS which means reaction efficiency and extents cannot always be directly determined, over-oxidation to the carboxylic product, as well as the use of hazardous oxidising reagents.⁸⁴

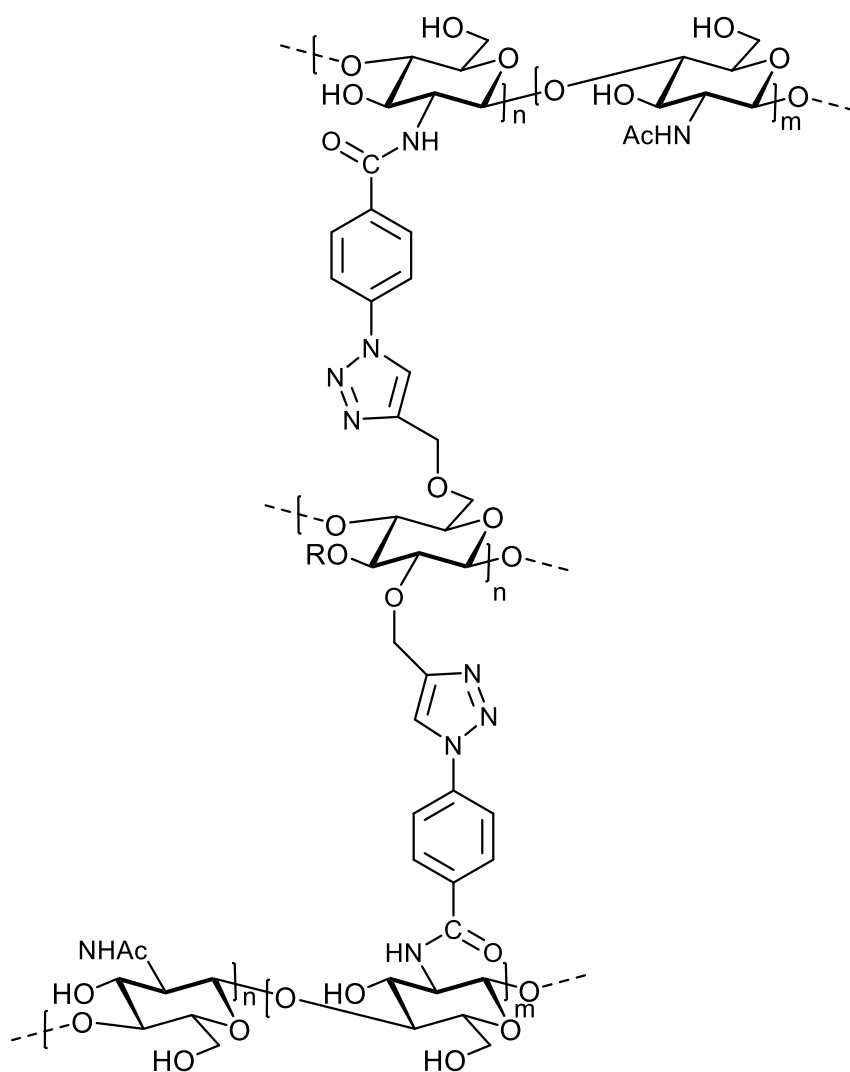
vi. Azidation and further derivatisation

The azidation of biopolymers has great significance because of the high reactivity of azide groups. Moreover, azide groups can partake in reactions of ‘click chemistry’, specifically the copper-catalysed azide-alkyne cycloaddition (CuAAC).⁸⁷ Click chemistry was independently introduced by Sharpless and Meldal in 2002 through the introduction of Cu(I) catalysis.^{88, 89} The main advantages of click chemistry are its reactions rates and regioselectivity.⁸⁷ Highly regioselective chitosan derivatives were prepared using click chemistry by Ifuku *et al.*⁹⁰ This was accomplished by a CuAAC reaction using a 6-azido-6-deoxy chitosan derivative (**Scheme 1.7**). Firstly, the C-2 amino group of chitosan was protected by 2-*N* regioselective phthaloylation. Secondly, bromination at the C-6 position of chitosan was performed. It is important to note that regioselective *N*-phthaloyl chitosan was insoluble due to its high crystallinity and bromination improved the polymer’s solubility. The bulky *N*-phthaloyl group at the C-2 position of chitosan contributes to the C-6 regioselective bromination due to steric hindrance.⁸⁷ In comparison, the reaction proceeded at the C-3 and C-6 position in cellulose.⁹¹ Subsequently, azidation of the 6-bromo-6-deoxy-*N*-phthaloyl chitosan was achieved by a nucleophilic displacement reaction with sodium azide.⁸⁷ Lastly, a click reaction between 6-azido-6-deoxy-*N*-phthaloyl chitosan and alkyne-terminated compounds (hydroxymethyl and phenyl groups) were performed in the presence of Cu(II) sulfate pentahydrate, triethylamine and sodium ascorbate to couple the two compounds together by formation of a triazole. The coupled product was deprotected using hydrazine to remove the phthaloyl group to yield 6-hydroxymethyltriazole (a) and 6-phenyltriazole-6-deoxy chitosan (b) (**Scheme 1.7**). The authors successfully demonstrated the potential for the regioselective introduction of functional modules with triazole linkers into chitosan using click chemistry. This synthetic strategy leads to many novel chitosan derivatives with new or enhanced properties.⁸⁷



Scheme 1.7. Synthetic scheme for the preparation of chitosan derivatives (a and b) by Ifuku *et al.*⁹⁰ Reagents and conditions: (i) phthalic anhydride, DMF/water (95:5), 120 °C, 8 h; (ii) NBS, TPP, NMP, 80 °C, 2 h; (iii) NaN₃, NMP, 80 °C, 4 h; (iv) 2-propyn-1-ol (a), or ethynyl benzene (b), CuSO₄·5H₂O, sodium ascorbate, TEA, DMSO, 70 °C, 48 h; (v) H₂NNH₂·H₂O, NMP, 100 °C, 4 h.

Peng *et al.* was the first to report cellulose bound to chitosan *via* click chemistry.⁹² A novel cellulose-*click*-chitosan polymer was synthesised as follows: firstly, propargyl cellulose was synthesised by etherification of bamboo *Phyllostachys bambusoide* cellulose with propargyl chloride in DMAc/LiCl in the presence of NaH. Secondly, the azidation of chitosan was performed by reacting chitosan with 4-azidobenzoic acid in [Amim]Cl/DMF. Lastly, the click product was obtained *via* CuAAC reaction between terminal propargyl-functionalised cellulose and the azido-functionalised chitosan. The cellulose-*click*-chitosan product (**Figure 1.8**) showed high thermal stability and are therefore candidates for applications of heat-tolerable materials. Furthermore, some hollow tubes with near millimeter length were also observed.⁹²



Where:

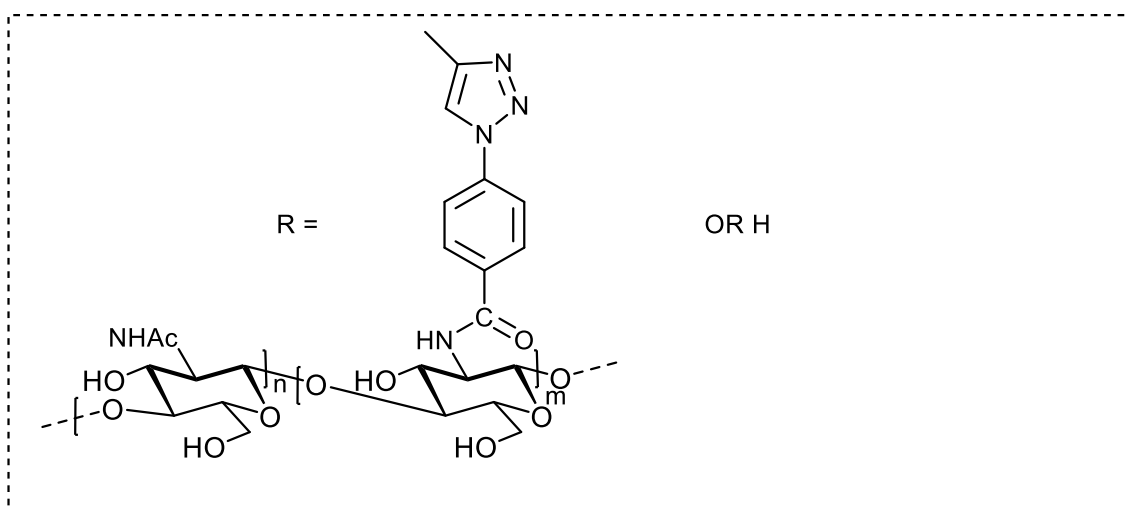


Figure 1.8. Structure of cellulose-*click*-chitosan by Peng *et al.*⁹²

1.5 Synthesis of aminated biopolymers

Some biopolymers naturally contain amino groups as part of their structure, e.g. chitosan. An example of the usefulness of the amine functionality in biopolymers is its application as hydrogels. The hydrophilic nature of these amine groups allows for high water absorption capacity which makes these biopolymers suitable for application as hydrogels.⁹³ Hydrogels have applications in cosmetics as well as the biomedical field.⁹⁴ The noteworthy properties of chitosan that makes it ideal for application as hydrogels in cosmetics are the hair fixing and film-forming properties.⁹⁵ The moisturising properties of chitosan hydrogels are dependent on its molecular weight and degree of deacetylation.⁹⁶

The synthetic introduction of amino groups into biopolymers are known to display improved solubility in aqueous and organic solvents, as well as enhanced properties of bioactivity and biocompatibility.⁹⁷ These properties make aminated biopolymers attractive for applications in many industries such as pharmaceuticals, drug delivery, cosmetics, food and beverage, amongst others. In **Chapter 3** the different methods of amination of biopolymers are introduced. Of particular interest, is the synthetic route that proceeds firstly by oxidation of the biopolymers and subsequent reductive amination to yield soluble aminated biopolymers. Koshani *et al.* explored this route whereby dialdehyde cellulose was synthesised and subsequently aminated *via* reductive amination using sodium borohydride and ammonium acetate to yield diamine cellulose. Lastly, diamine cellulose was subjected to acidic hydrothermal treatment which resulted in rod-like hairy aminated cellulose (**Figure 1.9**).⁹⁸ The limitations of current methods for the reductive amination of biopolymers are discussed in **Chapter 3**.

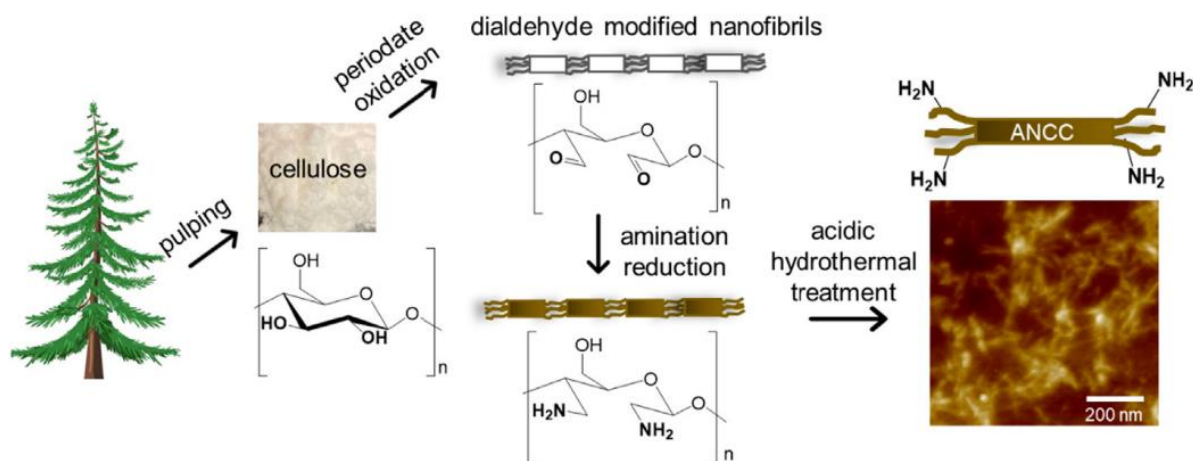


Figure 1.9. Graphical abstract on the synthesis of hairy aminated nanocrystalline cellulose by Koshani *et al.*⁹⁸

In this study, an improved method for the reductive amination of dialdehyde cellulose was sought after which inspired the discovery of a novel synthetic method towards the synthesis of C-6 aminated biopolymers following a similar oxidation-reductive amination approach.

1.6 Aims and objectives

1.6.1 Aims

The overall aim of this study is to develop improved synthetic methodologies towards aminated biopolymers. The aim is to achieve biopolymer amination *via* reductive amination of oxidised biopolymer derivatives. It is important that the method be green and sustainable, using less hazardous reagents and producing minimal waste; as well as be scalable and cost-effective. More specifically, an improved method aims at having a shorter synthetic route, using ‘greener’ or less hazardous solvents, as well as less solvent, and lastly milder reaction conditions such as lower temperatures and shorter reaction periods. Additionally, applications of these aminated biopolymers is to be explored in areas of cytotoxicity against brain cancer cell lines. A further explored ideal is the use of biopolymers as solid supports for the immobilisation of pyridoxal 5'-phosphate (PLP) for the non-enzymatic conversion of L-phenylalanine to phenylpyruvate.

1.6.2 Objectives

Objective 1: Synthesise and characterise dialdehyde cellulose.

Objective 2: Synthesise and characterise cellulose C-6 carbaldehyde.

Objective 3: Synthesise and characterise chitosan C-6 carbaldehyde.

Objective 4: Investigate the reductive amination of oxidised biopolymers.

Objective 5: Characterise aminated celluloses.

Objective 6: Evaluate the cytotoxicity of aminated celluloses against brain cancer cell lines.

Objective 7: Immobilise PLP on aminated biopolymer (Q188) *via* ionic bonding and explore its application in non-enzymatic deamination of L-phenylalanine to phenylpyruvate.

Objective 8: Immobilise PLP on biopolymers *via* covalent bonding and explore its application in non-enzymatic deamination of L-phenylalanine to phenylpyruvate.

1.7 References

1. S. K. Hoekman, *Renewable Energy*, 2009, **34**, 14-22.
2. H. S. Kim, M.-R. Park, Y. J. Jeon, S.-K. Kim, Y.-K. Hong and G.-T. Jeong, *Energy Technology*, 2018, **6**, 1747-1754.
3. S. Sayed and A. Jardine, *International journal of molecular sciences*, 2015, **16**, 9064-9077.
4. Biomass explained, <https://www.eia.gov/energyexplained/biomass/>, (accessed 4 February 2022).
5. E. A and A. Chvez-Hidalgo, in *Biomass Now - Sustainable Growth and Use*, 2013, DOI: 10.5772/54520, ch. Chapter 21.
6. G. Trends and S. Framework, *Waste and climate change*, , 2010.
7. F. M. Kerton, Y. Liu, K. W. Omari and K. Hawboldt, *Green Chemistry*, 2013, **15**.
8. D. Hall, in *Economics of ecosystems management*, Springer, 1985, pp. 207-226.
9. C. S. K. Lin, L. A. Pfaltzgraff, L. Herrero-Davila, E. B. Mubofu, S. Abderrahim, J. H. Clark, A. A. Koutinas, N. Kopsahelis, K. Stamatelatos and F. Dickson, *Energy & Environmental Science*, 2013, **6**, 426-464.
10. L. Lange, L. Bech, P. K. Busk, M. N. Grell, Y. Huang, M. Lange, T. Linde, B. Pilgaard, D. Roth and X. Tong, *IMA Fungus*, 2012, **3**, 87-92.
11. Waste hierarchy, https://en.wikipedia.org/wiki/Waste_hierarchy, (accessed 4 February 2022).
12. S. Sayed, PhD, University of Cape Town, 2018.
13. B. Bharathiraja, M. Chakravarthy, R. Ranjith Kumar, D. Yogendran, D. Yuvaraj, J. Jayamuthunagai, R. Praveen Kumar and S. Palani, *Renewable and Sustainable Energy Reviews*, 2015, **47**, 634-653.
14. M. Rabaçal, A. F. Ferreira, C. A. Silva and M. Costa, in *Biorefineries*, ed. N. Y. Biorefineries Springer International Publishing, 2017.
15. M. Carneiro and R. Martins, in *Life Below Water*, Springer, 2022, pp. 295-304.
16. K. Overton, T. Dempster, S. E. Swearer, R. L. Morris and L. T. Barrett, *Conservation Biology*, 2024, **38**, e14065.
17. D. K. P. K. Lavanya, Kulkarni, P.K., Dixit, M., Raavi, P.K. and Krishna, L.N.V., *International Journal of Drug Formulation and Research*, 2011, **2**, 19-38.
18. R. L. Crawford, *Lignin biodegradation and transformation.*, John Wiley and Sons, 1981.
19. R. Young, R. M. Rowell and *Structure, Modification and Hydrolysis*. John Wiley & Sons, New York, 1986.
20. A. Payen, *Comptes rendus*, 1838, 1052-1056.
21. T. Aziz, A. Farid, F. Haq, M. Kiran, A. Ullah, K. Zhang, C. Li, S. Ghazanfar, H. Sun and R. Ullah, *Polymers*, 2022, **14**, 3206.
22. A. Etale, A. J. Onyianta, S. R. Turner and S. J. Eichhorn, *Chemical reviews*, 2023, **123**, 2016-2048.
23. G. A. Roberts and G. A. Roberts, *Chitin chemistry*, 1992, 1-53.
24. J. H. Clark and F. e. Deswarte, *Introduction to Chemicals from Biomass*, John Wiley and Sons, West Sussex, UK, 1 edn., 2014.
25. R. A. Muzzarelli, J. Boudrant, D. Meyer, N. Manno, M. DeMarchis and M. G. Paoletti, *Carbohydrate polymers*, 2012, **87**, 995-1012.
26. A. Jardine and S. Sayed, *Current Opinion in Green and Sustainable Chemistry*, 2016, **2**, 34-39.

27. L. Soetemans, M. Uyttebroek and L. Bastiaens, *International Journal of Biological Macromolecules*, 2020, **165**, 3206-3214.
28. A. Pinkert, K. N. Marsh, S. Pang and M. P. Staiger, *Chemical reviews*, 2009, **109**, 6712-6728.
29. L. Feng and Z.-l. Chen, *Journal of Molecular Liquids*, 2008, **142**, 1-5.
30. A. Pinkert, K. N. Marsh and S. Pang, *Industrial & Engineering Chemistry Research*, 2010, **49**, 11121-11130.
31. P. M. Visakh and S. Thomas, *Waste and Biomass Valorization*, 2010, **1**, 121-134.
32. T. Rosenau, A. Potthast, H. Sixta and P. Kosma, *Progress in polymer science*, 2001, **26**, 1763-1837.
33. N. Mohd, S. Draman, M. Salleh and N. Yusof, 2017.
34. A. Citarella, A. Amenta, D. Passarella and N. Micale, *International Journal of Molecular Sciences*, 2022, **23**, 15960.
35. C. K. Pillai, W. Paul and C. P. Sharma, *Progress in polymer science*, 2009, **34**, 641-678.
36. H. Yi, L.-Q. Wu, W. E. Bentley, R. Ghodssi, G. W. Rubloff, J. N. Culver and G. F. Payne, *Biomacromolecules*, 2005, **6**, 2881-2894.
37. M. Rinaudo, G. Pavlov and J. Desbrieres, *Polymer*, 1999, **40**, 7029-7032.
38. K. M. Kim, J. H. Son, S. K. Kim, C. L. Weller and M. A. Hanna, *Journal of food science*, 2006, **71**, E119-E124.
39. M. Rinaudo, G. Pavlov and J. Desbrieres, *International Journal of Polymer Analysis and Characterization*, 1999, **5**, 267-276.
40. P. R. Austin, 1980. , ACS Publications, 1980.
41. P. R. Austin, *Journal*, 1975.
42. K. Prasad and M. Sharma, *Current Opinion in Green and Sustainable Chemistry*, 2019, **18**, 72-78.
43. S. Sayed, PhD Thesis, University of Cape Town, 2018.
44. M. R. Kasaai, *Carbohydrate polymers*, 2007, **68**, 477-488.
45. M. Lago, A. Rodríguez Bernaldo de Quirós, R. Sendón, A. Sanches-Silva, H. Costa, D. I. Sánchez-Machado, J. López-Cervantes, H. Soto Valdez, G. Aurrekoetxea and I. Angulo, *CyTA-Journal of Food*, 2011, **9**, 319-328.
46. J. Kumirska, M. Czerwicka, Z. Kaczyński, A. Bychowska, K. Brzozowski, J. Thöming and P. Stepnowski, *Marine drugs*, 2010, **8**, 1567-1636.
47. A. Tiwari and A. N. Nordin, *Advanced biomaterials and biodevices*, John Wiley & Sons, 2014.
48. S. C. Fox, B. Li, D. Xu and K. J. Edgar, *Biomacromolecules*, 2011, **12**, 1956-1972.
49. C. Brasselet, G. Pierre, P. Dubessay, M. Dols-Lafargue, J. Coulon, J. Maupeu, A. Vallet-Courbin, H. de Baynast, T. Doco, P. Michaud and C. Delattre, *Applied Sciences*, 2019, **9**.
50. M. Rodriguez-Vazquez, B. Vega-Ruiz, R. Ramos-Zuniga, D. A. Saldana-Koppel and L. F. Quinones-Olvera, *BioMed Research International*, 2015, **1**, 821279.
51. P. Ying, J. Yu and W. Su, *Advanced Synthesis & Catalysis*, 2021, **363**, 1246-1271.
52. M. A. Asrahwi, N. A. Rosman, N. N. M. Shahri, J. H. Santos, E. Kusriani, S. Thongratkaew, K. Faungnawakij, S. Hassan, A. H. Mahadi and A. Usman, *Carbohydrate Research*, 2023, **534**, 108971.
53. C. Van Poucke, A. Vandeputte, S. Mangelinckx and C. V. Stevens, *Green Chemistry*, 2023, **25**, 4271-4281.
54. D. Vallejo-Domínguez, E. Rubio-Rosas, E. Aguila-Almanza, H. Hernández-Cocolezzi, M. Ramos-Cassellis, M. Luna-Guevara, K. Rambabu, S. Manickam, H. S. H. Munawaroh and P. L. Show, *Ultrasonics Sonochemistry*, 2021, **72**, 105417.

55. J. Shokri and K. Adibki, in *Cellulose - Medical, Pharmaceutical and Electronic Applications*, 2013, DOI: 10.5772/55178, ch. Chapter 3.
56. J. You, X. Zhang, Q. Mi, J. Zhang, J. Wu and J. Zhang, *Cellulose*, 2022, **29**, 9583-9596.
57. H. Tu, M. Zhu, B. Duan and L. Zhang, *Advanced Materials*, 2021, **33**, e2000682.
58. T. Mahnaj, S. U. Ahmed and F. M. Plakogiannis, *Pharmaceutical development and technology*, 2013, **18**, 982-989.
59. P. Ahmadi, A. Jahanban-Esfahlan, A. Ahmadi, M. Tabibiazar and M. Mohammadifar, *Food Reviews International*, 2022, **38**, 685-732.
60. M. M. Costa, E. C. Cabral-Albuquerque, T. L. Alves, J. C. Pinto and R. L. Fialho, *Journal of agricultural and food chemistry*, 2013, **61**, 9984-9991.
61. M. Davidovich-Pinhas, S. Barbut and A. Marangoni, *Carbohydrate polymers*, 2015, **117**, 869-878.
62. A. Ain-Ai and P. K. Gupta, *International journal of pharmaceutics*, 2008, **351**, 282-288.
63. S. P. Hoo, Q. L. Loh, Z. Yue, J. Fu, T. T. Y. Tan, C. Choong and P. P. Y. Chan, *Journal of Materials Chemistry B*, 2013, **1**, 3107-3117.
64. B. Midmore, *Colloids and Surfaces A: Physicochemical and Engineering Aspects*, 1998, **132**, 257-265.
65. M. A. Repka and J. W. McGinity, *Journal of Controlled Release*, 2001, **70**, 341-351.
66. R. L. McMullen, S. Ozkan and T. Gillece, *Cosmetics*, 2022, **9**, 52.
67. B. Helferich and H. Koester, *Berichte der deutschen chemischen Gesellschaft (A and B Series)*, 1924, **57**, 587-591.
68. W. Hearon, G. D. Hiatt and C. R. Fordyce, *Journal of the American Chemical Society*, 1943, **65**, 2449-2452.
69. J. Honeyman, *Journal of the Chemical Society (Resumed)*, 1947, 168-173.
70. D. M. Hall and J. R. Horne, *Journal of Applied Polymer Science*, 1973, **17**, 2891-2896.
71. T. Kondo and D. G. Gray, *Carbohydrate research*, 1991, **220**, 173-183.
72. N. Ding, *Homogeneous etherification modification of chitosan and preparation of high-strength hydrogel*, IOP Publishing, 2022.
73. M. I. H. Mondal, *Cellulose and Cellulose Derivatives: Synthesis, Modification and Applications*, Nova Publishers, 2015.
74. S. Fischer, K. Thümmeler, B. Volkert, K. Hettrich, I. Schmidt and K. Fischer, *Macromolecular Symposia*, 2008, **262**, 89-96.
75. Y. Cheng, Z. Hu, Y. Zhao, Z. Zou, S. Lu, B. Zhang and S. Li, *International Journal of Molecular Sciences*, 2019, **20**, 3890.
76. K. Rahn, M. Diamantoglou, D. Klemm, H. Berghmans and T. Heinze, *Die Angewandte Makromolekulare Chemie: Applied Macromolecular Chemistry and Physics*, 1996, **238**, 143-163.
77. T. Heinze, K. Rahn, M. Jaspers and H. Berghmans, *Macromolecular Chemistry and Physics*, 1996, **197**, 4207-4224.
78. P.-H. Elchinger, P.-A. Faugeras, C. Zerrouki, D. Montplaisir, F. Brouillette and R. Zerrouki, *Green Chemistry*, 2012, **14**, 3126-3131.
79. C. L. McCormick and P. A. Callais, *Polymer*, 1987, **28**, 2317-2323.
80. S. Schmidt, T. Liebert and T. Heinze, *Green Chemistry*, 2014, **16**, 1941-1946.
81. U. T. Santoso, R. Nurmasari and D. Umaningrum, 2011.
82. K.-i. Furuhashi, K. Koganei, H.-S. Chang, N. Aoki and M. Sakamoto, *Carbohydrate research*, 1992, **230**, 165-177.

83. Y. Matsui, J. Ishikawa, H. Kamitakahara, T. Takano and F. Nakatsubo, *Carbohydrate research*, 2005, **340**, 1403-1406.
84. I. A. Duceac and S. Coseri, *Biotechnology Advances*, 2022, **61**, 108056.
85. H. Hamed, S. Moradi, S. M. Hudson, A. E. Tonelli and M. W. King, *Carbohydrate Polymers*, 2022, **282**, 119100.
86. T. Kondo, *Journal of Polymer Science Part B: Polymer Physics*, 1994, **32**, 1229-1236.
87. M. S. Singh, S. Chowdhury and S. Koley, *Tetrahedron*, 2016, **72**, 5257-5283.
88. V. V. Rostovtsev, L. G. Green, V. V. Fokin and K. B. Sharpless, *Angewandte Chemie International Edition*, 2002, **41**, 2596-2599.
89. C. W. Tornøe, C. Christensen and M. Meldal, *The Journal of organic chemistry*, 2002, **67**, 3057-3064.
90. S. Ifuku, M. Wada, M. Morimoto and H. Saimoto, *Carbohydrate Polymers*, 2011, **85**, 653-657.
91. K.-i. Furuhashi, H.-S. Chang, N. Aoki and M. Sakamoto, *Carbohydrate research*, 1992, **230**, 151-164.
92. P. Peng, X. Cao, F. Peng, J. Bian, F. Xu and R. Sun, *Journal of Polymer Science Part A: Polymer Chemistry*, 2012, **50**, 5201-5210.
93. N. A. Peppas, P. Bures, W. Leobandung and H. Ichikawa, *European journal of pharmaceuticals and biopharmaceutics*, 2000, **50**, 27-46.
94. S. Mitura, A. Sionkowska and A. Jaiswal, *Journal of Materials Science: Materials in Medicine*, 2020, **31**, 1-14.
95. I. Aranaz, N. Acosta, C. Civera, B. Elorza, J. Mingo, C. Castro, M. D. L. L. Gandía and A. Heras Caballero, *Polymers*, 2018, **10**, 213.
96. C. Qin, Y. Du, L. Xiao, Y. Liu and H. Yu, *Journal of applied polymer science*, 2002, **86**, 1724-1730.
97. A. Jardine, *Current Research in Green and Sustainable Chemistry*, 2022, **5**, 100309.
98. R. Koshani, J. Zhang, T. G. van de Ven, X. Lu and Y. Wang, *ACS Sustainable Chemistry & Engineering*, 2021, **9**, 10513-10523.

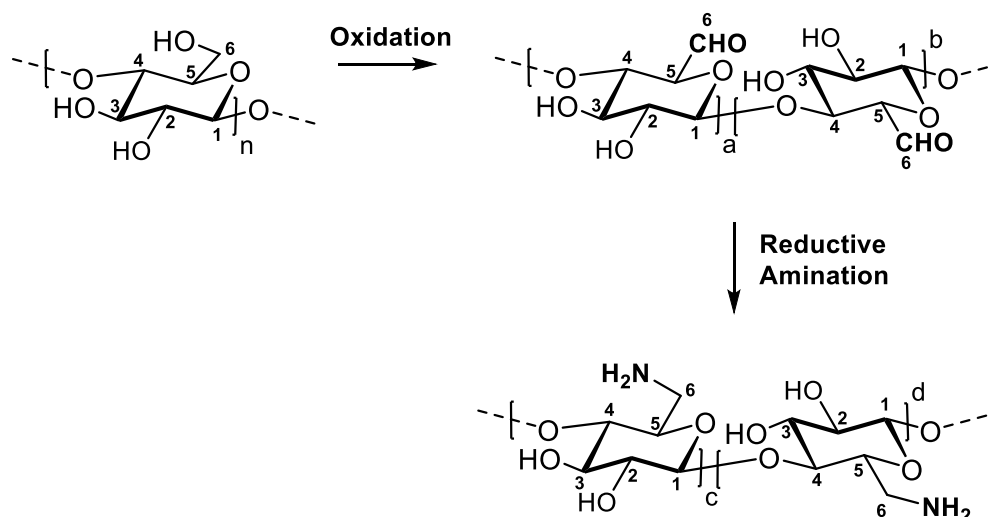
Chapter 2: Oxidation of Biopolymers

2.1 Literature review

Selective oxidation of cellulose and chitosan

The oxidation of biopolymers is a greatly advantageous chemical modification because the aldehyde or carboxyl moieties in the backbone allows for further chemical modifications such as Schiff base reactions, oxidation to carboxylic acids and reduction to alcohols.¹⁻³ Oxidation is an attested method for derivatisation because the structures and properties of the products it yields are dependent on the reaction medium and parameters, as well as substrate and reagents used.⁴

There are two main oxidation states of cellulose whereby primary and secondary hydroxyl groups are converted to oxidised functionalities, namely, carbonyl (aldehydes and ketones) and carboxyl groups.⁵ These different oxidation states of cellulose are dependent on the oxidising conditions such as nature of oxidant, temperature, pH and reaction period; and allow for different types of further chemical modifications.^{6, 7} Of particular interest, is the reductive amination of carbonyl functionalised cellulose to secondary or tertiary amines and carboxylic functionalised cellulose to primary amines (**Scheme 2.1**).



Scheme 2.1. Oxidation and Reductive Amination of Cellulose.

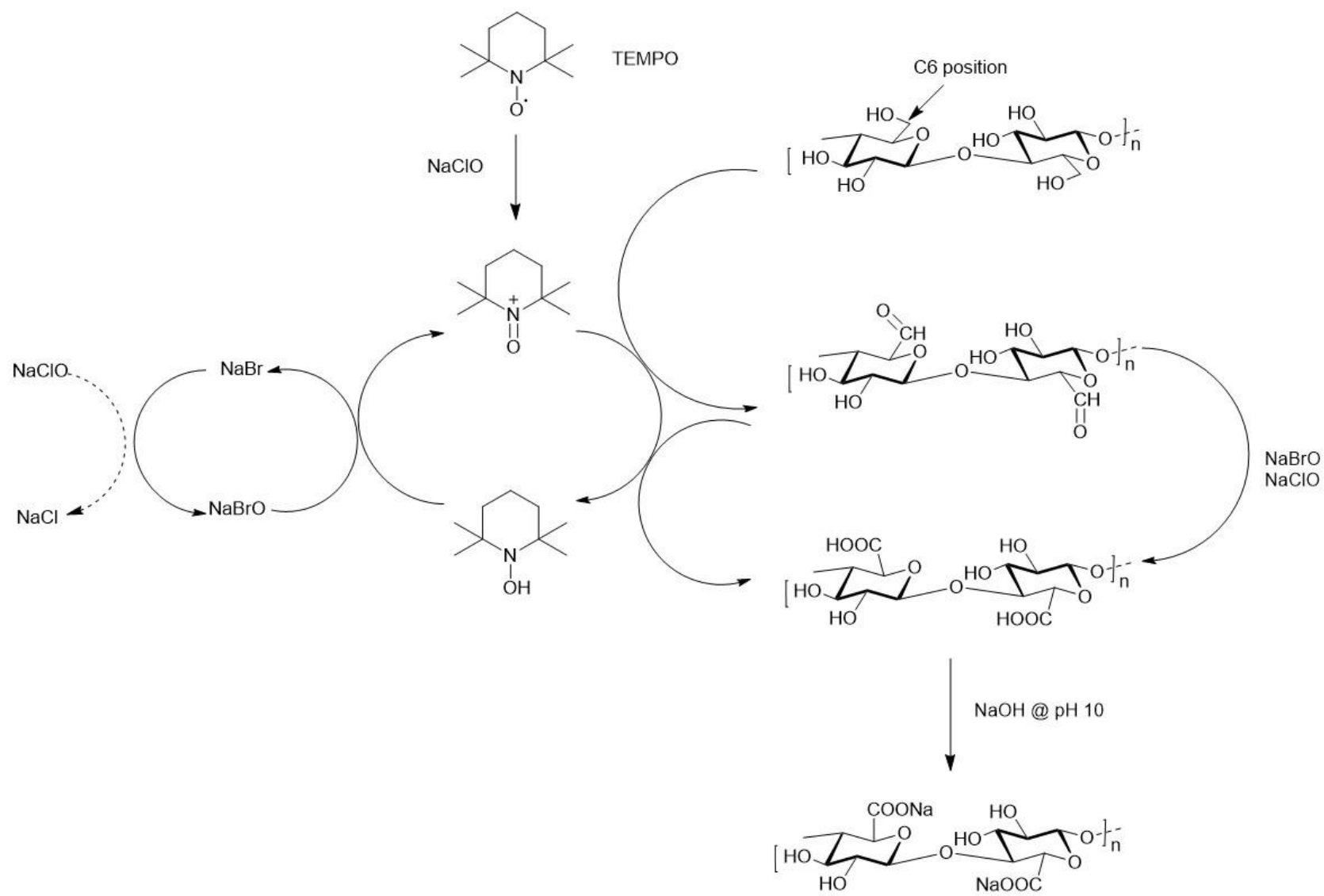
Primary oxidised cellulose has applications in many fields. Crawford *et al.* formed shear thinning gels from partially C-6 oxidised cellulose nanofibers in the presence of surfactants or salts which are used as materials in applications that require thickening of aqueous formulations. Partially C-6 oxidised cellulose that is dispersed is a cheap yet effective thickener that is made from renewable sources using minimal chemical processing and is suitable for use in personal care formulations amongst other aqueous formulations.⁸ A recent review by Zhang *et al.* highlights the use of oxidised cellulose as hemostatic materials with applications in surgical procedures.⁹ Oxidised cellulose, specifically C-6 carboxy cellulose, displays characteristics of compatibility and absorption which allows it to be biodegradable in the human body.^{10, 11} The degree of oxidation and structure of the original cellulose influences the degradation and resorption time in the body.¹² Oxidised cellulose with carboxyl acid content in the range of 16-24 % shows good hemostatic effects and has been used to control bleeding in many surgeries.¹³

A wide variety of further chemical reactions of oxidised cellulose are possible such as Schiff base reactions, sulfonation, silanisation, oxidation to carboxylic acids and reduction to alcohols.^{2, 3, 14-19} Lucia *et al.* reported a direct silanisation method for dialdehyde cellulose (DAC), which can be easily modified with (3-aminopropyl)triethoxysilane. After thermal treatment and lyophilisation, the product obtained showed condensation and cross-linking between hydroxyl group of DAC with the silanol groups and imine-type bonds between the amino group and aldehyde functions of the DAC.¹⁸ Rajalaxmi *et al.* reported the synthesis of novel water-soluble sulfonated cellulose following a periodation/sulfonation procedure at room temperature which can be utilised as a biocompatible and biodegradable material in the biomedical field.¹⁹

Two oxidation methods of interest are (2,2,6,6-tetramethylpiperidin-1-yl)oxyl (TEMPO)-mediated reactions for C-6 oxidation and periodate oxidation reactions for C-2,3 oxidation because of their mild conditions, increased regioselectivity, improved yield and degree of substitution, as well as great opportunities for further chemical modifications.⁴ The aforementioned methods for selective oxidation of cellulose and chitosan are briefly highlighted below.

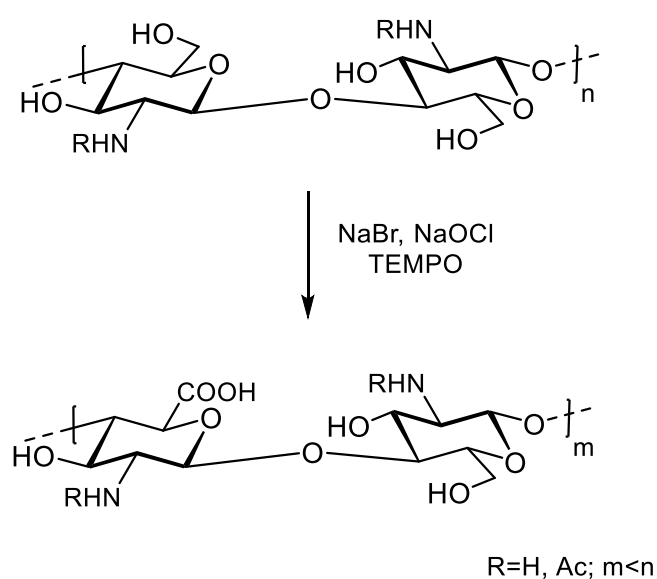
i. (2,2,6,6-Tetramethylpiperidin-1-yl)oxyl (TEMPO)-mediated C-6 oxidation

Tempo-mediated oxidation of cellulose is temperature- and pH-sensitive and utilises stable nitroxyl radicals as selective oxidants. The reaction converts the primary alcohol at C-6 in the anhydroglucose unit into carboxylic acid/salt moieties (polyuronic analogues), hence is highly regioselective as well as produces high yields and degrees of conversion. Other advantages of TEMPO-mediated oxidation are the preservation of the crystal width and crystallinity of cellulose. However, depending on the reaction conditions, some degree of depolymerisation occurs. The mechanism is presented in **Scheme 2.2**. Firstly, the reaction of 2,2,6,6-tetramethylpiperidine-*N*-oxyl (TEMPO) with an oxidising system, such as bromide salts and sodium hypochlorite yielding hypobromide anions which further oxidise TEMPO, generates the active oxidant species nitrosonium cation *in situ*. This intermediate undergoes reduction to the reduced form of TEMPO, *N*-hydroxy-2,2,6,6-tetramethylpiperidine, with concomitant oxidation of cellulose by the nitrosonium cation. The TEMPO-mediated oxidation of cellulose occurs at an alkaline pH of 10.5 which is a result of the presence of NaOH. Sodium hydroxide in the reaction medium is required for the neutralisation of the carboxylic acid moieties formed by oxidation. Although primary hydroxyl groups are converted to aldehyde groups in the first stage of cellulose oxidation, hemiacetal moieties form as well by intra- or intermolecular reactions between hydroxyl and aldehyde groups. NaOH is consumed in greater amounts than the carboxylic acid groups formed, which can be attributed to aldehydes turning into aldehyde hydrate sodium salts. Lastly, the oxidation of aldehyde hydrates and/or hemiacetals by oxoammonium cations occurs when sodium salts of the carboxylic acid moieties form in addition to the reduced form of TEMPO. This oxidation cycle can repeat when new nitroxyl radicals and oxoammonium cations form.^{4, 20, 21}



Scheme 2.2. Proposed mechanism of TEMPO-NaOCl- mediated oxidation of cellulose.^{4, 20}

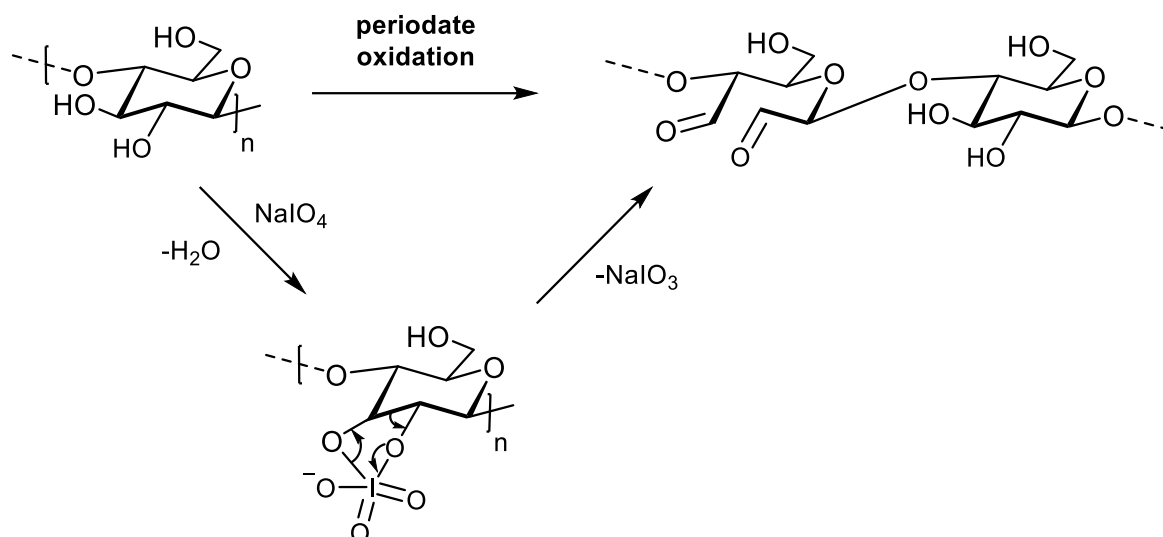
TEMPO-oxidation of chitosan follows a similar mechanism (**Scheme 2.3**). Yoo *et al.* investigated the effect of C-6-selective TEMPO-oxidation of chitosan on its physical and biological properties and found that the introduction of carbonyl groups into the chitosan structure resulted in improved water solubility; however, this enhanced water solubility was limited as it decreased as the degree of oxidation increased from 25 to 100 %. This could possibly be explained by the incorporation of negative charges on chitosan which interact with the positive charges from the C-2 amino groups of native chitosan, hence forms an aggregation of chitosan 6-carbaldehyde polymer molecules by charge-charge interactions.²² These intermolecular associations are similar to the H-bonding experienced by cellulose, causing the polymer chains to bind and crystallise resulting in an aggregate of 6-oxychitosan molecules and a decrease in aqueous solubility. The limited solubility as a consequence of the degree of oxidation (DO), coupled with degradation of the chitosan structure and low yields are major disadvantages of this method.^{22, 23} Gao *et al.* investigated the effects of acid swelling chitosan pretreatment on the rate of the specific oxidation of chitosan catalysed by the TEMPO-NaBr-NaOCl system. Results showed a significant increase in the rate of oxidation for pretreated chitosan as well as a reduction in degradation. Additionally, the oxidised chitosan was obtained in favourable yield, with great water solubility and a high DO.²³ The environmental impact and cost of using TEMPO as a catalyst for oxidation limits its use for industrial-scale oxidation.²⁴ Furthermore, TEMPO-mediated oxidation yields further oxidation of the C-6 aldehyde to carboxyl groups. The need arises for the investigation of an oxidation method for biopolymers that selectively stops at the aldehyde.



Scheme 2.3. Synthetic scheme for TEMPO-mediated oxidation of chitosan.²³

ii. Periodate oxidation of the C-2,3 diol

Sodium periodate can react with the vicinal secondary hydroxyl groups at C-2 and C-3 and split the C2-C3 bond in the anhydroglucose structural unit, thus forming two vicinal aldehyde groups, i.e. dialdehydes. Therefore, sodium periodate is a highly selective cellulose oxidant. Periodate oxidation occurs at an acidic pH of approximately 3, at temperatures close to room temperature (20 °C), and in the dark for 24 to 250 h.^{4, 25} The mechanism for sodium periodate-mediated selective oxidation of cellulose is shown in **Scheme 2.4**. During the cleavage reactions, a periodate ester firstly forms, which is a cyclic intermediate, and subsequently generates the dialdehyde.¹⁴ The periodate ester is temperature- and pH- sensitive, and the geometry of the substrate also influences its formation.^{14, 26-30} Compared to TEMPO-mediated oxidation, the periodate oxidation results in DAC with lower crystallinity dependent on the degree of oxidation, but with preservation of the microfibril shape.^{4, 25} Previous studies have shown that the introduction of aldehyde groups in regions of high molecular weight is a distinguishable characteristic of periodate oxidation. It was concluded that the periodate anion reacted with the C2-C3 bonds in the crystalline regions from the start of the reaction, therefore influencing the highly ordered alignment of macromolecules.⁴ The periodate-chlorite method is a selective oxidation method that occurs in the presence of hydrogen peroxide and sodium chlorite at a pH of 5, stirring at room temperature for 24 h. During this oxidation method, the aldehyde groups were converted to carboxylic groups and the fractions separated after analysis of each stage. Hence, it was concluded that the amorphous regions in cellulose (softwood cellulose pulp) were subjected to both oxidation reactions, resulting in a depolymerisation and subsequent dissolution which were evident by the crystallinity and morphology study. This was further supported by FTIR data for the fraction with the greatest number of carboxylic groups.^{4,}
³¹ In another experiment, cellulose was reacted with sodium periodate for 5 h in the dark at 55 °C to yield DAC. DAC (after isolation) was subjected to oxidation in the presence of sodium chlorite for 24 h at an acidic pH and the data collected showed near complete conversion of aldehyde groups into carboxylic groups.^{4, 32}



Scheme 2.4. Proposed mechanism of sodium periodate-mediated selective oxidation of cellulose.¹⁴

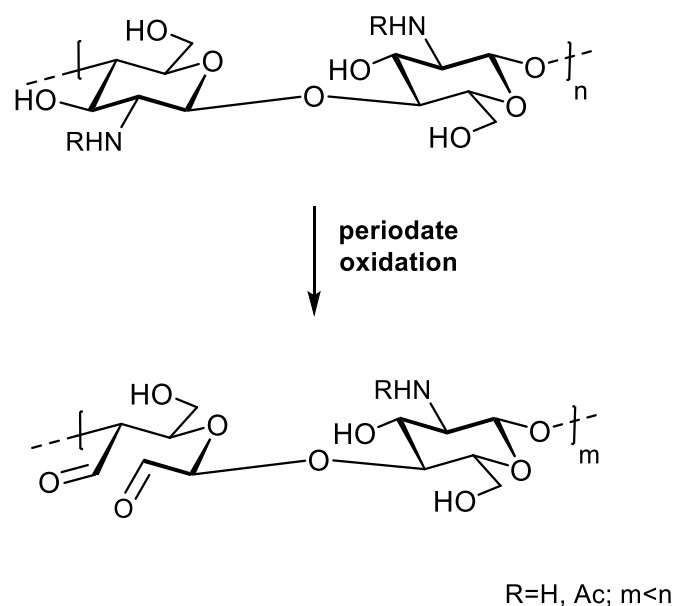
The physicochemical properties of DAC make it ideal for applications in the biomedical field such as tissue engineering, wound-care and drug delivery; as well as other fields such as packaging, chromatography and energy storage. A recent review by Dalei *et al.* highlights the versatility of DAC in various applications.¹⁴ A few noteworthy properties of DAC include solubility, thermal properties, antibacterial attributes and the potential to be used as intermediates for further functionalisation using the aldehyde as a handle.

There are two broad strategies for the synthesis of DAC: Criegee glycol cleavage and the Malaprade reaction. The Criegee glycol cleavage utilises the toxic lead tetracetate as oxidising agent, whereas the Malaprade reaction uses the relatively less toxic periodate.^{14, 33-37} The reaction is performed at low temperatures in acidic environments. Advantages of the periodate oxidation method include mild reaction conditions and great selectivity for the cleavage of the C2-C3 bond of cellulose.^{14, 38} The DO can also be controlled by changing the reaction conditions of the periodate reaction.^{4, 39-45} Unfortunately, its application is limited on large scale due to cellulose's high crystallinity and the formation of hemiacetals. Other disadvantages of periodate oxidation are the iodinated products that result after oxidation that are hazardous and require removal.

Therefore, the commercial scalability of DAC is an issue due to the reusability of the periodate. Studies have been conducted on the reusability of periodate by Koprivica *et al.* who regenerated used iodate by ozone treatment in alkaline medium; and Dang *et al.* who used an

electrochemically-assisted system for the synthesis of DAC with a regeneration efficiency of used periodate of 93.4 %.^{14, 46, 47}

Periodate oxidation of chitosan is an understudied area of research (**Scheme 2.5**). This method has been used to confirm the structure of chitosan and chitin, but chitosan with intermediate degrees of acetylation were not studied.^{48, 49} It is an understudied research area because of the amino group of chitosan. Vold *et al.* demonstrated that the behaviour of periodate oxidised chitosan is greatly dependent on the degree of *N*-acetylation. It was observed that the rate of oxidation is indirectly proportional to the fraction of acetylated units, F_A , which may be attributed to the decreasing charge density with increasing F_A . This results in a weaker electrostatic attraction between the cationic chitosan and the anionic periodate, hence increasing the effective concentration of periodate in proximity to the polymer chain.⁴⁹ The rate of depolymerisation and the overconsumption of periodate decreased as F_A increases. The reason for this ‘protective’ effect of *N*-acetylated residues, which are oxidation-resistant, is not yet known.⁴⁹ Chitosan also experiences an oxidation limit, like cellulose and other polysaccharides, due to the formation of hemiacetals.^{49, 50} Chitosan experiences more extensive depolymerisation by periodate oxidation than cellulose.^{49, 51} These attributes of periodate oxidised chitosan could be explained by a unique chitosan-specific degradation mechanism connected to the free amino groups of chitosan.⁴⁹ A study by Kirui *et al.* explored the prospective applications of dialdehyde chitosan, which was synthesised from chitosan extracted from the black soldier fly followed by periodate oxidation. Dialdehyde chitosan exhibited enhanced inhibition growth of *A. brasiliensis* and *C. albicans* fungi relative to chitosan which was attributed to the enhanced interaction between the dialdehyde groups and fungal cells, possibly a consequence of its properties of increased crystallinity.⁵²



Scheme 2.5. Periodate oxidation of chitosan.⁵²

Although TEMPO- and periodate-oxidation are the most common methods for selective oxidation of biopolymers, they both have concerning drawbacks, mainly depolymerisation and over-oxidation. Selective C-6 oxidation of biopolymers to the aldehyde remains a challenge. In addition to the over-oxidation to the carboxyl group during TEMPO oxidation, other drawbacks such as the degradation of cellulose using halogens in the TEMPO/NaBr/NaClO (TBN) oxidation reaction; and the limitation of carbonyl groups formed in the TEMPO/laccase/O₂ (TLO)-oxidation because of laccase degradation caused by the TEMPO⁺ formed which competes with the oxidation of cellulose.^{53, 54} Therefore, the need arises for a new method for selective, mild oxidation of biopolymers to the aldehyde level displaying minimal if not any depolymerisation.

2.2 Results and discussion

2.2.1 Synthesis of dialdehyde cellulose (DAC)

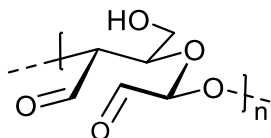
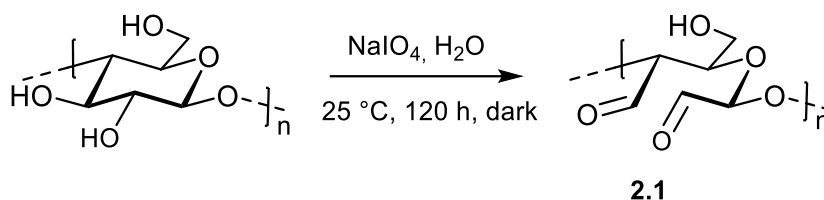


Figure 2.1. Structure of dialdehyde cellulose (DAC) (**2.1**).

Dialdehyde cellulose (DAC) (**2.1**) was prepared *via* a periodate oxidation reaction with cellulose in distilled water at 25 °C for 120 h in the dark since periodate is light-sensitive (**Scheme 2.6**). Periodate oxidation generates equimolar amounts of iodate as well as excess toxic periodate. A common work-up procedure for the decomposition of excess periodate is glycol quenching using either ethylene glycol or glycerol.^{55, 56} This method has significant drawbacks such as the possible occurrence of side reactions with the formaldehyde formed. The formaldehyde and excess glycol could react with the hydroxyl or aldehyde groups of DAC. Therefore, a simple washing with distilled water was performed, as suggested by Simon *et al.*, as it also removes excess periodate and does not encourage any side reactions with organic contaminants.⁵⁶ DAC (**2.1**) was obtained as a white solid with a high mass yield of 75 %.



Scheme 2.6. Reaction scheme for formation of DAC (**2.1**).

DAC (**2.1**) was characterised by FT-IR spectroscopy (**Figure 2.2**) which shows the diagnostic absorption band at 880 cm^{-1} of the hemiacetal.^{25, 57} The presence of a carbonyl group is not distinguishable in the spectrum, possibly due to the formation of hemiacetals, hemialdals and hydrates which are all masked forms of the aldehyde.⁵⁸ The lower intensity of the absorption band occurring at 3334 cm^{-1} , as well as the presence of the hemiacetal band, are due to the lower hydroxyl content resulting from the formation of hemiacetals and hemialdals.^{59, 60} Possible aldehyde hydration is suggested by the absorption band at 1628 cm^{-1} which is a slight shift from 1640 cm^{-1} observed for the adsorbed water of cellulose.

DAC was mildly oxidised with a DO of 9.20 mmol.g^{-1} , which was determined by means of a quantitative oximation reaction with hydroxylamine hydrochloride, as described in **Chapter 6**.⁶¹

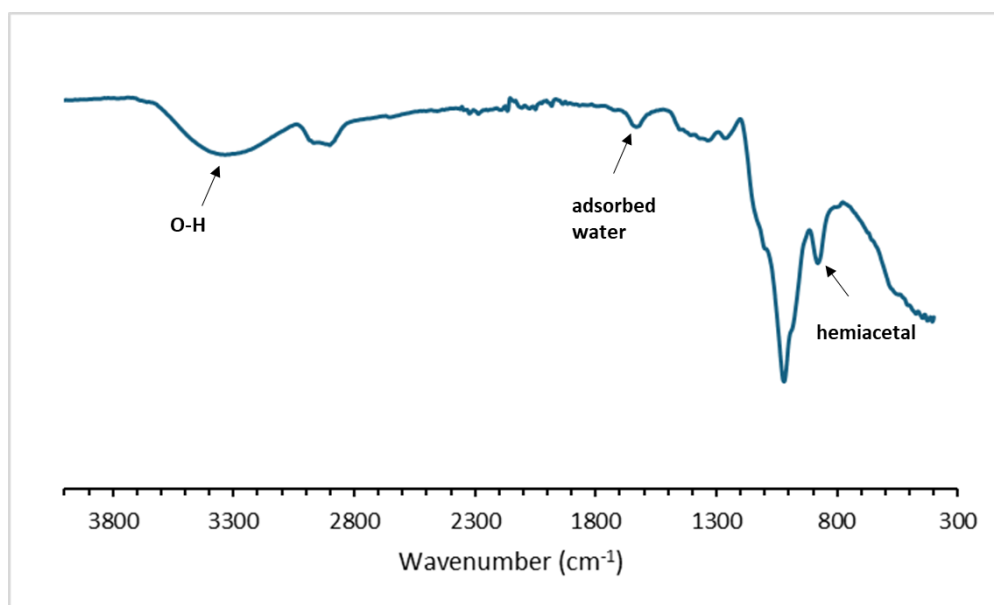


Figure 2.2. IR spectrum of DAC (2.1)

The crystallinity of DAC relative to microcrystalline cellulose was examined using PXRD (**Figure 2.3**). Cellulose shows three diffraction peaks at 2θ of 15.45° , 22.76° and 35.03° , respectively, in agreement with literature.⁶² The strongest peak at 22.76° is associated with the crystallinity planes of (2 0 0).⁶³ The PXRD pattern changes after oxidation. The diffraction pattern displays one broad peak with a 2θ of 18.92° which is indicative of a fully amorphous and highly oxidised polymer.^{1, 62} DAC loses the high crystallinity of cellulose when the highly ordered structure of cellulose is disrupted due to the opening of the rings of AGUs caused by periodate oxidation.⁶⁴

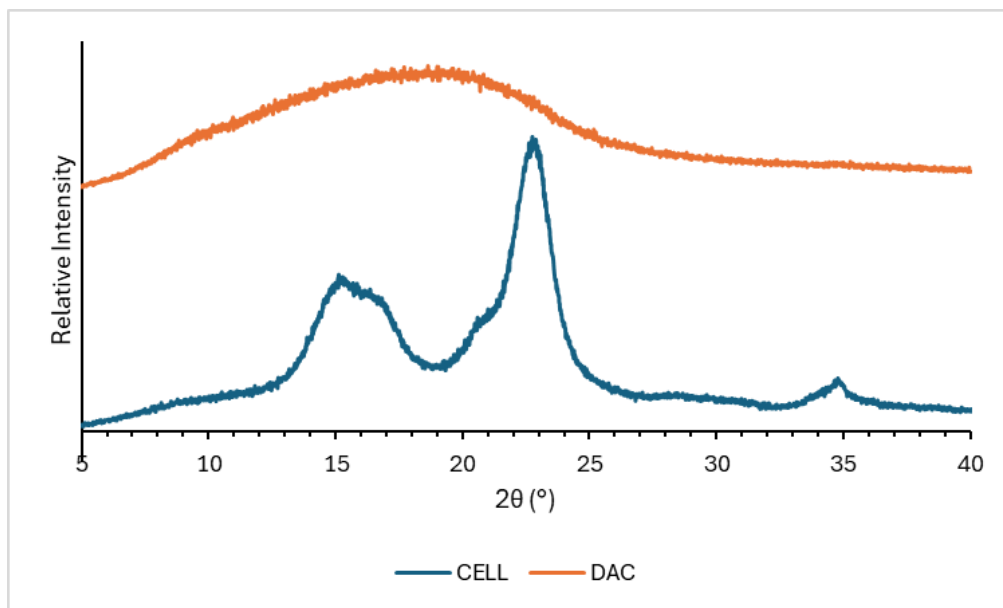


Figure 2.3. PXRD spectrum of cellulose (**CELL**) and dialdehyde cellulose (**DAC**) (**2.1**).

The TGA and DSC curves for DAC is shown in **Figure 2.4**. The TGA thermogram depicts three degradation stages which are similar to that reported in literature.⁶⁵ Firstly, the loss of adsorbed water which occurs under 100 °C and then the thermal degradation of oxidised cellulose at 190 °C, and lastly the pyrolysis process starting at 220 °C. The decomposition temperature of DAC shifts to a lower temperature (190 °C) than that of microcrystalline cellulose (MCC) (352 °C) because of the decrease in crystallinity of DAC caused by cleavage of the glucopyranose ring and disorder in the packing order of cellulose molecules after oxidation.^{64, 66} The DSC was used to confirm the thermal stability of the polymer and displays two endothermic peaks at 89 °C and 190 °C, corresponding to weight losses of 9 % and 4 %, respectively. The majority of the weight loss (64 %) occurs during the third degradation step at 220 °C which is attributed to the depolymerisation and pyrolysis of DAC.

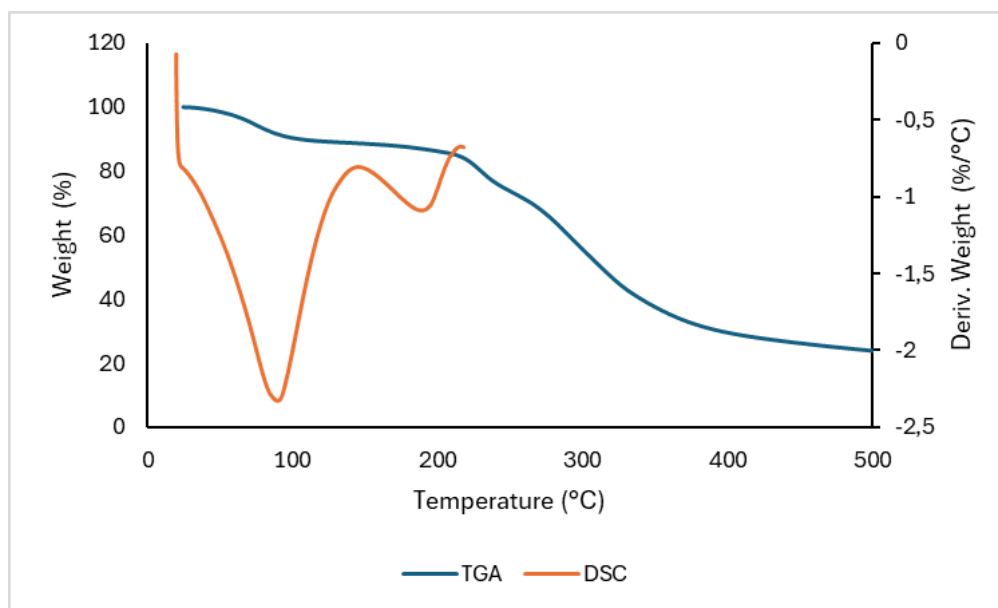
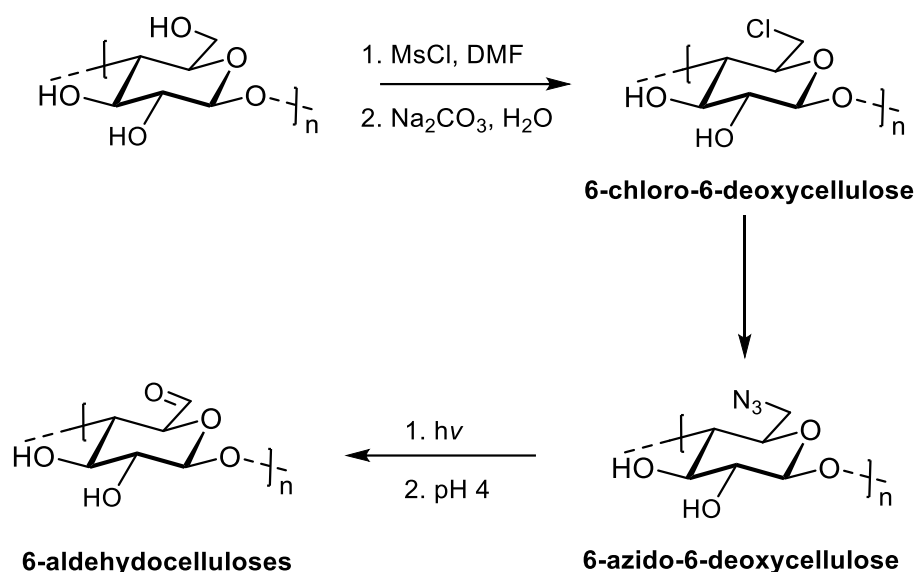


Figure 2.4. The TGA and DSC curves of DAC (**2.1**).

2.2.2 Selective C-6 oxidation of cellulose

The selective oxidation of cellulose to unsubstituted 6-aldehydocellulose and 6-carboxycellulose was reported by Horton *et al.* by photolysis of 6-azido-6-deoxycellulose (**Scheme 2.7**). In this reported method, C-6-chlorinated cellulose was prepared using methanesulfonyl chloride in DMF; a method of introducing the good leaving-group chlorine without protection of the secondary hydroxyl groups. Secondly, the 6-chloro-6-deoxycellulose was converted to 6-azido-6-deoxycellulose by means of a reaction with sodium azide in water or dimethyl sulfoxide.

Finally, 6-aldehydocellulose was obtained by photolysis of the 6-azido product, where the authors explored various conditions of photolysis. The 6-aldehydocellulose with DO of 60% was water soluble and characterised by oxidation to 6-carboxycellulose, reduction to cellulose, by copper number and by the method of deuteration-mass spectroscopy.⁶⁷

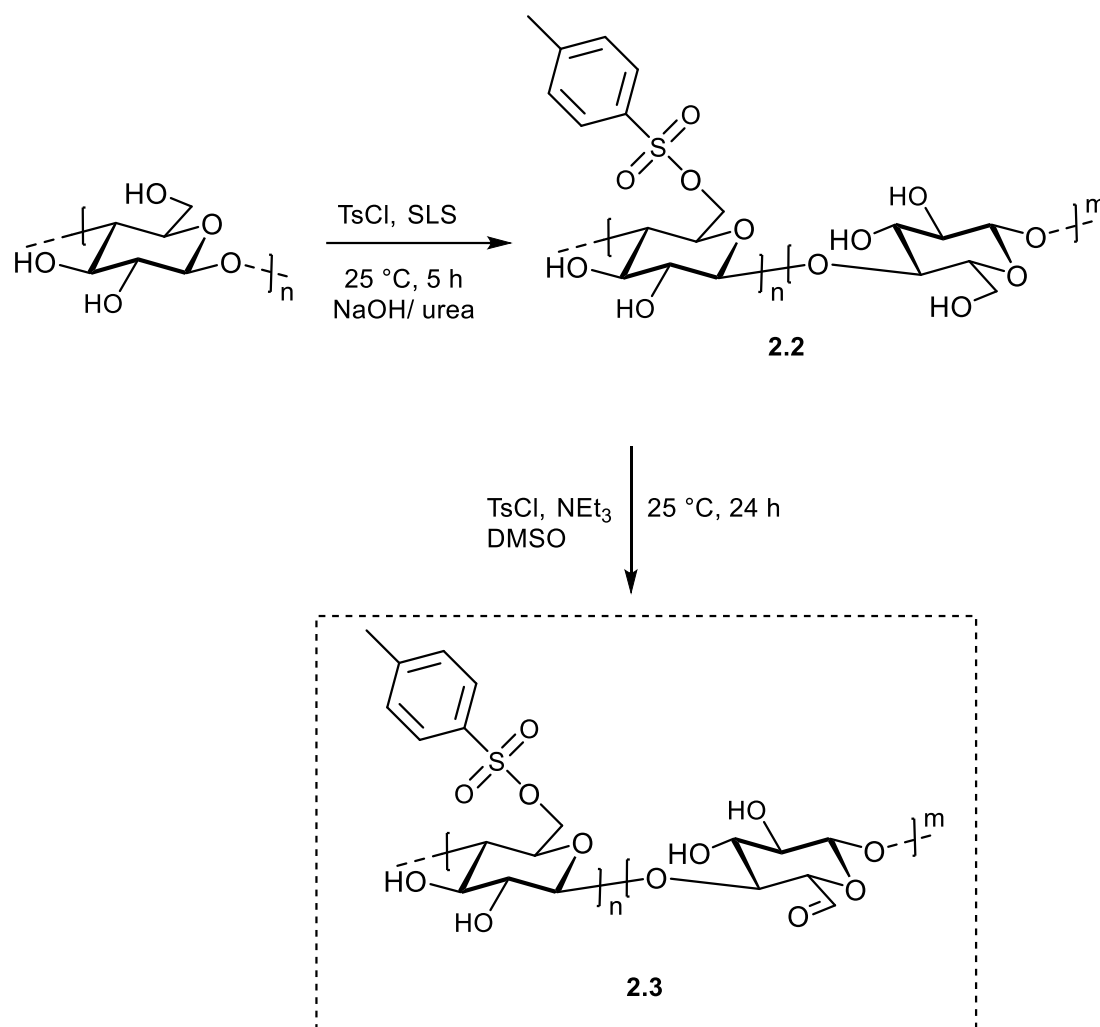


Scheme 2.7. Synthesis of 6-aldehydocelluloses by Horton *et al.*⁶⁷

This reported synthesis of C-6 selective oxidation of cellulose has major disadvantages. There was a significant decrease in DS from the 6-azido to the aldehyde product, possibly due to the loss of water-soluble fragments in the wash solutions as well as in the hydrolysis media during the isolation of the aldehyde product. This loss of yield was further evident in the decrease of weight-yields as the DS increases. Additionally, product was also lost during the reduction of the aldehyde to yield cellulose. Aldehyde groups might have also been reductively transformed by the formation of amino groups during photolysis.⁶⁷ Therefore, the need arises for a new, shorter and greener method for C-6 selective oxidation of cellulose that bypasses these limitations as well as the use of hazardous chlorinating reagents like methanesulfonyl chloride and the formation of harmful azido products.

In this study, a more green and sustainable method for the synthesis of soluble C-6 selectively oxidised cellulose which utilises green solvent systems and is easily scalable and cost-effective is proposed (**Scheme 2.8**). Cellulose is insoluble in most common solvent systems but is known to be soluble in LiCl/DMAc, hence tosylation of cellulose usually occurs in this solvent system. Therefore, cellulose is firstly tosylated using TsCl in the presence of the surfactant sodium lauryl sulfate (SLS) in a green NaOH/urea solvent system to yield cellulose tosylates (**2.2**) with a DS high enough to disrupt the crystallinity of cellulose and improve the solubility in DMSO.

The solubility of tosyl cellulose in DMSO is important because it is the solvent choice for Swern-type oxidation reactions. Partially tosylated cellulose is subsequently subjected to a Swern-like oxidation, using TsCl in the presence of triethylamine in DMSO, to obtain the target C-6 selectively oxidised C-6 tosyl cellulose product (**2.3**). To confirm the successful synthesis of C-6 selectively oxidised C-6 tosyl cellulose, a Schiff base reaction (**2.4**) is performed using benzylamine in DMSO where the characteristic imine bond formed is identified using NMR and IR spectroscopy.



Scheme 2.8. Overall synthetic scheme for the synthesis of C-6 selectively oxidised C-6 tosyl cellulose (**C-6 OXID CELL**) (**2.3**).

Tosylation of cellulose

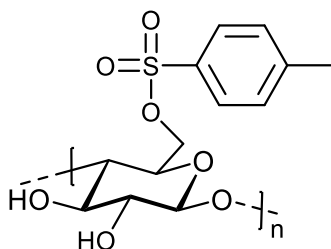


Figure 2.5. Structure of tosyl cellulose (2.2).

Tosyl cellulose (2.2) was synthesised following a modified literature method by Schmidt *et al.* as shown in **Scheme 2.8**.⁶⁸ The authors reported the use of a green NaOH-urea solvent system and the nonionic surfactant polyethylene glycol alkyl-(C₁₁-C₁₅) ether (Imbetin) to yield soluble tosyl cellulose. They found that the use of anionic surfactants e.g. sodium laurate sulfate (SLS) cannot improve the solubility of tosyl cellulose.⁶⁸ However, in this study soluble tosyl cellulose was successfully synthesised using SLS as a surfactant. The drawback of using SLS is that it requires excessive water and ethanol washing to remove it from the reaction mixture. Herein, DMSO-soluble tosyl cellulose with a good yield of 72 % is reported. The IR, ¹H-NMR and ¹³C-NMR spectra (**Figures 2.6, 2.7 and 2.8** respectively) confirm the structure of tosyl cellulose (2.2). The IR spectrum shown in **Figure 2.6** suggests the structure of tosyl cellulose (TS CELL). The absorption bands at 1354 and 1174 cm⁻¹ corresponding to the asymmetric and symmetric stretching of SO₂, respectively; as well as the signal for S-O-C at 812 cm⁻¹, are indicative of the introduction of the tosyl moiety of tosyl cellulose.

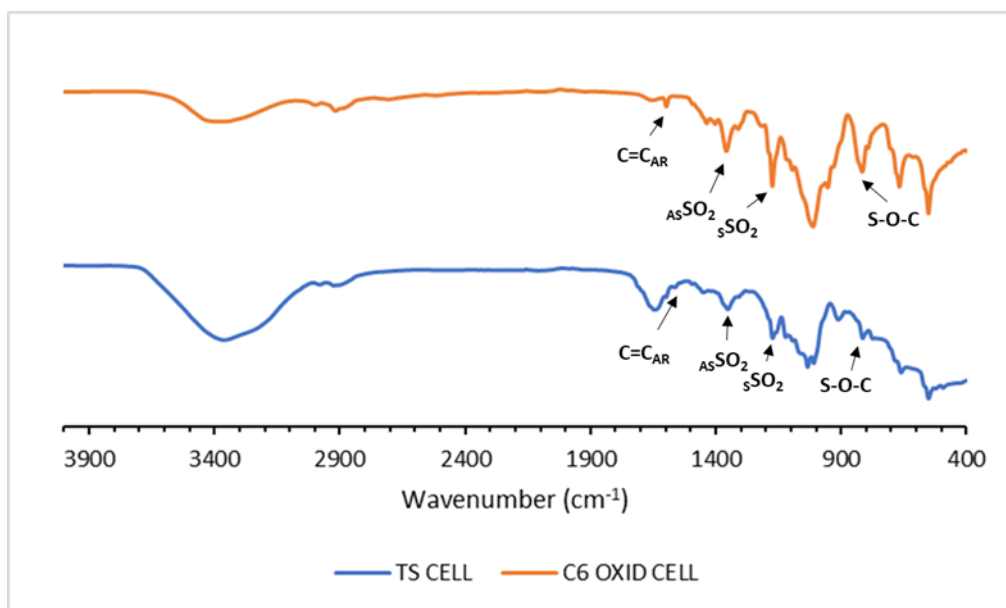


Figure 2.6. IR spectra of tosyl cellulose (TS CELL) (2.2) and C-6 oxidised C-6 tosyl cellulose (C-6 OXID CELL) (2.3).

In the $^1\text{H-NMR}$ spectrum, the signals of the tosyl moiety are evident at δ 7.10 to 7.78 ppm integrating for the four aromatic protons assigned H-8 and H-9; and at δ 2.42 ppm integrating for the three methyl protons assigned H-11. The cellulose backbone protons, assigned H-1 to H-6, are all present in the region δ 3.07 to 4.33 ppm. The $^{13}\text{C-NMR}$ spectrum displays signals for the *p*-substituted toluene ring in the region δ 125.46 to 137.56 ppm. The signal for the methyl group of the tosyl moiety, C-11, is observed at δ 21.02 ppm. The aromatic moiety of tosyl cellulose experiences desymmetrisation of C-8 and C-9 due to the chirality of the cellulose backbone. The signals at δ 60.26 to 102.44 ppm are assigned to the carbons of the cellulose backbone. Tosylation of cellulose occurs mainly at the C-6 primary hydroxyl group because it is the least sterically hindered. There is no evidence for substitution at the C-2 and C-3 positions as there is no visible signal at δ 78 ppm as reported by Schmidt *et al.* Furthermore, the signal assigned to C-1 at δ 102.44 ppm does not experience splitting which is generally attributed to tosylation at C-2.^{68, 69}

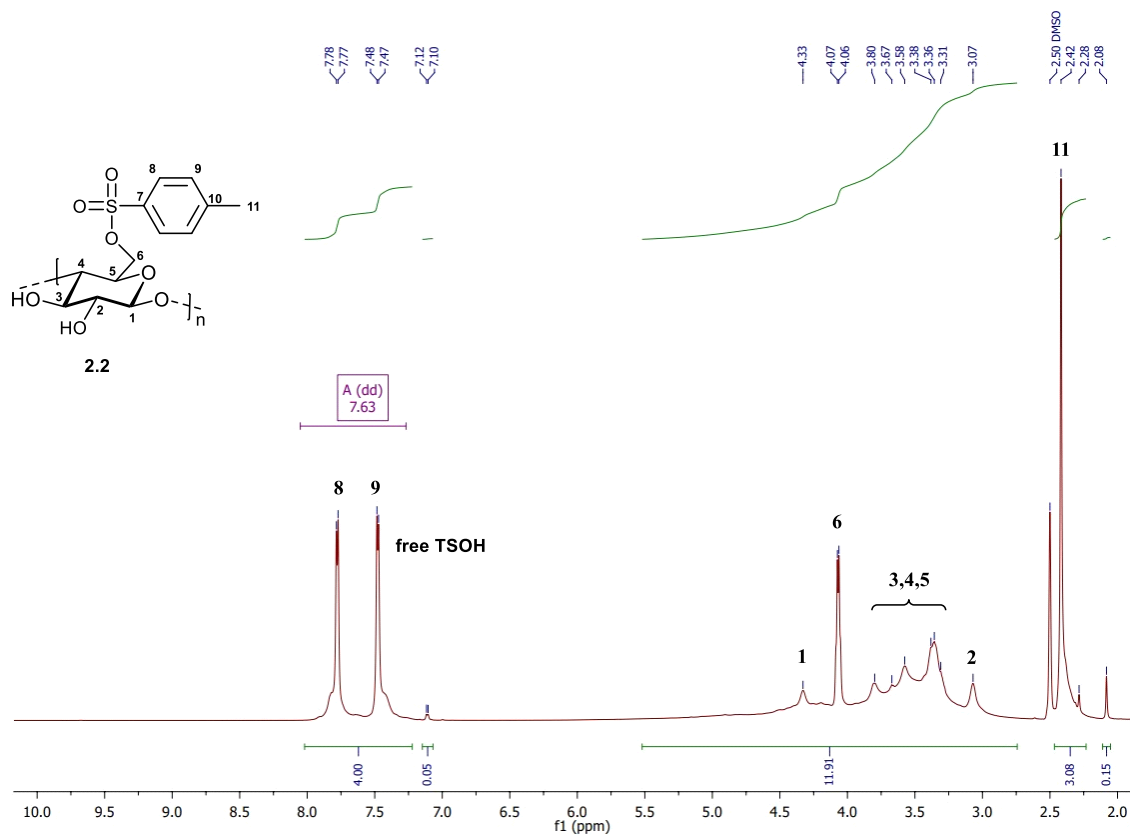


Figure 2.7. ¹H NMR spectrum of partially tosylated cellulose (2.2) in DMSO-d₆.

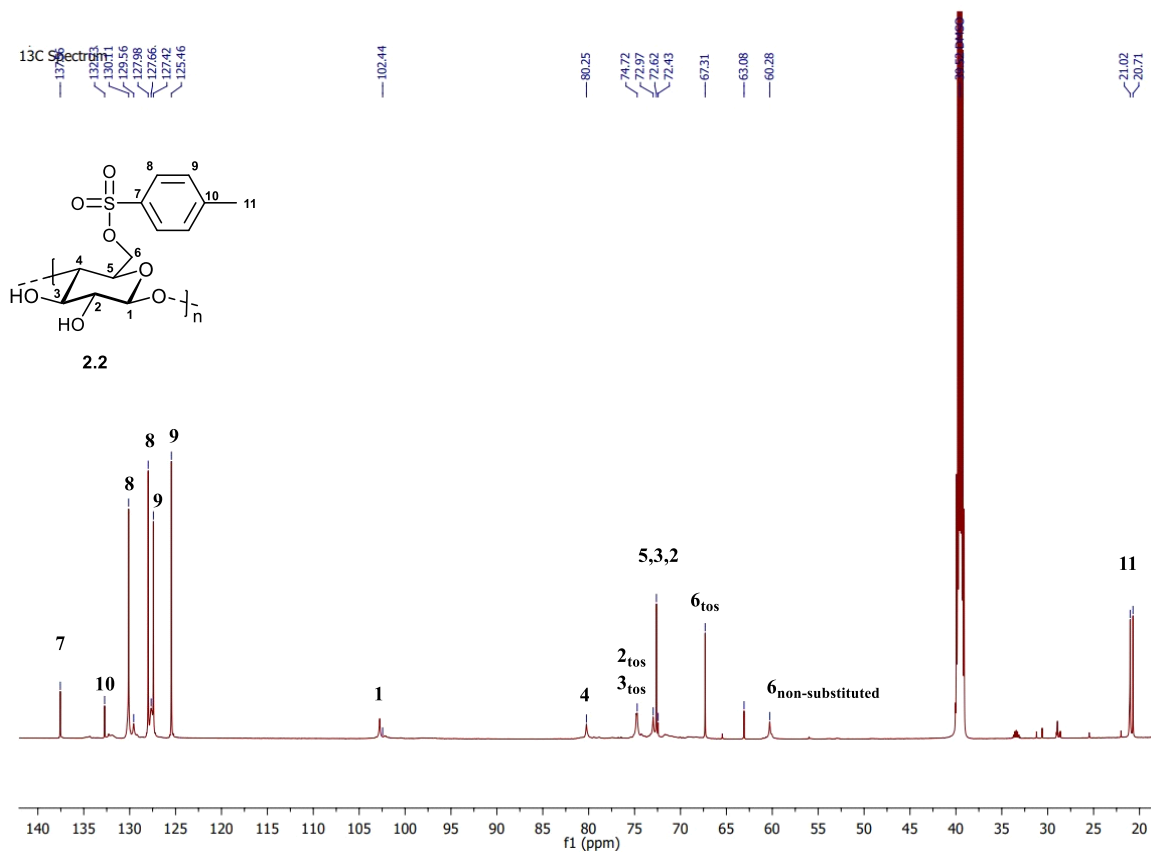


Figure 2.8. ¹³C NMR spectrum of partially tosylated cellulose (2.2) in DMSO-d₆.

A degree of tosylation (DS_{TOS}) of 0.59 was determined by elemental analysis. The DS_{TOS} was comparable to that obtained in literature of 0.43 for the same ratio of TsCl/AGU of 3.⁶⁸

The PXRD spectrum of tosyl cellulose (**2.2**) shown in **Figure 2.9** displays two sharp peaks at $2\theta = 20.97^\circ$ and 21.51° which are assigned to the (021) of amorphous cellulose (II).^{70, 71} This differs from the diffraction pattern shown in literature of one broad peak at $\sim 21^\circ$.⁷² The tosyl cellulose prepared here has a crystallinity index (CrI) of 5.07 % which is a great decrease from the CrI of MCC of 67 – 80 %.⁷³ This is due to the dissolution of cellulose in the NaOH/urea solvent system.⁷⁴⁻⁷⁶ This differs from the diffraction pattern shown in literature of one broad peak at $\sim 21^\circ$ with a CrI of 19.9 %, possibly due to a higher DS_{TOS} as well as the presence of excess reagents.⁷² Peaks were observed at a 2θ of 7.32° , 15.94° and 28.00° which imply a higher degree of crystallinity attributed to contaminants of excess TsCl and triethylamine.

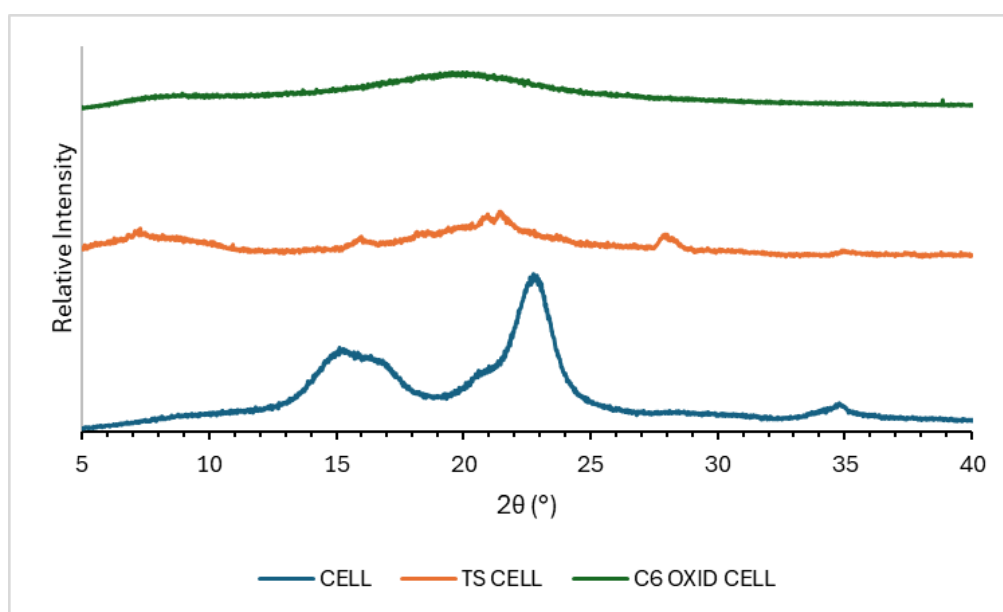


Figure 2.9. PXRD spectrum of cellulose (**CELL**), tosyl cellulose (**TS CELL**) (**2.2**) and C-6 oxidised C-6 tosyl cellulose (**C6 OXID CELL**) (**2.3**).

Thermal analysis of tosyl cellulose (**2.3**) is shown in **Figure 2.10**. The TGA thermogram is characterised by a visible thermal decomposition between 145 and 290 °C, mass loss of 46 %; and a peak of speed mass loss is observed at 200 °C.⁶⁹ The thermal stability of the polymer over a range of 0 – 250 °C was confirmed by DSC. The DSC thermogram displays an endothermic peak at 74 °C and an exothermic peak at 183 °C.

The endothermic peak is attributed to the free water loss of the polymer (mass loss of 8 %) and the exothermic peak is due to crystallisation of the polymer.⁷⁷ The DSC differs from that reported in literature of an endothermic peak around 210 °C assigned to the major decomposition stage of tosyl cellulose, possibly due to the difference in preparation methods and the presence of excess reagents and contaminants in the product obtained.

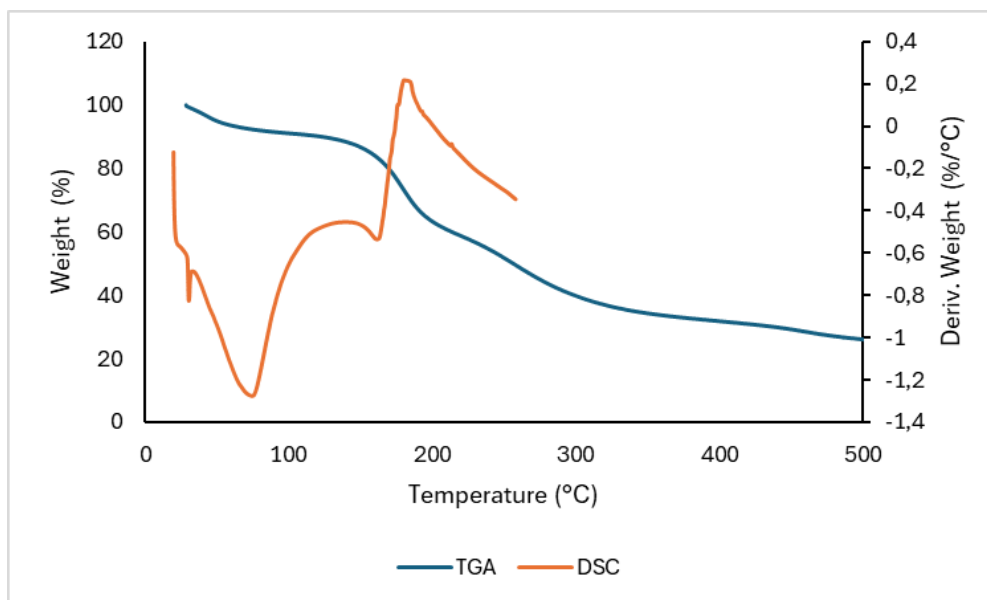


Figure 2.10. The TGA and DSC curves of tosyl cellulose (2.3).

In summary, DMSO-soluble partially tosylated cellulose with a DS_{TOS} of 0.59 was obtained with high yield using the eco-friendly solvent system of NaOH-urea in the presence of the anionic surfactant SLS. This solubility as well as the moderate-level of tosylation makes the tosyl cellulose obtained ideal for further chemical reactions of selective oxidation.

C-6 Oxidation of C-6 tosyl cellulose

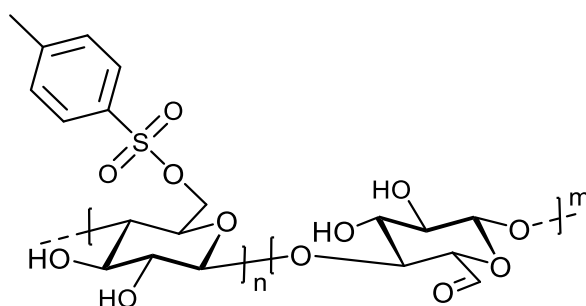
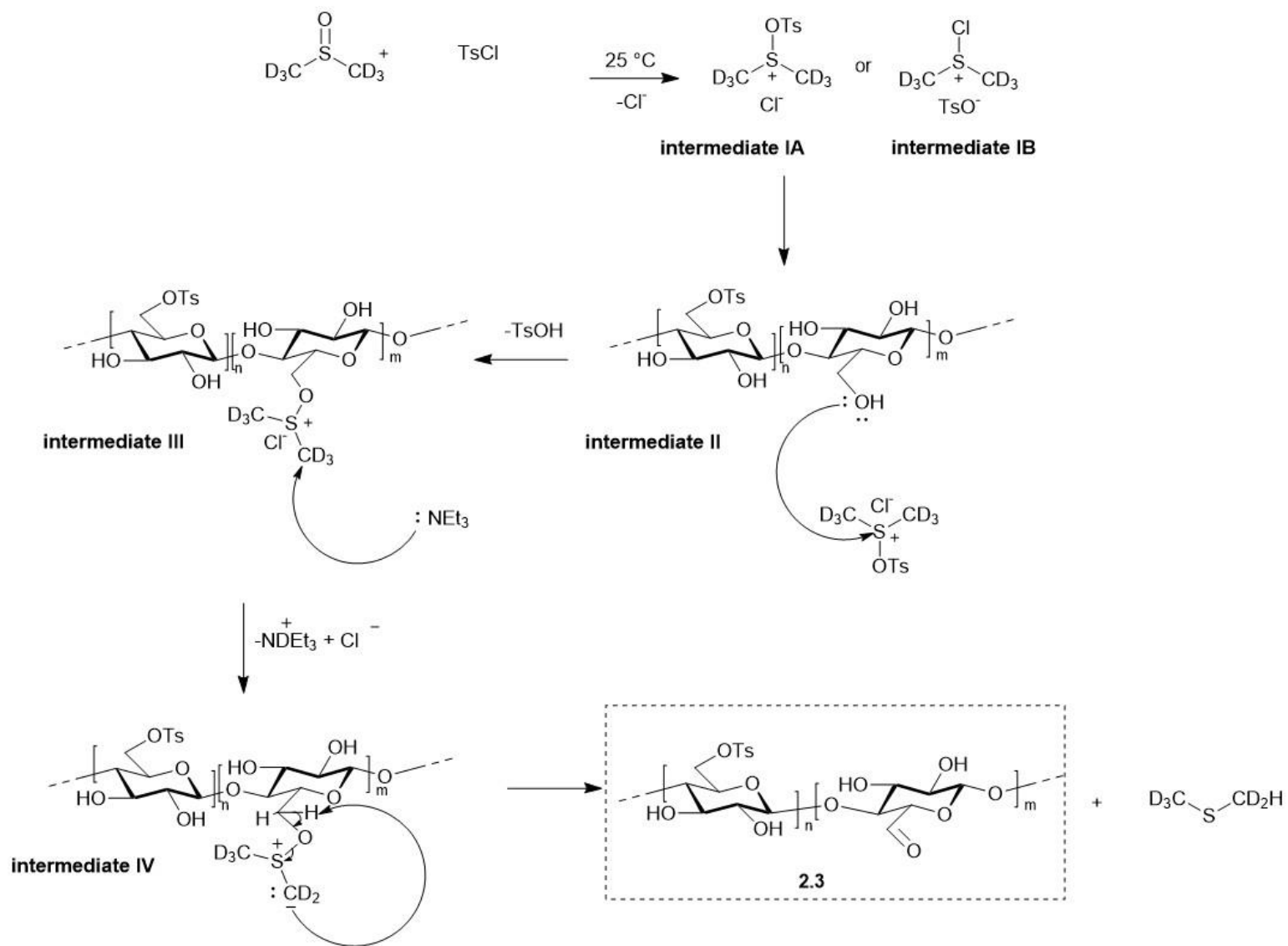


Figure 2.11. Structure of C-6 oxidised C-6 tosyl cellulose (**2.3**).

After having successfully synthesised DMSO-soluble tosyl cellulose, a Swern-like oxidation reaction was performed to yield C-6 oxidised C-6 tosyl cellulose. Tosyl cellulose (**2.2**) was selectively oxidised at the C-6 position using a mixture of TsCl in DMSO in the presence of triethylamine at 25 °C for 24 h (**Scheme 2.8**). The C-6 oxidised C-6 tosyl cellulose product (**2.3**) was obtained as a white crystalline solid with a mass yield of 81 %. The product was purified by means of ethanol and water washing, followed by lyophilisation. The mixed C-6 oxidised C-6 tosyl cellulose (**2.3**) obtained was soluble in DMSO, however, it is of note that when dialysis was performed, a highly crystalline white solid formed which was insoluble because of strong inter-polymer strand hydrogen bonding due to the formation of hemiacetals.

The Swern-like oxidation mechanism for the formation of C-6 oxidised C-6 tosyl cellulose (**2.3**) in DMSO- d_6 is shown in **Scheme 2.9**. Firstly, DMSO- d_6 (in excess) reacts with TsCl to form the key intermediates tosyloxydimethylsulfonium chloride (**intermediate IA**) and chloridimethylsulfonium tosylate (**intermediate IB**). The activated intermediate then reacts with the alcohol group of partially tosylated cellulose to yield the alkoxydimethylsulfonium salt (**intermediate II**). Finally, triethylamine deprotonates the α -proton of **intermediate II** to give **intermediate III**, which is subsequently converted to C-6 oxidised C-6 tosyl cellulose (**2.3**) and dimethyl sulfide (DMS- d_5).⁷⁸



Scheme 2.9. Swern-like oxidation mechanism for the formation of C-6 oxidised C-6 tosyl cellulose (**2.3**) in DMSO-d_6 .

The IR spectrum shown in **Figure 2.6** depicts a chemical shift from **C-6 OXID CELL (2.3)** relative to **TS CELL (2.2)**. The characteristic absorption bands for the aldehyde group of **C-6 OXID CELL** are not visible due to the formation of hemiacetals, but the absorbance bands for the tosyl group experiences a slight shift relative to **TS CELL** due to the presence of the electron-withdrawing carbonyl group.

The successful synthesis of mixed C-6 oxidised C-6 tosyl cellulose (**2.3**) was confirmed by conducting a NMR experiment in DMSO- d_6 . The diagnostic aldehyde proton and by-product DMS is evident in deuterated DMSO whereas it is not visible in the NMR spectra of the isolated product due to hemiacetal formation (**Figure 2.12**). The formation of the aldehyde occurs instantly when the solution of TsCl in DMSO- d_6 is added to the NMR reaction mixture as shown by the two signals at δ 9.88 and 9.61 ppm at $t(0)$. These two signals are attributed to the C-6 aldehyde and the terminal aldehyde of cellulose. The aromatic protons of the tosyl moiety experience a downfield shift from $t(\text{initial})$ to $t(24\text{h})$ and this could be attributed to the addition of more TsCl in the oxidation reaction which interacts more strongly with the polymer than the unreacted initial sample. The signal for DMS resonates at δ 2.51 ppm. Due to overlap in the region with signals of triethylamine hydrochloride protons and the methyl protons of the tosyl moiety, a 1D DOSY experiment of the 24 h NMR study sample of C-6 oxidised C-6 tosyl cellulose was performed to identify DMS- d_5 . The 1D DOSY shows signals of high MW compounds, hence filters out the small molecule signals resulting in a spectrum of the biopolymer alone. This was stacked with a ^1H -NMR spectrum of the 24 h NMR study sample of C-6 oxidised C-6 tosyl cellulose to assign the signal for DMS- d_5 . It appears that the small molecules (triethylamine and excess tosyl chloride) are reacting with the polymer structure because their signals are still evident in the 1D DOSY (**Figure 2.13**). Et_3N and TsCl could tosylate the cellulose, however, the intermediates IA and IB would form instantly.

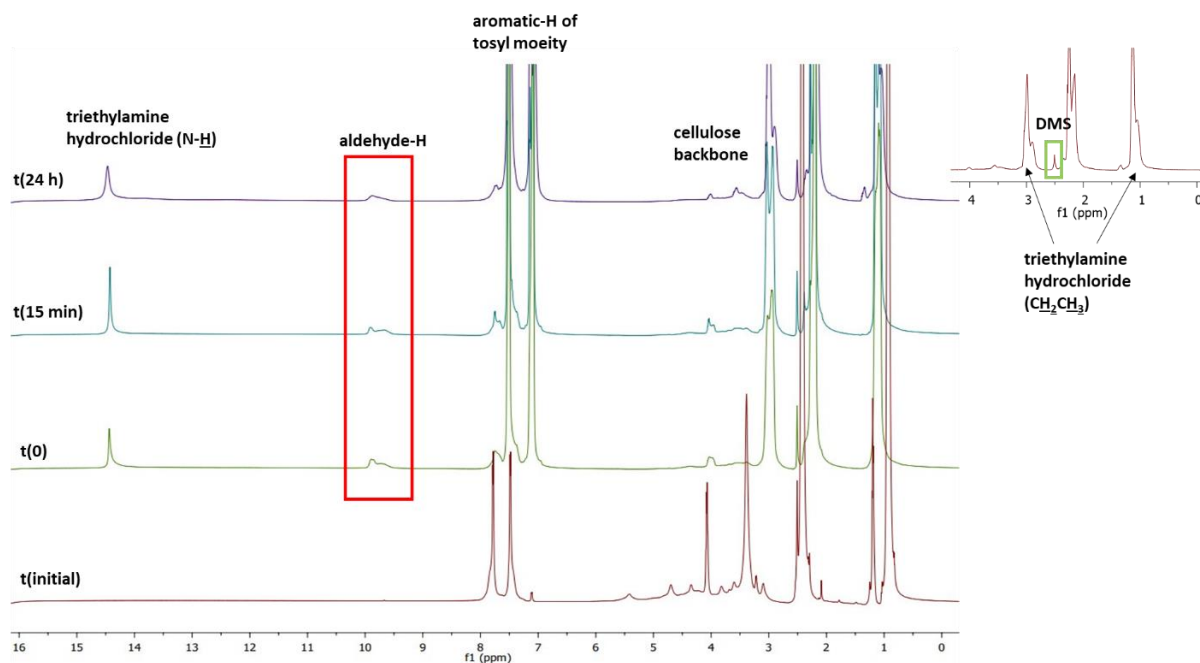


Figure 2.12. Stacked ^1H NMR spectrum displaying the formation of C-6 oxidised C-6 tosyl cellulose (**2.3**) in DMSO-d_6 over a 24 h period.

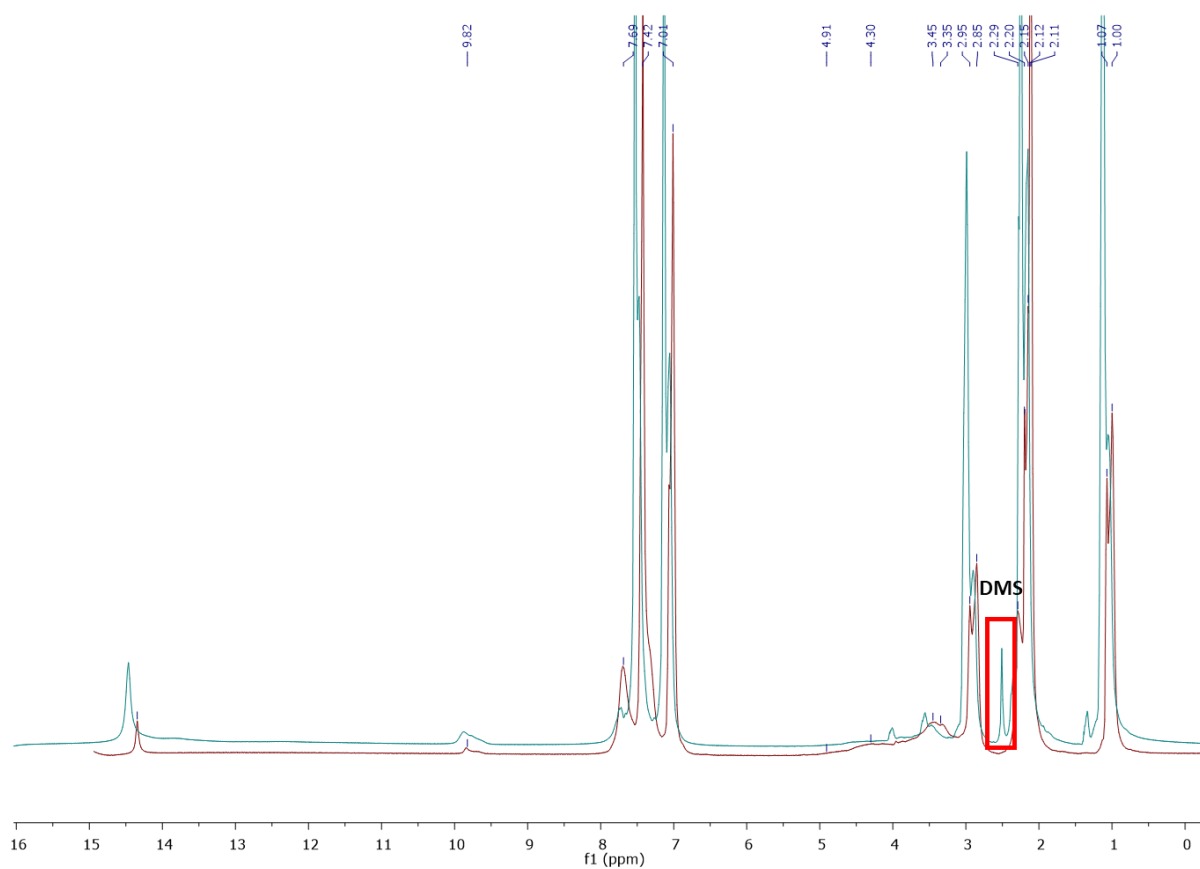


Figure 2.13. Stacked spectra of 1D DOSY (red) and ^1H -NMR (blue) of 24 h sample of C-6 oxidised C-6 tosyl cellulose (**2.3**) in DMSO-d_6 for identification of DMS signal.

C-6 oxidised C-6 tosyl cellulose (**2.3**) has a DO of 1.63 mmol.g^{-1} as determined by means of oxime formation with hydroxylamine hydrochloride.⁶¹

A Schiff base formation test was conducted to further confirm the successful synthesis of C-6 oxidised C-6 tosyl cellulose (**2.3**). C-6 oxidised C-6 tosyl cellulose (**2.3**) was reacted with benzylamine in DMSO to yield the Schiff base product (**2.4**) which was characterised by ¹H-NMR spectroscopy and Infrared spectroscopy. The ¹H-NMR spectrum depicts the characteristic imine signal at δ 8.50 ppm for H-6' and the IR spectrum shows the $\nu(\text{C}=\text{N})$ absorption band at 1643 cm^{-1} (see **Appendix**).

PXRD shows the diffraction patterns of C-6 selectively oxidised tosyl cellulose (**2.3**) and displays one broad peak with a 2θ of 20.21° which suggests a more highly amorphous polymer than that of tosyl cellulose (**2.2**) (**Figure 2.9**).

Thermal studies were conducted to evaluate if a change in thermal properties occurred upon oxidation of tosyl cellulose at the C-6 position. The TGA thermogram (**Figure 2.14**) displays three characteristic degradation stages: at 0 to 94°C which is attributed to the loss of free water from the polymer, at 185 to 200°C which resulted from depolymerisation of the polymer with a mass loss of 20 %, and lastly at 205 to 357°C which resulted from the greatest mass loss of 30 % due to depolymerisation of the polymer. The DSC further confirms the TGA results by the presence of two peaks, an endothermic peak at 94°C for the loss of residual water from the polymer and an exothermic peak at 200°C which is possibly due to a phase transition in which tosyl cellulose undergoes crystallisation to form the highly crystalline solid C-6 oxidised C-6 tosyl cellulose.

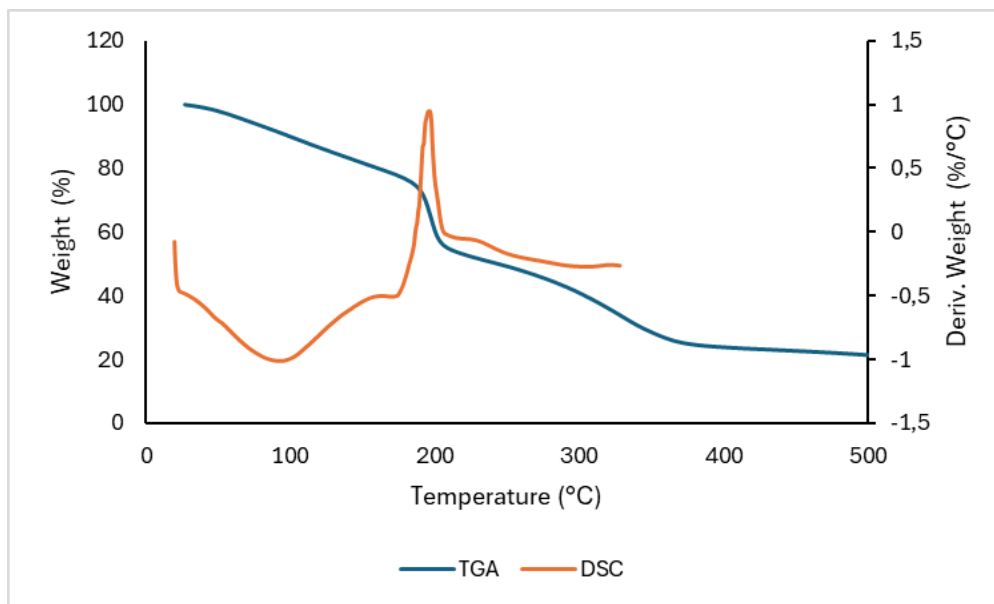


Figure 2.14. The TGA and DSC curves of C-6 oxidised C-6 tosyl cellulose (**2.4**).

In summary, a novel route towards selective C-6 oxidation to the aldehyde level of cellulose has been reported. Firstly, cellulose was tosylated using a green solvent system of NaOH-urea in the presence of the surfactant SLS to achieve a polymer that is soluble in DMSO. The soluble tosyl cellulose was further subjected to a Swern-like oxidation reaction in DMSO using TsCl as activator. The resulting C-6 oxidised C-6 tosyl cellulose displayed solubility in DMSO and was characterised *via* NMR and IR spectroscopy. A $^1\text{H-NMR}$ spectroscopic study in DMSO-d_6 was conducted to visibly depict the aldehyde and DMS-d_5 signals. Lastly, a Schiff base reaction with the C-6 oxidised C-6 tosyl cellulose and benzylamine was performed to provide further evidence that tosyl cellulose was indeed oxidised.

This novel method of selective C-6 oxidation of cellulose was attempted on chitosan derivatives to selectively oxidise chitosan to 6-aldehyde-chitosan.

2.2.3 Selective C-6 oxidation of chitosan

The selective C-6 oxidation of chitosan mediated by TEMPO was studied by Bordenave *et al.*⁷⁹ The amino groups present in chitosan limits its reactivity during direct oxidation, possibly due to the nucleophilic character of nitrogen and reactivity. Therefore, the protection of amino groups was explored. The authors investigated three methods of protection, namely, *N*-acetylation, *N*-phthaloylation and *N,N,N*-trimethylation. *N*-acetylation and *N*-phthaloylation

proved to be ineffective methods of protection. For *N*-acetylation, the deprotection of the amino group by means of deacetylation had too harsh reaction conditions and for *N*-phthaloylation, the phthaloyl groups were removed from chitosan during oxidation. Hence, the permanent modification of *N,N,N*-trimethylation was used which allowed selective C-6 oxidation of chitosan. However, the reported yields were low.⁷⁹ Azevedo *et al.* reported the preparation of aldehyde-functionalised chitosan by the reaction of chitosan with nitrogen oxides generated *in situ* from a HNO₃/H₃PO₄– NaNO₂ mixture. This method has milder reaction conditions than previous methods, with slower depolymerisation and simpler purification processes. The aldehyde-functionalised chitosan synthesised was characterised by FTIR and ¹³C-NMR spectroscopy. The aldehyde-containing polymer was able to self-cross-link with the free amine groups of chitosan to form Schiff bases at a pH of 6. The aldehyde-functionalised chitosan prepared with a reaction time of 6 h formed a gel *in situ* and could potentially be used as a vehicle for drug delivery.⁸⁰

The aim of this study was to implement the selective C-6 oxidation method that was developed using cellulose, on chitosan. Although *N*-phthaloylation protection of chitosan was deemed unsuccessful for TEMPO-oxidation, it was attempted nonetheless as amino-group protection of chitosan, because the Swern-like oxidation reaction conditions are expected to be milder and not result in depolymerisation.

Attempt to oxidise *N*-phthaloyl chitosan

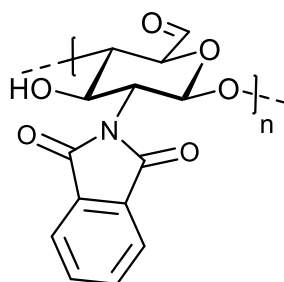
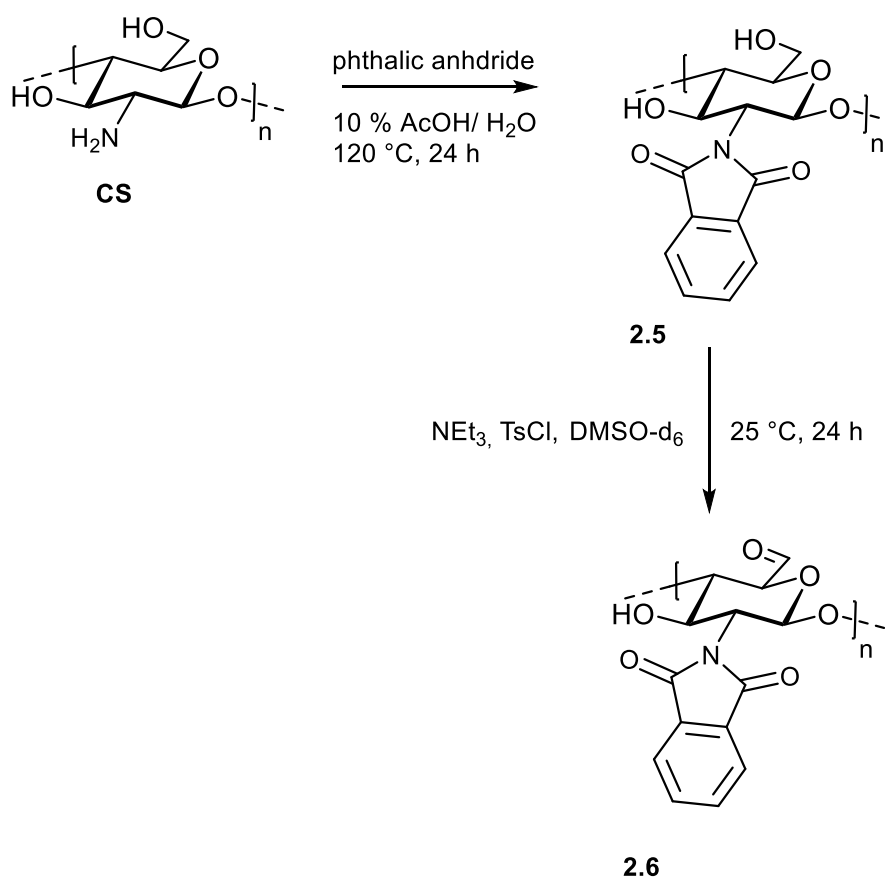


Figure 2.15. Structure of C-6 oxidised *N*-phthaloyl chitosan (2.6).

N-phthaloyl chitosan (2.5) was synthesised by refluxing chitosan with phthalic anhydride in 10% AcOH/H₂O at 120 °C for 24 h (Scheme 2.10). The precipitate was collected by centrifugation and washed with water and ethanol. Lastly, the solid was allowed to stir in acetone to dissolve any unreacted phthalic anhydride and subsequently dialysed against

deionised water and dried to obtain the product as a brown powder with a low mass yield of 19 %.⁸¹



Scheme 2.10. Reaction scheme for formation of oxidised *N*-phthaloyl chitosan (2.6).

The structure of *N*-phthaloyl chitosan (2.5) was confirmed by ¹H-NMR spectroscopy as shown in **Figure 2.16**. The characteristic signals assigned to the pyranose protons occur in the region δ 4.12 to 5.51 ppm. The diagnostic signals of the *N*-phthaloyl aromatic groups were present between δ 7.47 and 8.19 ppm. Furthermore, these signals confirm the selective formation of *N*-phthaloyl chitosan as signals attributed to *O*-phthaloyl chitosan are not evident in the region δ 7.30 to 7.50 ppm.⁸²

C-6 selective oxidation of *N*-phthaloyl chitosan using TsCl in the presence of triethylamine in DMSO was attempted and deemed unsuccessful as seen in **Figure 2.16**. A ¹H-NMR spectroscopy study was conducted in DMSO-d₆ and there was no evidence for the formation of an aldehyde or the by-product of DMS. A possible reason for this could be the poor solubility of *N*-phthaloyl chitosan in DMSO.

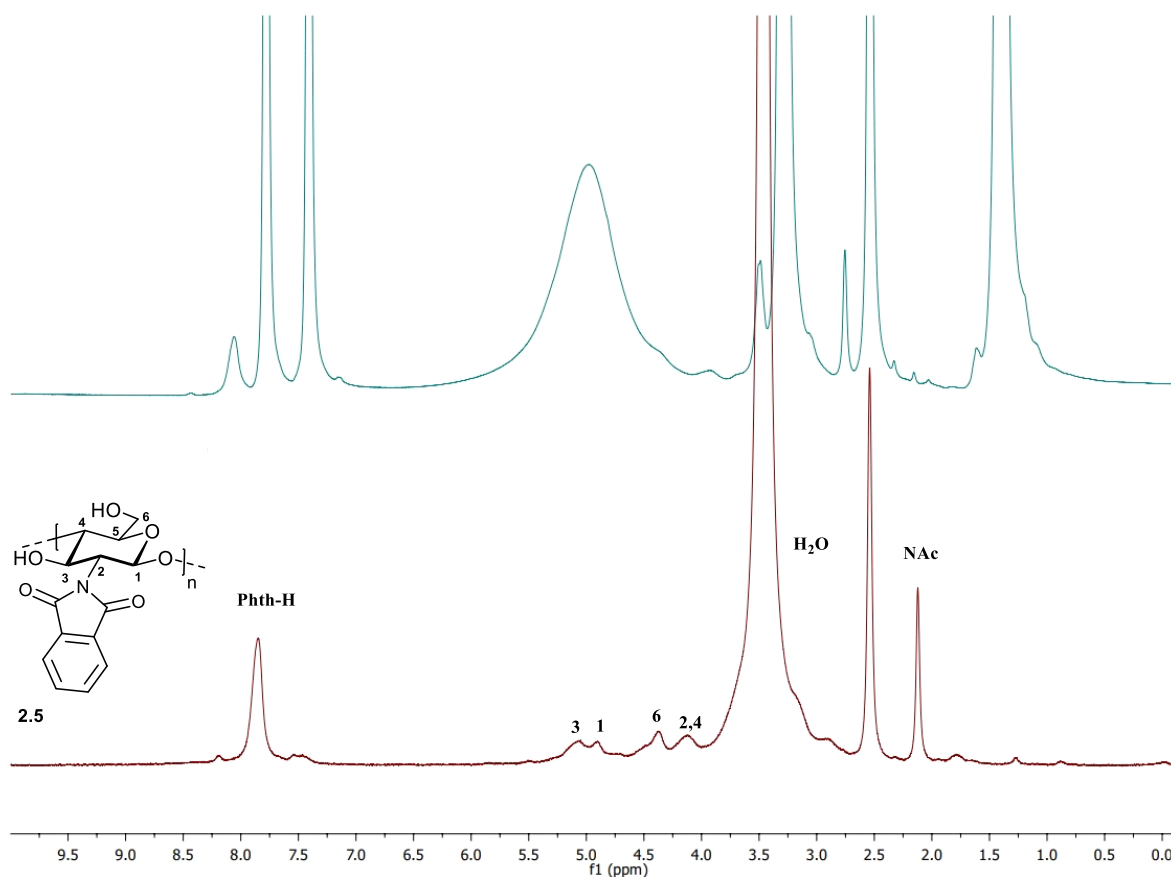


Figure 2.16. Stacked $^1\text{H-NMR}$ spectra of *N*-phthaloyl chitosan (**2.5**) (bottom) and attempt at oxidised *N*-phthaloyl chitosan (top) in DMSO-d_6 .

Attempt to oxidise *N*-succinyl chitosan

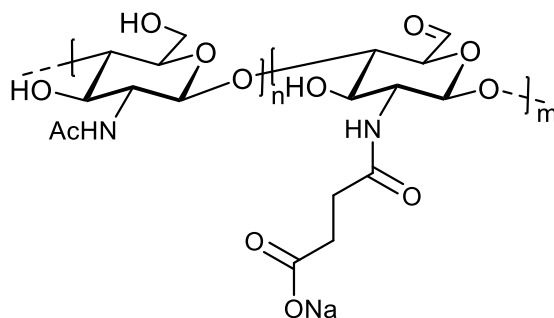
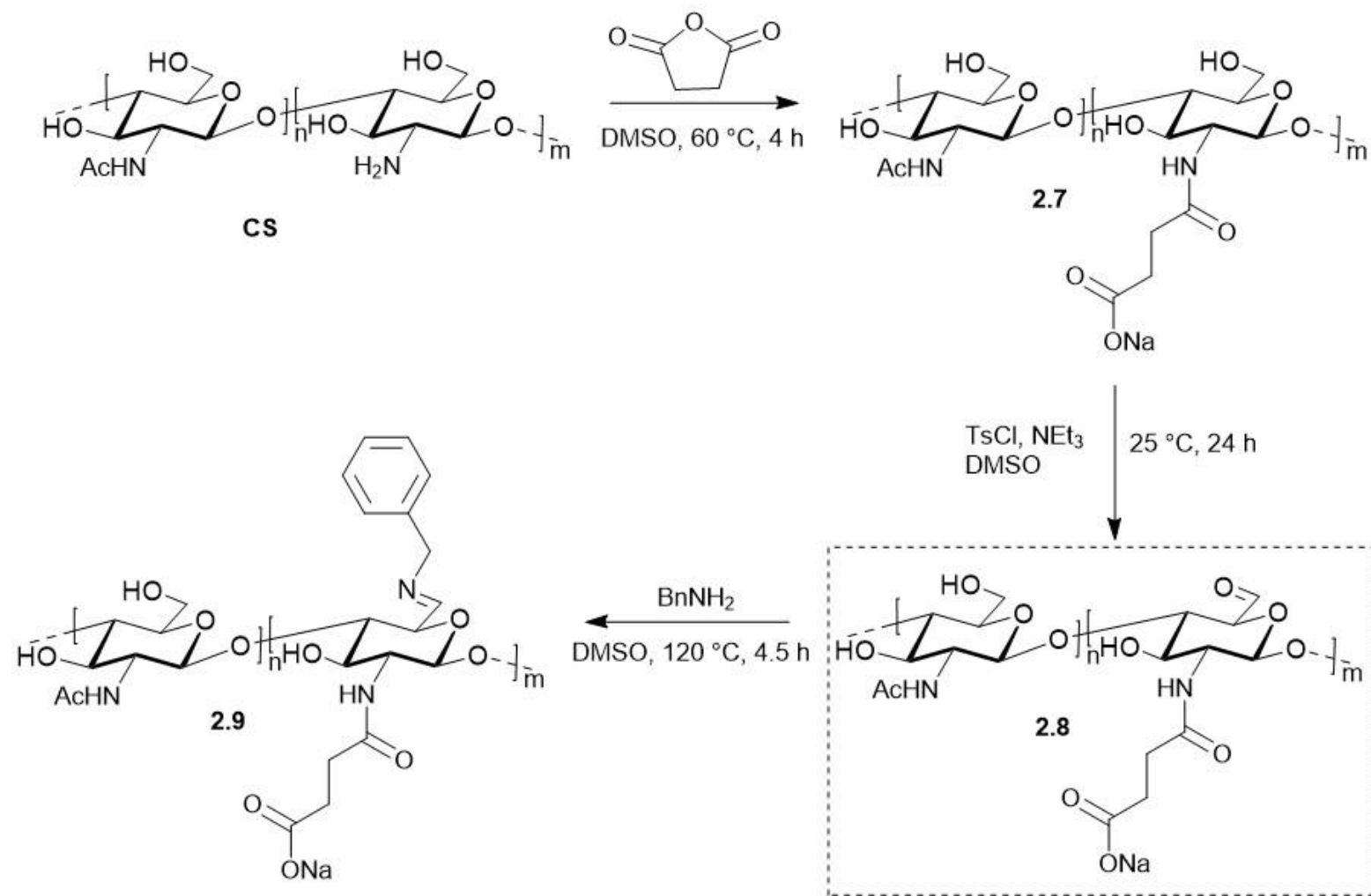


Figure 2.17. Structure of C-6 oxidised *N*-succinyl chitosan (**2.8**).

To overcome the solubility issue experienced by *N*-phthaloyl chitosan, chitosan was modified by *N*-succinylation. *N*-Succinyl chitosan (NSCS) (**2.7**) was prepared by the treatment of chitosan with succinic anhydride in DMSO at $60\text{ }^\circ\text{C}$ for 4 h.⁸³

Literature reports water soluble NSCS but the product (**2.7**) that was obtained following the literature method was insoluble and could not be characterised by $^1\text{H-NMR}$ spectroscopy. The synthesised NSCS (**2.7**) was oxidised using a mixture of TsCl and DMSO- d_6 in the presence of triethylamine at 25 °C for a period of 24 h (**Scheme 2.11**). The reaction was performed in deuterated NMR solvent to avoid hemiacetal formation and visibly depicts the proton signals of the aldehyde. The $^1\text{H-NMR}$ spectrum is shown in **Figure 2.18**. An aldehyde-H signal (H-6') is present at δ 9.45 ppm but the Swern-like oxidation by-product DMS- d_5 is unidentifiable as it occurs in a region that overlaps with the *p*- CH_3 signals of TsCl and DMSO- d_6 . To confirm the formation of C-6 oxidised *N*-succinyl chitosan (**2.8**), a Schiff base reaction was performed using benzylamine in the presence of DMSO at 120 °C for 4.5 h. The resulting Schiff base product (**2.9**) was washed with ethanol and water, dialysed against deionised water and lyophilised to yield a yellow solid. However, after NMR analysis it was concluded that a Schiff base did not form. This could possibly be due to the insolubility of C-6 oxidised *N*-succinyl chitosan (**2.8**) as well as deprotection of the succinyl protecting group during the oxidation reaction.



Scheme 2.11. Overall reaction scheme for the attempted oxidation of *N*-succinyl chitosan (**2.8**).

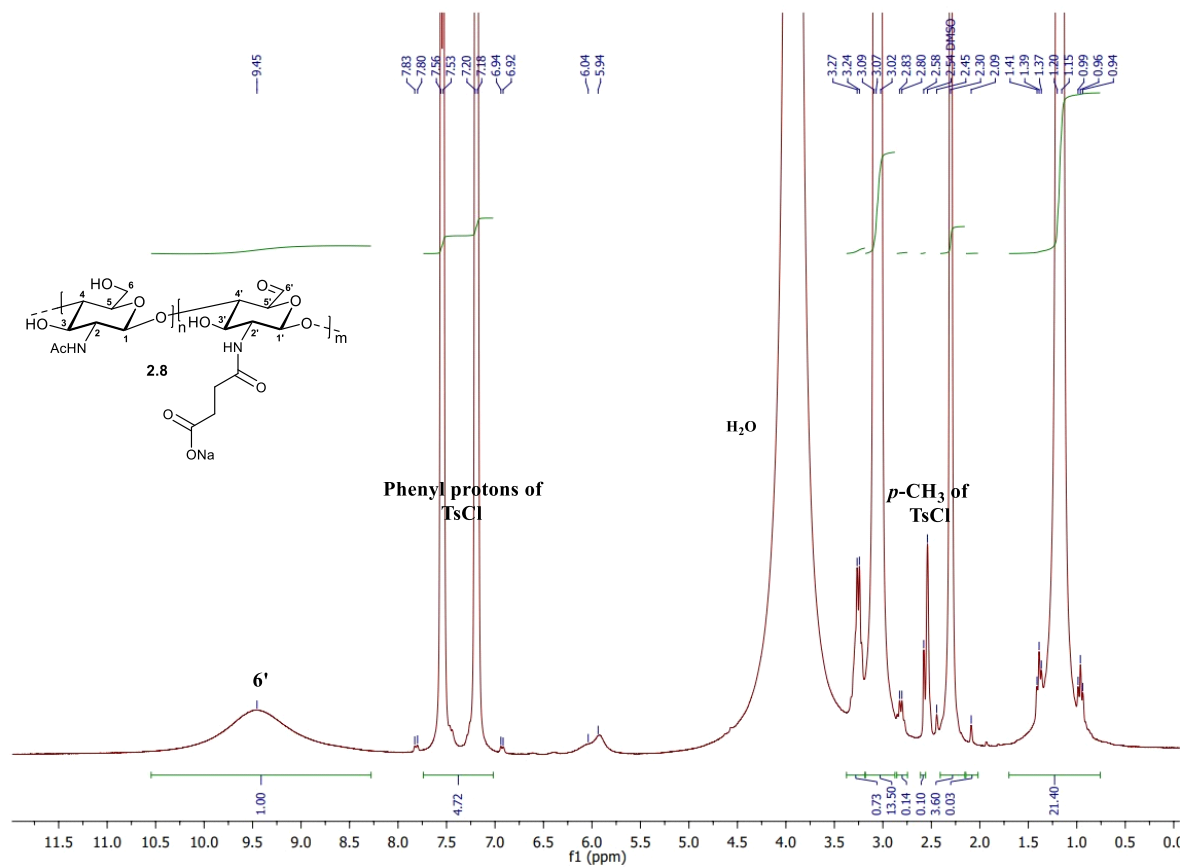


Figure 2.18. $^1\text{H-NMR}$ spectrum of the attempted oxidation of *N*-succinyl chitosan (**2.8**) in DMSO-d_6 .

2.3 Conclusion

Periodate oxidation of cellulose was explored for the synthesis of DAC. A novel method was designed and developed for the selective C-6 oxidation of cellulose whereby cellulose is firstly tosylated in the green solvent system of NaOH-urea in the presence of the anionic surfactant SLS to yield soluble cellulose tosylates. Secondly, tosyl cellulose undergoes a Swern-like oxidation reaction using TsCl in DMSO in the presence of triethylamine. The selective C-6 oxidised cellulose obtained was soluble in DMSO and could be further chemically modified in reactions such as reductive amination to yield water-soluble aminocelluloses. This new two-step method of oxidation has advantages of avoiding the use of hazardous reagents such as TEMPO, as well as avoids the formation of toxic by-products that is generated by sodium hypochlorite, and lastly avoids over-oxidation to the carboxyl product as reported in literature methods of TEMPO-oxidation for selective C-6 oxidation of biopolymers. Further important elements of this new method are that it yields soluble oxidised cellulose products and is scalable for commercial purposes.

In addition, an attempt to selectively oxidise chitosan using this method was made. However, the oxidation of chitosan requires the protection of the amino group beforehand. This was done by *N*-phthaloylation and *N*-succinylation. Oxidation of both these amino group-protected polymers were unsuccessful, possibly due to reasons of deprotection and insolubility in DMSO.

To far our knowledge, selective C-6 oxidation of cellulose following a Swern-like oxidation mechanism has not been reported in literature, except for aliphatic small molecule alcohols.

This chapter described the synthesis of DAC using periodate oxidation thus indirectly providing readily access to aminated polymers *via* reductive amination of aldehyde, which will be further discussed in **Chapter 3**.

2.4 References

1. U.-J. Kim and S. Kuga, *Thermochimica Acta*, 2001, **369**, 79-85.
2. S. M. Keshk, A. M. Ramadan and S. Bondock, *Carbohydrate polymers*, 2015, **127**, 246-251.
3. W. Kasai, T. Morooka and M. Ek, *Cellulose*, 2014, **21**, 769-776.
4. I. A. Duceac, F. Tanasa and S. Coseri, *Materials*, 2022, **15**.
5. D. Jaušovec, R. Vogrinčič and V. Kokol, *Carbohydrate polymers*, 2015, **116**, 74-85.
6. E. Toshikj, A. Tarbuk, K. Grgić, B. Mangovska and I. Jordanov, *Cellulose*, 2019, **26**, 777-794.
7. A. Aktekin, I. Sahin, U. Aydemir Sezer, M. Gulmez, S. Ozkara and S. Sezer, *Cellulose*, 2016, **23**, 3145-3156.
8. R. J. Crawford, K. J. Edler, S. Lindhoud, J. L. Scott and G. Unali, *Green chemistry*, 2012, **14**, 300-303.
9. S. Zhang, J. Li, S. Chen, X. Zhang, J. Ma and J. He, *Carbohydrate polymers*, 2020, **230**, 115585.
10. J. M. Jetten, R. Van Den Dool, W. Van Hartingsveldt and A. C. Besemer, *Journal*, 2004.
11. *USA Pat.*, 7,662,801, 2010.
12. B. Martina, K. Kateřina, R. Miloslava, G. Jan and M. Ruta, *Advances in Polymer Technology: Journal of the Polymer Processing Institute*, 2009, **28**, 199-208.
13. J. M. He, Y. D. Wu, F. W. Wang, W. L. Cheng, Y. D. Huang and B. Fu, *Fibers and Polymers*, 2014, **15**, 504-509.
14. G. Dalei, S. Das and M. Pradhan, *Cellulose*, 2022, **29**, 5429-5461.
15. M. Wu and S. Kuga, *Journal of applied polymer science*, 2006, **100**, 1668-1672.
16. U.-J. Kim and S. Kuga, *Journal of Chromatography A*, 2001, **919**, 29-37.
17. E. Maekawa and T. Koshijima, *Journal of Applied Polymer Science*, 1990, **40**, 1601-1613.
18. A. Lucia, M. Bacher, H. W. van Herwijnen and T. Rosenau, *Molecules*, 2020, **25**, 2458.
19. D. Rajalaxmi, N. Jiang, G. Leslie and A. J. Ragauskas, *Carbohydrate research*, 2010, **345**, 284-290.
20. C.-F. Huang, C.-W. Tu, R.-H. Lee, C.-H. Yang, W.-C. Hung and K.-Y. A. Lin, *Polymer Degradation and Stability*, 2019, **161**, 206-212.
21. Y. Kato, R. Matsuo and A. Isogai, *Carbohydrate Polymers*, 2003, **51**, 69-75.
22. S.-H. Yoo, J.-S. Lee, S. Y. Park, Y.-S. Kim, P.-S. Chang and H. G. Lee, *International Journal of Biological Macromolecules*, 2005, **35**, 27-31.
23. K. Gao, J. Zhan, Y. Qin, S. Liu, R. Xing, H. Yu, X. Chen and P. Li, *Carbohydrate Polymers*, 2021, **265**, 118073.
24. A. Balea, N. Merayo, E. De La Fuente, C. Negro and Á. Blanco, *Industrial crops and products*, 2017, **97**, 374-387.
25. U.-J. Kim, S. Kuga, M. Wada, T. Okano and T. Kondo, *Biomacromolecules*, 2000, **1**, 488-492.
26. C. Bunton and V. Shiner, *Journal of the Chemical Society (Resumed)*, 1960, 1593-1598.
27. G. Buist, C. Bunton and W. Hipperson, *Journal of the Chemical Society B: Physical Organic*, 1971, 2128-2142.
28. S. Eyley and W. Thielemans, *Nanoscale*, 2014, **6**, 7764-7779.
29. W. Ding and Y. Wu, *Carbohydrate Polymers*, 2020, **248**, 116801.

30. S. Mayer, M. Tallawi, I. De Luca, A. Calarco, N. Reinhardt, L. A. Gray, K. Drechsler, A. Moeini and N. Germann, *Carbohydrate Polymers*, 2021, **272**, 118506.
31. H. Yang, M. N. Alam and T. G. van de Ven, *Cellulose*, 2013, **20**, 1865-1875.
32. A. Salama, H. A. Aljohani and K. R. Shoueir, *Materials Letters*, 2018, **230**, 293-296.
33. R. Criegee, *Berichte der Deutschen Chemischen Gesellschaft* 1931, **64**, 260-266.
34. L. Malaprade, *Bulletin de la Societe Chimique de France*, 1928, **43**, 683-696.
35. L. Malaprade, *Bulletin de la Société Chimique de France*, 1934, **5**, 833-852.
36. J. L. de O. Domingos, G. V. de A. Vilela, P. R. Costa and A. G. Dias, *Synthetic communications*, 2004, **34**, 589-598.
37. S. C. Dakdouki, D. Villemain and N. Bar, *Journal*, 2011.
38. J. Bobbitt, in *Advances in carbohydrate chemistry*, Elsevier, 1956, vol. 11, pp. 1-41.
39. S. Xu, D. Huo, K. Wang, Q. Yang, Q. Hou and F. Zhang, *Carbohydrate Polymers*, 2021, **266**, 118118.
40. E. Maekawa and T. Koshijima, *Journal of Applied Polymer Science*, 1991, **42**, 169-178.
41. V. Crescenzi, M. Dentini, C. Meoli, B. Casu, A. Naggi and G. Torri, *International Journal of Biological Macromolecules*, 1984, **6**, 142-144.
42. A. Varma, V. Chavan, P. Rajmohan and S. Ganapathy, *Polymer degradation and stability*, 1997, **58**, 257-260.
43. B. Casu, A. Naggi, G. Torri, G. Allegra, S. Meille, A. Cosani and M. Terbojevich, *Macromolecules*, 1985, **18**, 2762-2767.
44. M. Kobayashi, I. Suzawa and E. Ichishima, *Agricultural and biological chemistry*, 1990, **54**, 1705-1709.
45. T. Koshijima, R. Tanaka, E. Muraki, A. Yamada and F. Yaku, *Cellulose chemistry and technology*, 1973, **7**, 197.
46. S. Koprivica, M. Siller, T. Hosoya, W. Roggenstein, T. Rosenau and A. Potthast, *ChemSusChem*, 2016, **9**, 825-833.
47. X. Dang, P. Liu, M. Yang, H. Deng, Z. Shan and W. Zhen, *Cellulose*, 2019, **26**, 9503-9515.
48. R. Jeanloz and E. Forchielli, *Helvetica Chimica Acta*, 1950, **33**, 1690-1697.
49. I. M. Vold and B. E. Christensen, *Carbohydrate research*, 2005, **340**, 679-684.
50. M. Cantley, L. Hough and A. Pittet, *Journal of the Chemical Society (Resumed)*, 1963, 2527-2535.
51. T. J. Painter, *Carbohydrate research*, 1988, **179**, 259-268.
52. G. K. Kirui, E. S. Madivoli, D. M. Nzilu, P. G. Kareru and W. Waudo, *Biomass Conversion and Biorefinery*, 2024, 1-15.
53. H. Chen, J. Jiang, S. Zhang, J. Yu, L. Liu and Y. Fan, *Industrial Crops and Products*, 2022, **176**, 114295.
54. J. Jiang, W. Ye, L. Liu, Z. Wang, Y. Fan, T. Saito and A. Isogai, *Biomacromolecules*, 2017, **18**, 288-294.
55. U.-J. Kim, M. Wada and S. Kuga, *Carbohydrate polymers*, 2004, **56**, 7-10.
56. J. Simon, L. Fliri, F. Drexler, M. Bacher, J. Sapkota, M. Ristolainen, M. Hummel, A. Potthast and T. Rosenau, *Carbohydrate Polymers*, 2023, **310**, 120691.
57. S. Vicini, E. Princi, G. Luciano, E. Franceschi, E. Pedemonte, D. Oldak, H. Kaczmarek and A. Sionkowska, *Thermochimica Acta*, 2004, **418**, 123-130.
58. Q. Fan, D. Lewis and K. Tapley, *Journal of Applied Polymer Science*, 2001, **82**, 1195-1202.
59. S. F. Plappert, S. Quraishi, N. Pircher, K. S. Mikkonen, S. Veigel, K. M. Klinger, A. Potthast, T. Rosenau and F. W. Liebner, *Biomacromolecules*, 2018, **19**, 2969-2978.

60. D. C. Du Chao, L. M. Liu MengRu, L. B. Li BingYun, L. H. Li HaiLong, M. Q. Meng QiJun and Z. H. Zhan HuaiYu, *BioResources*, 2016, **11**, 4017-4024.
61. R. Koshani, J. Zhang, T. G. van de Ven, X. Lu and Y. Wang, *ACS Sustainable Chemistry & Engineering*, 2021, **9**, 10513-10523.
62. L. Zhang, H. Ge, M. Xu, J. Cao and Y. Dai, *Cellulose*, 2017, **24**, 2287-2298.
63. B. Sun, Q. Hou, Z. Liu and Y. Ni, *Cellulose*, 2015, **22**, 1135-1146.
64. H. Li, B. Wu, C. Mu and W. Lin, *Carbohydrate Polymers*, 2011, **84**, 881-886.
65. E. S. Madivoli, P. G. Kareru, A. N. Gachanja, S. M. Mugo and D. S. Makhanu, *SN Applied Sciences*, 2019, **1**, 1-7.
66. L. Zhang, P. Yan, Y. Li, X. He, Y. Dai and Z. Tan, *Industrial Crops and Products*, 2020, **145**, 112126.
67. D. Horton, A. E. Luetzow and O. Theander, *Carbohydrate Research*, 1973, **26**, 1-19.
68. S. Schmidt, T. Liebert and T. Heinze, *Green Chemistry*, 2014, **16**, 1941-1946.
69. L. El Hamdaoui, A. Es-said, M. El Marouani, M. El Bouchti, R. Bchitou, F. Kifani-Sahban and M. El Moussaouiti, *ChemistrySelect*, 2020, **5**, 7695-7703.
70. N. S. El-Sayed, M. Abd El-Aziz, S. Kamel and G. Turkey, *Synthetic Metals*, 2018, **236**, 44-53.
71. K.-i. Furuhashi and H. Ikeda, *Reactive and Functional Polymers*, 1999, **42**, 103-109.
72. M. H. Do, K. Van Thi Khuat, P. T. Huynh, L. N. T. Nguyen, B. H. Do, P. D. Pham, H. D. Nguyen, H. M. Nguyen and U. D. Thach, *Biomass Conversion and Biorefinery*, 2023, **13**, 10595-10603.
73. A. F. Tarchoun, D. Trache, T. M. Klapötke, M. Derradji and W. Bessa, *Cellulose*, 2019, **26**, 7635-7651.
74. F. Nazir and M. Iqbal, *Polymers*, 2020, **12**, 2634.
75. A. F. Tarchoun, D. Trache, T. M. Klapötke, B. Krumm, A. Mezroua, M. Derradji and W. Bessa, *Cellulose*, 2021, **28**, 6107-6123.
76. A. F. Tarchoun, D. Trache, T. M. Klapötke, M. Belmerabet, A. Abdelaziz, M. Derradji and R. Belgacemi, *Industrial & Engineering Chemistry Research*, 2020, **59**, 22677-22689.
77. K. Cieřla, H. Rahier and G. Zakrzewska-Trznadel, *Journal of thermal analysis and calorimetry*, 2004, **77**, 279-293.
78. F. Saadati and K. Yousefi, *Synthetic Communications*, 2014, **44**, 2818-2825.
79. N. Bordenave, S. Grelier and V. Coma, *Biomacromolecules*, 2008, **9**, 2377-2382.
80. E. P. Azevedo, S. S. Mariappan and V. Kumar, *Carbohydrate polymers*, 2012, **87**, 1925-1932.
81. S. Sayed, T. Millard and A. Jardine, *Carbohydrate polymers*, 2018, **196**, 187-198.
82. X. Zhou, X. Zhang, J. Zhou and L. Li, *RSC advances*, 2017, **7**, 12247-12254.
83. A. Li, Q. Xue, Y. Ye, P. Gong, M. Deng and B. Jiang, *Molecules*, 2020, **25**, 4698.

Chapter 3: Amination of Cellulose and a Study of its Properties

3.1 Literature review

Aminated biopolymers are biopolymers modified by amino-functionalisation and have significant advantages of improved solubility in protic, aprotic and aqueous solvents. This improved solubility provides opportunities for further chemical modifications. The additional charge density of the amino-group facilitates properties of anticancer, antimicrobial, antioxidant and gene transfection.¹ A recent review by Jardine *et al.* discusses the synthesis, properties and applications of amino-functionalised polysaccharides, specifically 6-deoxy-6-aminocellulose and 6-deoxy-6-aminochitosan.¹

Water soluble 6-deoxy-6-amino derivatives of cellulose and chitosan have potential applications in the fields of antimicrobials, biomedicine, cosmetics, haemostatics, packaging, textiles and water purification amongst others (**Figure 3.1**).¹

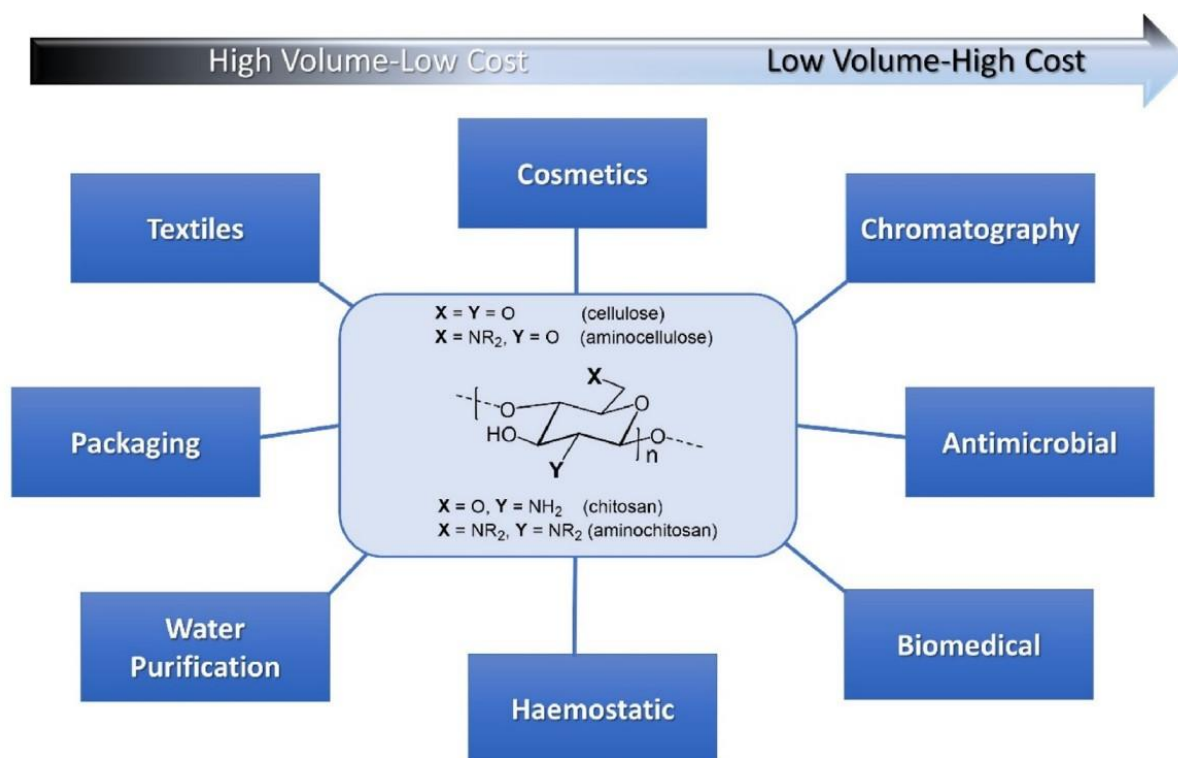


Figure 3.1. Various applications of 6-deoxy-6-amino derivatives of cellulose and chitosan.¹

There are different routes explored in literature for the synthesis of water soluble 6-deoxy-6-amino biopolymers (**Scheme 3.1**). They all require conversion of the 6-hydroxy group *via* a

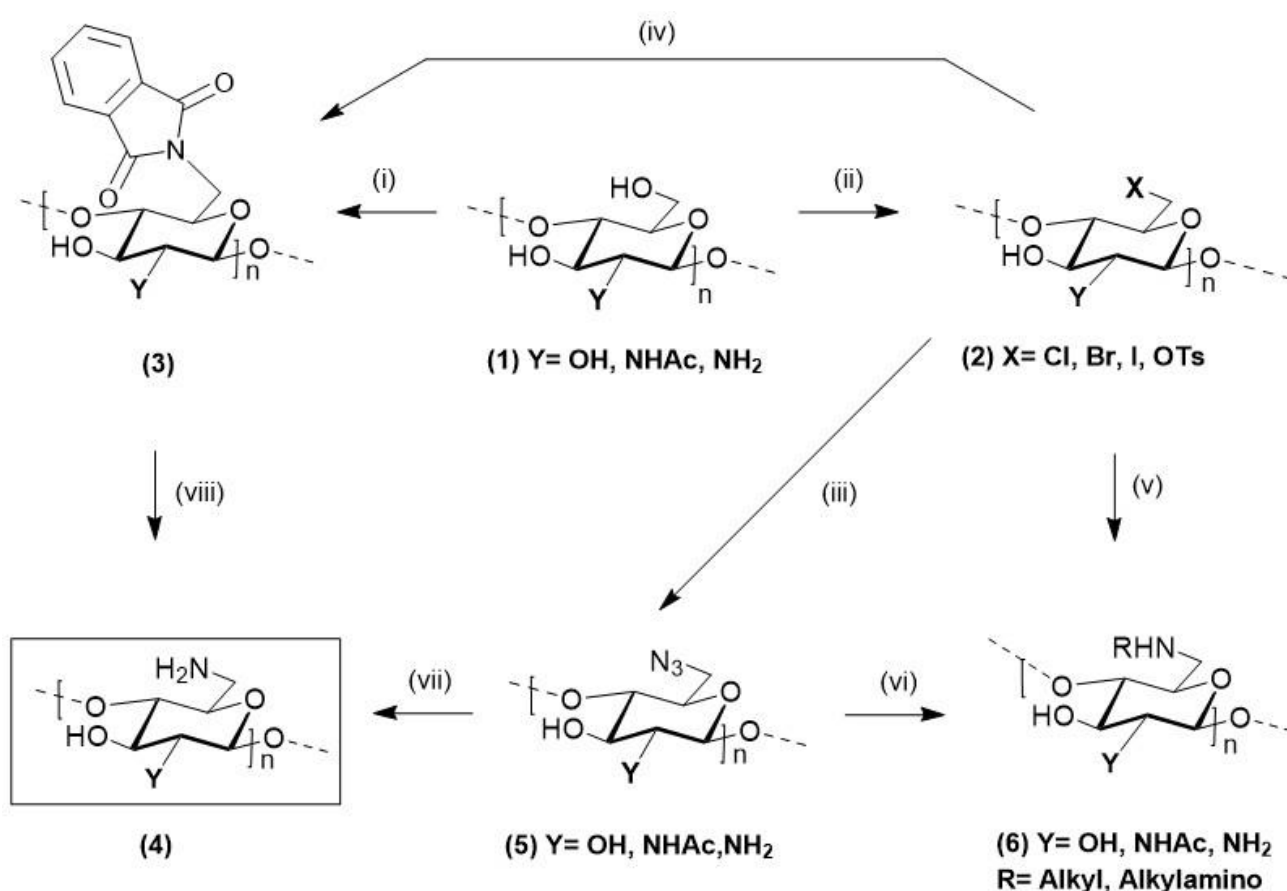
S_N2 reaction, generally tosylation or halogenation. The most popular method for tosylation of biopolymers is the homogenous reaction of biopolymer dissolved in DMAc/LiCl with TsCl in the presence of an organic base.^{1,2} The 6-tosyl is a good leaving group which readily undergoes substitution with a nucleophile.

Direct halogenation of polysaccharides is possible by the phosphonium leaving groups produced by homogenous reactions using triphenylphosphine/*N*-halosuccinimide mixtures.^{1, 3, 4} Three commonly explored 6-deoxy-6-halo celluloses are *N*-bromo, *N*-chloro and *N*-iodo. The 6-deoxy-6-bromo cellulose is well-researched as it can easily undergo substitution reactions, however, displays poor solubility in organic solvents relative to 6-tosyl cellulose. Moreover, the removal of residual Ph₃PO and Ph₃P from the polymer is a greater challenge.¹ To halogenate chitosan, protection of the amino group, generally through use of *N*-phthaloyl groups, is needed before subsequent conversion of the 6-hydroxy group into a 6-halo group using Ph₃P/NXS (X = Cl, Br, I) in solvents such as DMF, DMSO or NMP.^{1,5}

The synthesis of 6-deoxy-6-amino derivatives *via* azidation of 6-tosyl or 6-deoxy-6-halo polysaccharides is a commonly used method. More often, reduction of the 6-azido groups to 6-amino groups is done by Staudinger Ph₃P or simply hydride reduction. When direct substitution of the 6-tosyl or 6-halo groups with nucleophilic amino groups were performed, a broad variety of amino polysaccharides were produced.¹ Previous methods for the synthesis of 6-deoxy-6-amino polysaccharides have disadvantages of the use of hazardous solvents (pyridine, DMF, NMP) and contamination with residual aromatics. Incomplete tosylation, as well as Ph₃PO, leads to impurities during Staudinger reduction of the 6-azido groups. Furthermore, poor deprotection of the phthaloyl groups occurred when 6-deoxy-6-aminochitosan was synthesised from chitosan, which results in poor aqueous solubility of the amino product. Limitations in the scale up arises, such as toxicity and sodium azide waste, when azidation is used in DMF to introduce the C-6 amino group.¹

Direct amination of C-6 activated biopolymers is an attractive strategy due to its simplicity. An alkylamino group at the C-6 position is of particular interest due to the known properties of 6-amino derivatives and nucleophilicity of the amine that allows selective reactivity relative to hydroxyls. Ideally, direct tosyl substitution with the alkylamine as both reagent and solvent would solve the problem of the removal of residual triphenylphosphine oxide that results from Staudinger reduction of azido-polysaccharides.¹ An example of this is 6-deoxy-6-isobutylaminocellulose that was synthesised by amination of 2,3-di-*O*-acetyl-6-*O*-tosyl

cellulose using isobutylamine as both reagent and solvent.^{1,6} An extended linker, such as an alkylamino group, is often used in immobilisation to avoid non-specific polymer support type interference with biopolymers or immobilised molecules. 6-deoxy-6-alkylaminocellulose with varying alkyl chain lengths was used as a support surface for covalent enzyme immobilisation with different coupling reagents.^{1,7} Sayed *et al.* synthesised 6-deoxy-6-(2-aminoethyl)amino chitin and 6-deoxy-6-(2-aminoethyl)amino chitosan by treating 6-deoxy-6-tosyl chitin and 6-tosyl 2-phthaloyl chitosan with neat ethylenediamine at reflux. Ethylenediamine played the roles of reagent, solvent and deprotecting agent.^{1,8}



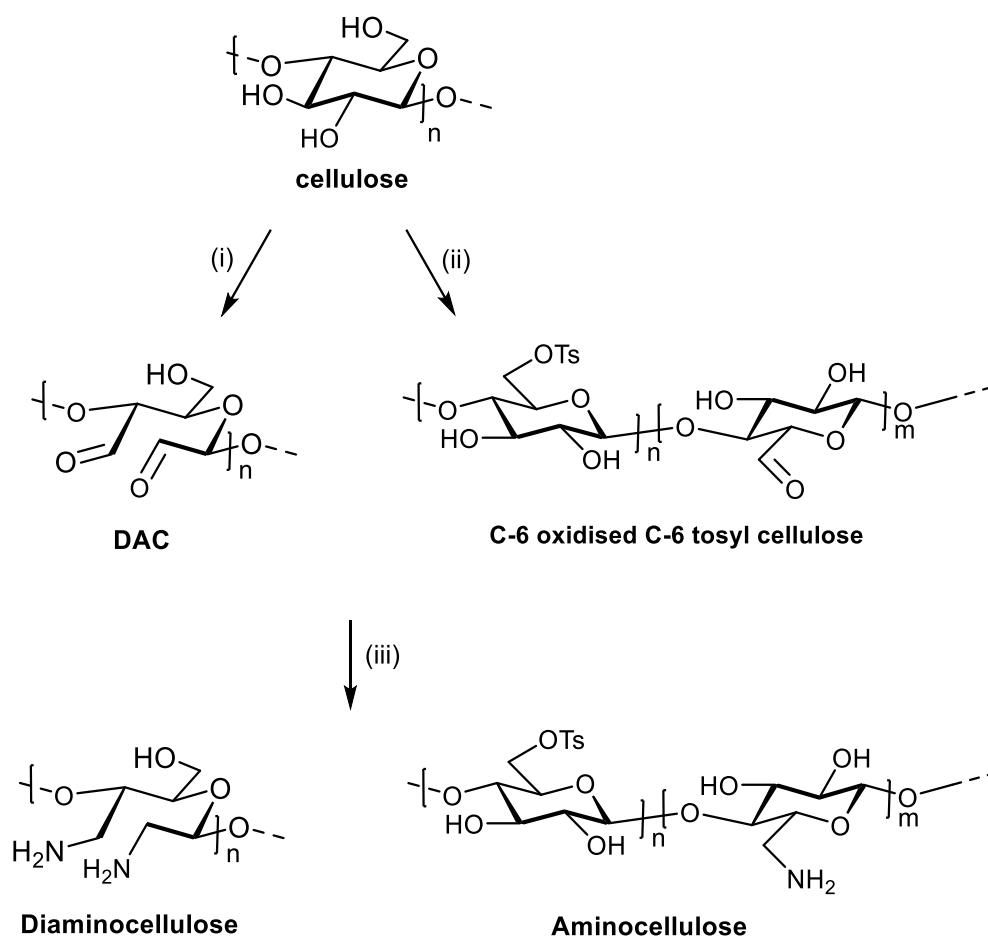
Scheme 3.1. Different synthetic routes towards the amination of cellulosic polysaccharides. (i) Ph₃P/ DIAD/ Phthalimide; (ii) Ph₃P/ NXS (X = Cl, Br, I) or TsCl/ Et₃N/DMAc/LiCl; (iii) NaN₃; (iv) K⁺ Phthalimide⁻; (v) RNH₂; (vi) Ph₃P and RCHO/NaCNBH₃; (vii) Ph₃P/ NH₂NH₂ or Ph₃P or LiAlH₄ or NaBH₄.¹

The major limitations for the synthesis of C-6 aminated biopolymers are the use of high boiling point toxic solvents like DMF and NMP, hazardous reagents like sodium azide, the production of liquid process waste streams, incomplete deprotection steps, inconsistent yields and degree

of substitution (DS), as well as depolymerisation. Importantly, challenges in economies of scale, solubility and DS, are reasons why more research needs to be conducted on the amination of biopolymers.¹ There is a commercial need for green and sustainable synthetic methods for the amination of biopolymers to yield soluble aminated biopolymers products that have consistent yields and DS, with minimal or no depolymerisation as well as with minimal or recyclable waste streams. The method needs to follow the 12 Green Chemistry principles, be scalable in a cost-effective manner, and should have short, simple synthetic steps.⁹

Diamino biopolymers, such as diaminocellulose and 6-deoxy-6-aminochitosan, contain two amino groups with a net positive charge at physiological pH which influences its binding and stabilisation through electrostatic interactions with negatively charged molecules.^{10, 11} Diaminocellulose is utilised in fields such as thermoplastics and as an immobilisation support for target aldehyde molecules through Schiff base formation.^{12, 13} Diaminocellulose is commonly synthesised in a two-step process: firstly oxidation of cellulose to yield DAC and secondly, reductive amination of DAC to obtain the desired diaminocellulose product.¹²

In this study, methods for reductive amination of oxidised biopolymers, specifically C-6 oxidised cellulose and DAC have been explored (**Scheme 3.2**). Different Schiff base reductants, namely picoline borane, sodium borohydride and sodium hypophosphite, were used in a one-pot reductive amination reaction to yield aqueous soluble 6-deoxy-6-aminocellulose and diaminocellulose. The aminated cellulose products synthesised using the ideal, most effective reductant was characterised *via* NMR, IR, EA, PXRD, TGA and DSC. A ninhydrin Kaiser test was used to qualitatively determine whether the biopolymers were successfully aminated by means of a blue colour change. Lastly, the bioactivity of the aminated biopolymers synthesised using the best method of the three explored, were evaluated in studies of cytotoxicity against brain cancer cell lines. The ‘best’ method of reductive amination of biopolymers would be the one of the three explored which produces soluble aminated biopolymers with a significant degree of substitution, as well as uses green reagents and solvents. The 12 Green Chemistry Principles that this study adheres to are the use of less hazardous chemical syntheses and safer solvents.



Scheme 3.2. Overall synthetic route towards the synthesis of diaminocellulose and 6-deoxy-6-aminocellulose. (i) NaIO_4 ; (ii) (a) $\text{TsCl}/\text{Et}_3\text{N}/\text{DMSO}/\text{SLS}$; (b) $\text{TsCl}/\text{Et}_3\text{N}/\text{DMSO}$; (iii) (a) pic-BH_3 ; (b) NaBH_4 ; (c) NaH_2PO_2 using NH_4Ac as amine source.

3.2 Results and discussion

3.2.1 Synthesis of diaminocellulose

There are literature reports on the synthesis of diaminocellulose, each proceeding by firstly synthesising DAC, which was discussed in **Chapter 2**, followed by reductive amination.¹³ Hitherto, there have been no comparative studies that evaluate the most effective reductant of the three explored for the synthesis of diaminocellulose. The ideal reductant should produce soluble diamino products with minimal depolymerisation in a ‘one-pot’ method whereby the imine is formed followed by *in situ* reduction. In this study, a comparative investigation on the use of three different reducing agents for the reductive amination of DAC was explored, namely, picoline borane, sodium borohydride and sodium hypophosphite.

Synthesis of diaminocellulose using 2-picoline borane as a reductant

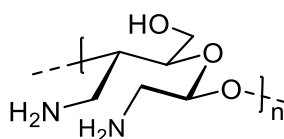
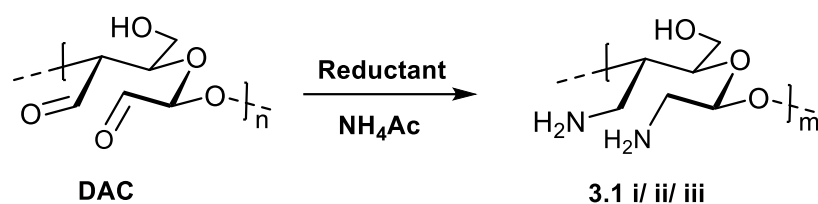


Figure 3.2. Structure of diaminocellulose.

Diaminocellulose (**3.1i**) was synthesised by the reduction of DAC using 2-picoline borane and ammonium acetate in an acidic aqueous media (pH 4.5) at 45 °C for 24 h (**Scheme 3.3i**).¹² The resulting mixture was washed with methanol and subsequently dialysed against water and lyophilised to yield a white solid. The major advantage of using 2-picoline borane for reductive amination reactions is that it is water soluble and therefore the reduction can occur in aqueous medium. The other significant advantage is that 2-picoline borane can be used in a ‘one-pot’ reductive amination of DAC as reported in literature.^{11, 12} 2-Picoline borane-mediated reduction occurs under slightly acidic reaction conditions which aids in the prevention of beta-elimination mediated depolymerisation side reactions as well as increases DAC’s reactivity by shifting the equilibria between masked (hemiacetal) and free aldehyde groups.¹⁴⁻¹⁶



Scheme 3.3. Synthesis of diaminocellulose using different reducing conditions (i) pic-BH₃/ NH₄Ac/ DI (pH 4.5)/ 45 °C for 24 h to yield (**3.1i**); OR NaBH₄/ NH₄Ac/ NH₄OH/ EtOH/ 80 °C for 18 h to yield (**3.1ii**); OR NaH₂PO₂/ NH₄Ac/ EtOH/ 40 °C for 19 h to yield (**3.1iii**).

A Kaiser ninhydrin test was performed on the diaminocellulose (**3.1i**) to confirm the presence of primary amines as shown in **Table 3.1**. The Kaiser ninhydrin test is a qualitative method to test for the presence of primary amines by a blue/purple colour change indicative of a positive result. This negative result was not in agreement with the increase in N:C ratio as determined by elemental analysis. A possible reason for the negative result is complexation between pic-BH₃ and the polymer by the formation of a borane ester. The increase in nitrogen content could be attributed to the nitrogen of pic-BH₃. Another reason for the unsuccessful reaction could be the insolubility of DAC in water.

Table 3.1: Table showing the degree of substitution and Kaiser ninhydrin test result for diaminocellulose and aminocellulose synthesised using different reductants.







No.	Reagent	Elemental Composition				Degree of Substitution (%)	Kaiser Test Image	Kaiser Test Result	
		C(%)	H(%)	N(%)	S(%)			Outcome	Solubility
3.1i	pic-BH ₃	45.29	6.26	14.83	-	-		NEGATIVE	-
3.1ii	NaBH ₄	40.98	7.27	1.66	-	0.096		POSITIVE	INSOLUBLE
3.1iii	NaH ₂ PO ₂	34.53	4.71	5.27	-	0.31		POSITIVE	SOLUBLE

Table 3.1: Table showing the degree of substitution and Kaiser ninhydrin test result for diaminocellulose and aminocellulose synthesised using different reductants.

No.	Reagent	Elemental Composition				Degree of Substitution (%)	Kaiser Test Image	Kaiser Test Result	
		C(%)	H(%)	N(%)	S(%)			Outcome	Solubility
3.2i	pic-BH ₃	44.90	6.00	0.26	6.70	-		NEGATIVE	-
3.2ii	NaBH ₄	46.57	6.06	0.29	7.22	0.034		POSITIVE	INSOLUBLE
3.2iii	NaH ₂ PO ₂	39.65	5.13	0.19	6.19	0.022		POSITIVE	SOLUBLE

Synthesis of diaminocellulose using sodium borohydride as a reductant

Sodium borohydride is a commonly used reductant but due to the known depolymerisation of DAC at alkalinity, it was not the first choice of reductant for DAC.¹⁷ However, in this study the use of sodium borohydride as an alternative reductant for DAC was explored because there is evidence in literature of its successful reduction of DAC to produce water-soluble aminated cellulose. Koshani *et al.* synthesised and characterised hairy aminated nanocrystalline cellulose whereby cellulose fibers are subjected to a two-step oxidation-reductive amination process and subsequently a hydrothermal treatment to form novel hairy nanocellulose.¹³ They report amination through a Schiff base reaction between the aldehyde groups of DAC and ammonia, followed by reduction of the resulting imine to primary amines using sodium borohydride as a reductant.¹³ The synthesis of diaminocellulose using sodium borohydride as a reducing agent (**3.1ii**) is shown in **Scheme 3.3ii**. DAC and NH₄Ac were allowed to stir in ethanol at 80 °C under reflux conditions for 18 h. The reaction mixture was subsequently cooled using an ice bath and NaBH₄ was added and allowed to stir for an additional 1 h. The resulting product was washed with water, dialysed against deionised water and lyophilised to obtain a brown powder with a mass yield of 34 %.

The Kaiser ninhydrin test confirmed the successful reductive amination of DAC as evident by the dark blue colour (Kaiser positive) (**Table 3.1**). Furthermore, elemental analysis indicated a DS of 0.10. Thus, the amount of available aldehyde groups of DAC converted to amino-groups was 93 %. Albeit the successful reductive amination of DAC using sodium borohydride, the resulting diamino product obtained was insoluble in common organic and aqueous solvents, and hence could not be characterised by solution ¹H-NMR spectroscopy. The IR spectrum of diaminocellulose (**DIAM CELL**) (**3.1ii**) (**Figure 3.3**) displayed the characteristic absorption band for C-NH₂ at 1634 cm⁻¹.

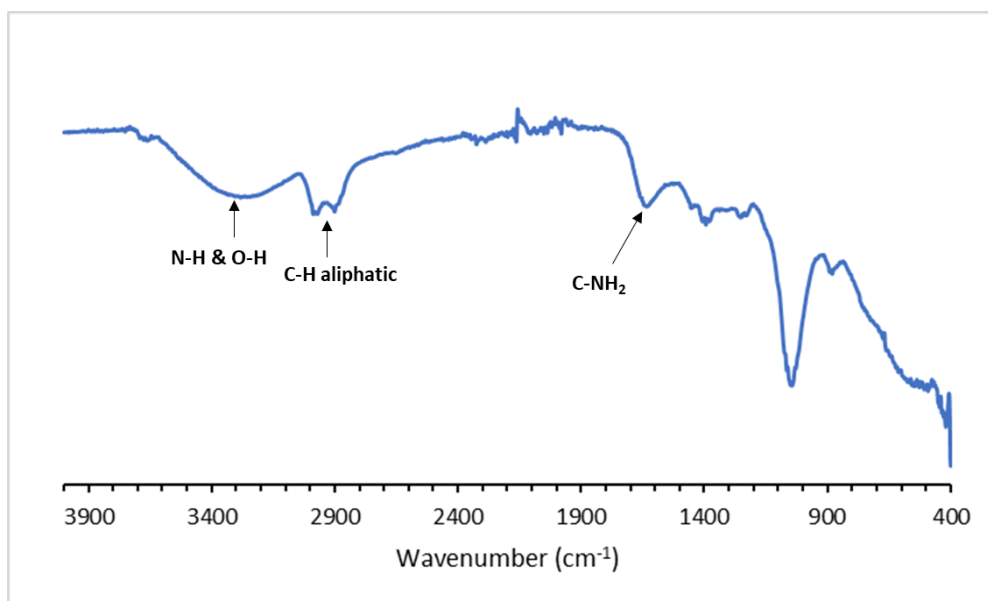


Figure 3.3. IR spectrum of diaminocellulose (**DIAM CELL**) synthesised using reductant NaBH₄ (**3.1ii**).

Synthesis of diaminocellulose using sodium hypophosphite as a reductant

Hitherto, DAC was subjected to reductive amination using pic-BH₃ and NaBH₄ as reductants. When pic-BH₃ was used as a reductant, a negative result for the presence of primary amines in the product was observed *via* the Kaiser ninhydrin test. The diaminocellulose product obtained using NaBH₄ produced a positive Kaiser ninhydrin test result, however, the resulting biopolymer was insoluble in aqueous and common organic solvents. Therefore, the search for a green, stable and effective reductant for amination of DAC was further investigated using sodium hypophosphite. Previously, NaH₂PO₂ was used as a reductant for a series of different combinations of carbonyl compounds and amines. The authors reported that reductive amination using NaH₂PO₂ proceeded optimally under neat conditions at a temperature of 130 °C using half an equivalent of reductant. Most notably, NaH₂PO₂ is stable, nontoxic, cheaply accessible in large quantities and green.¹⁸ These characteristics makes NaH₂PO₂ an attractive candidate for the reductive amination of DAC.

The literature method by Kliuev *et al.* was modified accordingly for DAC. The reported stoichiometric ratio of reactants was implemented using relative mass ratios (DAC/ NH₄Ac/ NaH₂PO₂ = 1/1.25/0.5). NaH₂PO₂ was dissolved in water, followed by the addition of DAC and NH₄Ac in ethanol and allowed to stir at 40 °C for 19 h (**Scheme 3.3iii**). The reaction

mixture was dialysed against deionised water, the solid collected by centrifugation and lyophilised to obtain the diaminocellulose product (**3.1iii**) in a mass yield of 33 %.

The diaminocellulose (**3.1iii**) tested positive for the presence of primary amines by means of the Kaiser ninhydrin test, as evident by the dark blue colour change (**Table 3.1**). The diaminocellulose product obtained was soluble in DMSO and displayed a DS of 0.31 as determined by elemental analysis and 90 % of available aldehyde groups were converted to amino-groups.

The IR spectrum (**Figure 3.4**) suggests the structure of diaminocellulose (**DIAM CELL**) (**3.1iii**) by the diagnostic absorption band of C-NH₂ at 1632 cm⁻¹. The expected absorption bands of the primary amine groups in the region 3400 to 3250 cm⁻¹ overlaps with absorption bands of cellulose (O-H and C-H at 3300 and 2900 cm⁻¹, respectively), therefore the amine groups cannot be clearly detected.¹³

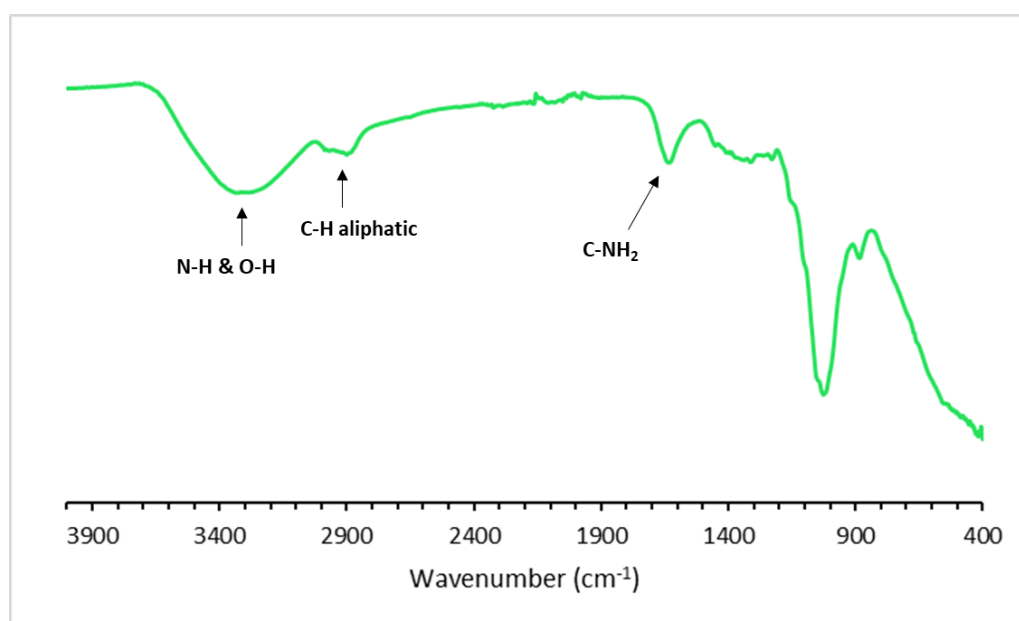


Figure 3.4. IR spectrum of diaminocellulose synthesised using reductant NaH₂PO₂ (**DIAM CELL**) (**3.1iii**).

The solid-state NMR spectrum (**Figure 3.5**) confirms the structure of diaminocellulose (**3.1iii**). Broad signals are present in the region δ 60 to 110 ppm, in accordance to literature, for the cellulose backbone of DAC which are attributed to the highly amorphous nature of DAC.^{19, 20} For the aminated subunit of diaminocellulose, the signal assigned C-1 is less deshielded at δ 97.75 ppm relative to the C-1' signal of the hydrated DAC subunit at δ 103.63 ppm. Furthermore, the same effect is observed for the signals C-4 of the aminated subunit and C-4'

of the hydrated DAC subunit at δ 82.84 and 87.74 ppm, respectively; as well as for the signals assigned C-6 at 59.92 ppm and C-6' at 64.15 ppm. This is evidence of the presence of both aminated and non-aminated hydrated DAC subunits in the diaminocellulose product. Signals for the rest of the cellulose backbone of the product, assigned C-2/3/5 and C-2'/3'/5' are found to overlap in the region δ 70.33 to 73.78 ppm.

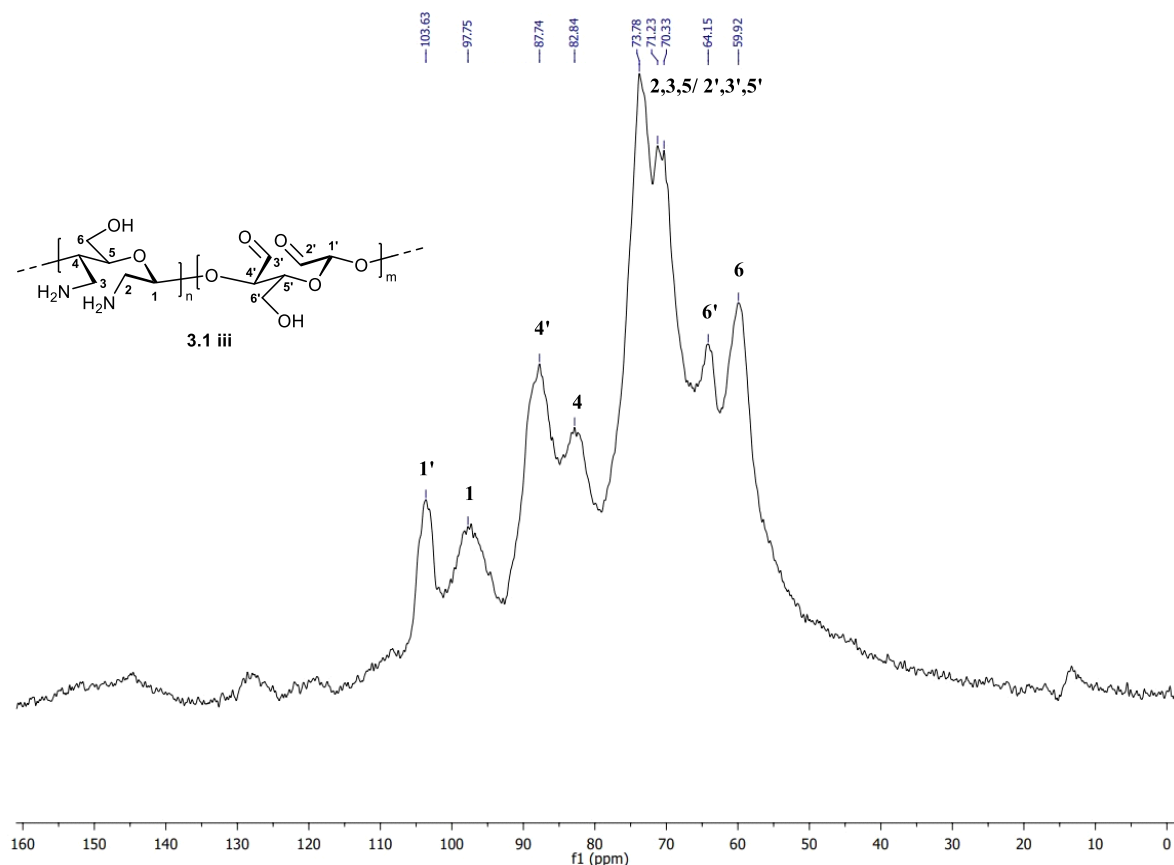


Figure 3.5. Solid state ^{13}C NMR spectrum of diaminocellulose using reductant NaH_2PO_2 (**3.1iii**).

The crystallinity of diaminocellulose (**3.3**) was evaluated using PXRD (**Figure 3.6**). The diffraction pattern displays one broad peak with a 2θ of 16° which is characteristic of an amorphous polymer. The relative intensity of diaminocellulose to DAC has decreased significantly, suggesting a more amorphous polymer than DAC. This could be explained by the reductive amination of the aldehyde groups to amino groups. Amino groups are more flexible in conformation and can behave as both hydrogen bond acceptors and donors whereas carbonyl groups are more rigid and planar and can behave as hydrogen bond acceptors; therefore, diaminocellulose is more likely to undergo cross-linking than DAC and thus displays a more

amorphous diffraction pattern as it is expected to experience more structural disorganisation. The increasing structural disorganisation of the amorphous phase of aminated cellulose derivatives is known to cause long range spacing of polymeric chains which leads to a decrease in the crystallinity of cellulose.²¹

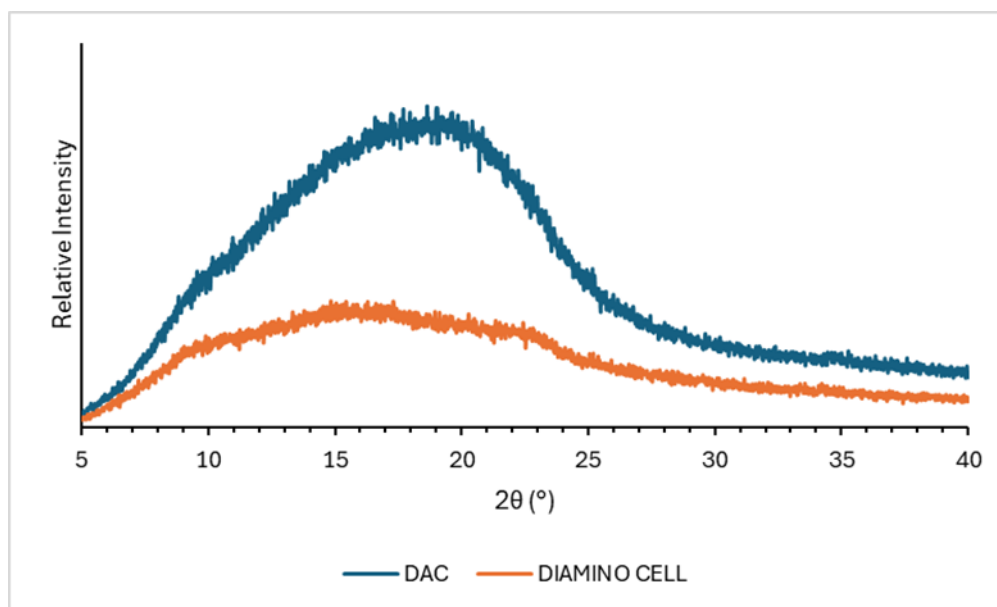


Figure 3.6. PXRD spectrum of dialdehyde cellulose (**DAC**) (**2.1**) and diaminocellulose (**DIAM CELL**) (**3.1iii**).

Thermal analysis of diaminocellulose (**3.1iii**) was conducted to evaluate its thermal stability (**Figure 3.7**). There are three main degradation processes evident in the TGA thermogram: at 0 to 80 °C due to the loss of free water from the polymer (13% mass loss), at 81 to 212 °C (6 % mass loss), and at 215 to 350 °C attributed to pyrolysis of the polymer (the greatest mass loss of 32 %). The DSC thermogram displays an endothermic peak at 75 °C which suggests that diaminocellulose is less thermally stable than DAC which shows no degradation until 90 °C. The decrease in thermal stability could be due to the decrease in crystallinity of diaminocellulose, as evident by the PXRD shown in **Figure 3.6**.

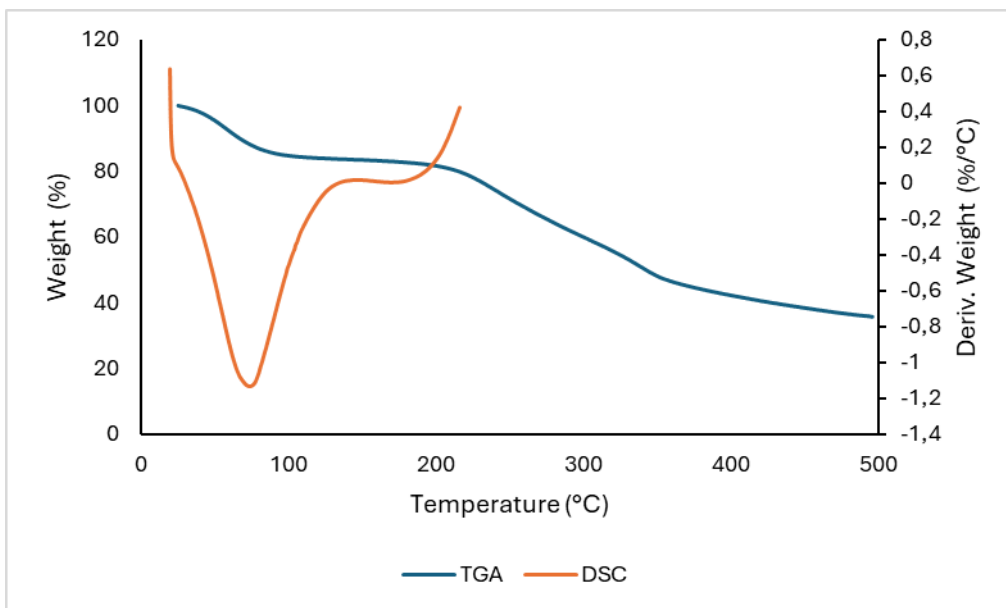


Figure 3.7. The TGA and DSC curves of Diaminocellulose (**3.1iii**).

Diaminocellulose was successfully synthesised using NaH_2PO_2 as a reductant. This is the first time that NaH_2PO_2 -mediated reductive amination was applied to a polymer. The aminated product obtained had a degree of amination of 0.31. The polymer tested positive for the presence of primary amines *via* the Kaiser ninhydrin test. The diaminocellulose was DMSO-soluble and its structure was confirmed by NMR and IR spectroscopy. Furthermore, diaminocellulose was found to be amorphous as determined by PXRD and thermally stable at temperatures below 80 °C.

3.2.2 Synthesis of aminocellulose

The synthesis of aminocellulose has been well reported in literature, as discussed previously in this chapter. Sirviö *et al.* has combined regioselective oxidation and reductive amination to yield amino-modified nanocrystals with modifiable hydrophobicity.²² The authors investigated the fabrication of amphiphilic CNCs with adjustable hydrophobicity by the introduction of linear amines of increasing chain length into the backbone of cellulose using periodate oxidation and 2-picoline borane-mediated reductive amination in an aqueous environment.²²

The synthesis of aminocellulose by reductive amination of mixed C-6 oxidised C-6 tosyl cellulose (**2.3**) has not been explored in literature. In this study, mixed C-6 oxidised C-6 tosyl cellulose (**2.3**) (**Figure 3.8**) is subjected to reductive amination using different reductants to yield aminocellulose. A similar protocol to the investigation of the best reducing agent for the synthesis of diaminocellulose was performed, using 2-picoline borane, sodium borohydride and sodium hypophosphite.

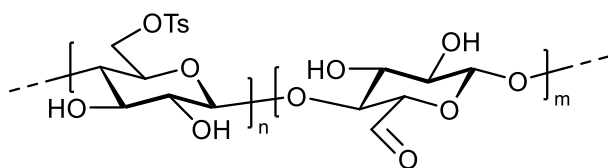


Figure 3.8. Structure of C-6 oxidised C-6 tosyl cellulose (**2.3**).

Synthesis of aminocellulose using 2-picoline borane as a reductant

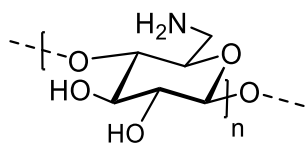
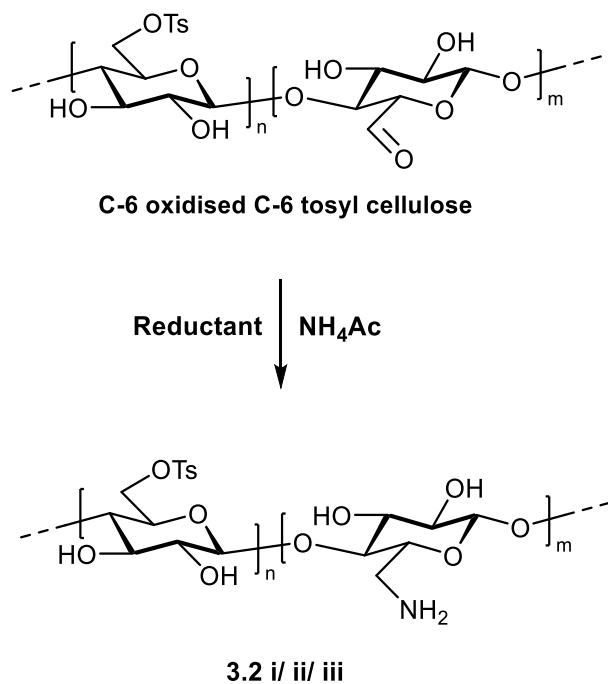


Figure 3.9. Structure of aminocellulose.

Aminocellulose (**3.2i**) was synthesised by a one-step reductive amination reaction of C-6 selectively oxidised tosyl cellulose using 2-picoline borane and ammonium acetate in an acidic aqueous media (pH 4.5) at 45 °C for 24 h (**Scheme 3.4i**). The reaction mixture was allowed to stir in methanol and dialysed against deionised water, followed by lyophilisation to obtain aminocellulose (**3.2i**) as a white solid.



Scheme 3.4. Synthesis of aminocellulose using different reducing agents (i) pic-BH₃/ NH₄Ac/ DI (pH 4.5)/ 45 °C for 24 h to yield (**3.2i**); OR (ii) NaBH₄/ NH₄Ac/ NH₄OH/ EtOH/ 80 °C for 18 h to yield (**3.2ii**); OR NaH₂PO₂/ NH₄Ac/ EtOH/ 40 °C for 19 h to yield (**3.2iii**).

A Kaiser ninhydrin test was performed on aminocellulose (**3.2i**) to confirm the presence of primary amines and displayed a negative result as shown in **Table 3.1**. This negative test result indicated that the reductive amination reaction of C-6 selectively oxidised tosyl cellulose using pic-BH₃ was unsuccessful. Further evidence that the reaction did not work is provided by elemental analysis where the C:N ratio of 44.90: 0.26 shows that the nitrogen content of the polymer did not increase. A possible reason for the reaction not working is the poor aqueous solubility of C-6 oxidised C-6 tosyl cellulose (**2.3**).

Synthesis of aminocellulose using sodium borohydride as a reductant

Mixed C-6 oxidised C-6 tosyl cellulose (**2.3**) was aminated following a reductive amination procedure whereby it was allowed to stir with NH₄Ac in ethanol at 80 °C under reflux conditions for 18 h. The reaction mixture was cooled using an ice bath and NaBH₄ was added and allowed to stir for an additional 1 h (**Scheme 3.4ii**). The resulting product was washed with water, dialysed against deionised water and lyophilised to obtain a white solid with a mass yield of 20 %. It is of note that the percentage mass yield was calculated based on the conversion

of tosyl cellulose to aminocellulose because C-6 oxidised C-6 tosyl cellulose was not dialysed and may contain excess starting materials and other impurities.

The Kaiser ninhydrin test confirmed the successful amination of mixed C-6 oxidised C-6 tosyl cellulose (**2.3**) by a visible dark blue colour change as shown in **Table 3.1**. The aminocellulose (**3.2ii**) was observed to have a DS of 0.034 as determined by elemental analysis, indicating a 72 % conversion of available aldehyde groups to amino-groups. However, structural characterisation of the polymer was limited to IR spectroscopy due to its insolubility in aqueous and organic solvents as the amination caused stronger inter-strand hydrogen bonding. The IR spectrum (**Figure 3.10**) shows absorption bands corresponding to $\nu(\text{N-H \& O-H})$ at 3396 cm^{-1} , $\nu(\text{C-H aliphatic})$ at 2918 cm^{-1} and $\nu(\text{C-NH}_2)$ at 1624 and 1596 cm^{-1} which confirms the presence of amino group in the polymer.

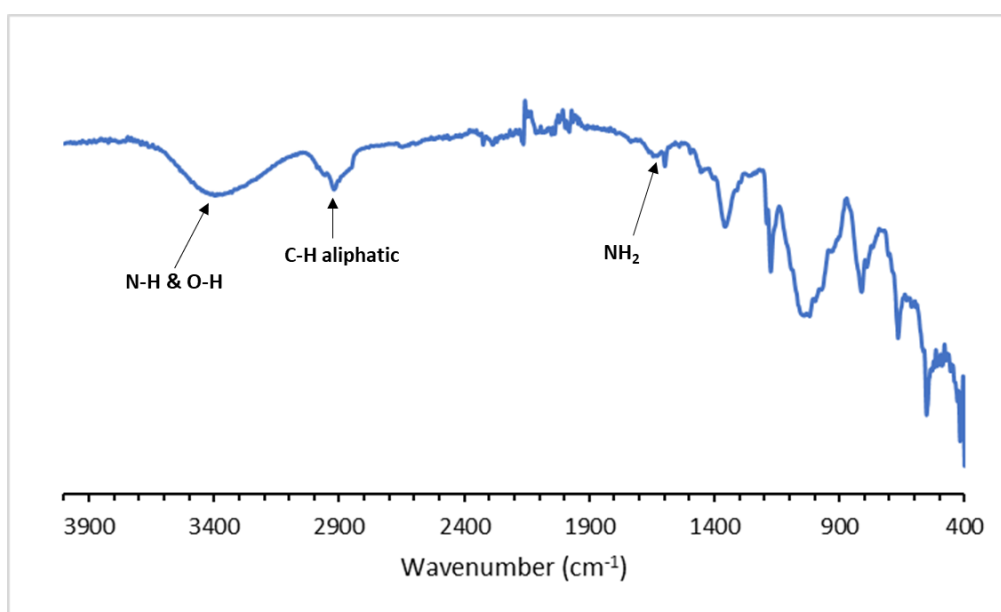


Figure 3.10. IR spectrum of aminocellulose synthesised using reductant NaBH₄ (AMINO CELL) (**3.2ii**).

Synthesis of aminocellulose using sodium hypophosphite as a reductant

The aim of this investigation was to find the ideal reducing agent for the reductive amination of mixed C-6 oxidised C-6 tosyl cellulose (**2.3**) to obtain soluble aminocellulose with a significant DS. Thus far, two reductants were evaluated in one-pot reductive amination reactions of C-6 oxidised C-6 tosyl cellulose (**2.3**), namely, pic-BH₃ and NaBH₄. The product

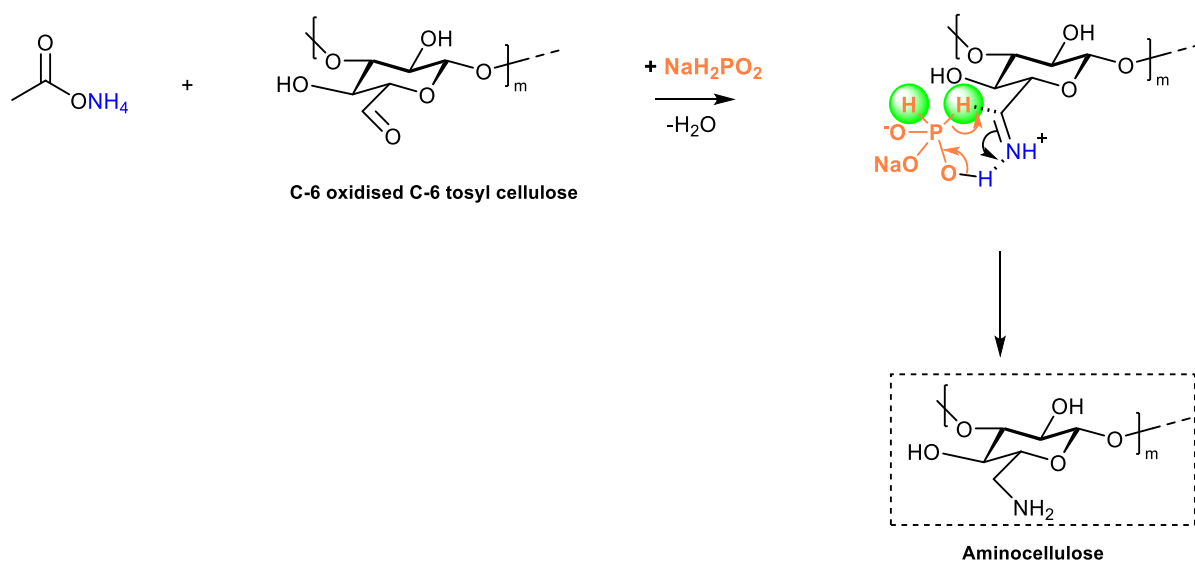
obtained from the reaction with pic-BH₃ tested negative for the Kaiser ninhydrin test, hence was unsuccessfully aminated; whereas the product obtained from the use of NaBH₄ produced a positive Kaiser ninhydrin test for the presence of primary amines but the resulting polymer was insoluble in aqueous and organic solvents.

Thus, there was still a need for the successful synthesis of soluble aminocellulose using a reductant that overcomes the challenges of the use of pic-BH₃ and NaBH₄. The use of NaH₂PO₂ as a reducing agent of mixed C-6 oxidised C-6 tosyl cellulose (**2.3**) to yield aminocellulose was explored.

A similar method to that reported for the synthesis of diaminocellulose (**3.2iii**) was employed for mixed C-6 oxidised C-6 tosyl cellulose (**2.3**). The literature method by Kliuev *et al.* was modified accordingly.¹⁸ The reported stoichiometric ratio of reactants was implemented using relative mass ratios (C-6 OXID CELL/ NH₄Ac/ NaH₂PO₂ = 1/1.25/0.5). NaH₂PO₂ was dissolved in water, followed by the addition of C-6 OXID CELL and NH₄Ac in ethanol and allowed to stir at 40 °C for 19 h (**Scheme 3.4iii**). The reaction mixture was dialysed against deionised water, the solid collected by centrifugation and lyophilised to obtain the aminocellulose product (**3.2iii**) in a mass yield of 34 %.

The aminocellulose product (**3.2iii**) obtained tested positive for the presence of primary amines *via* Kaiser ninhydrin test, as evident by a dark blue colour change (**Table 3.1**). The aminocellulose was soluble in DMSO and had a DS of 0.022 as determined by elemental analysis, indicating that 81 % of aldehyde content were converted to amino-groups.

The mechanism for the reductive amination of C-6 oxidised C-6 tosyl cellulose follows the proposed mechanism by Kliuev *et al.* (**Scheme 3.5**). Noting that 0.5 eq. of NaH₂PO₂ is sufficient to achieve the full conversion, it is assumed that NaH₂PO₂ acts as a 4e reductant which is able to reduce two molecules of the substrate. The H-P bond serves as a hydride source. Firstly, NaH₂PO₂ reduces one molecule of iminium ion formed from the starting amine (ammonium acetate) and carbonyl (C-6 oxidised C-6 tosyl cellulose) and yields the phosphorous acid derivative. The phosphorous acid derivative may reduce one more equivalent of the C=N bond.¹⁸



Scheme 3.5. Proposed mechanism for reductive amination of C-6 oxidised C-6 tosyl cellulose (**2.3**) using NaH_2PO_2 as reductant.

IR spectroscopy identifies the key functionalities of aminocellulose (**3.2iii**). Key absorption bands are present at 3371 cm^{-1} for ν (N-H & O-H), 2876 cm^{-1} for ν (C-H aliphatic) and at 1648 cm^{-1} & 1596 cm^{-1} for ν (NH_2) (**Figure 3.11**).

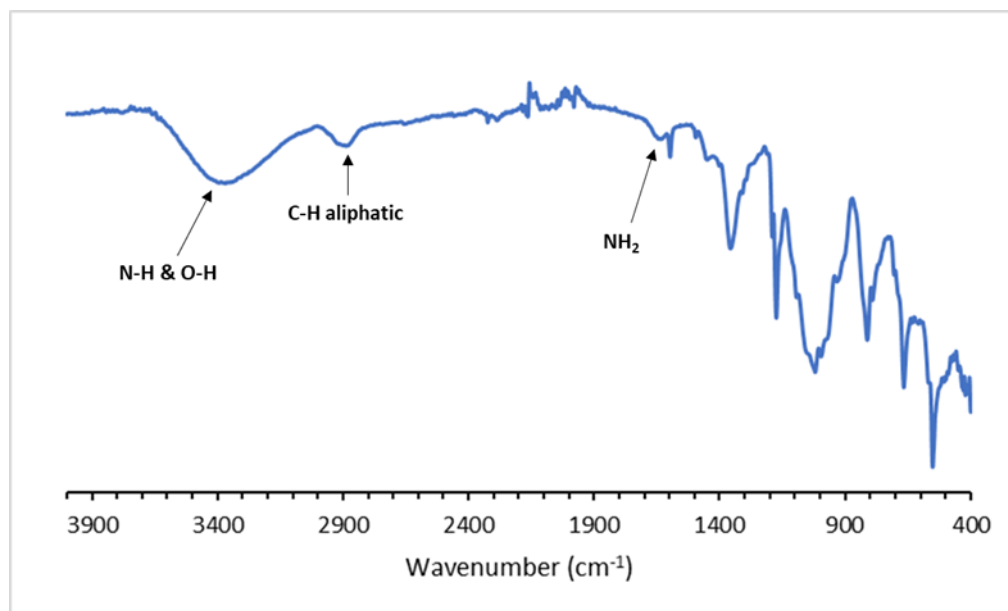


Figure 3.11 IR spectrum of aminocellulose synthesised using reductant NaH_2PO_2 (AMINO CELL) (**3.2iii**).

The structure of aminocellulose (**3.2iii**) was confirmed by various NMR spectroscopy techniques. The ^1H -NMR spectrum shown in **Figure 3.12** depicts the diagnostic shielded signal for the NH_2 -group at δ 1.22 ppm, and signals for the cellulose backbone in the region δ 3.06 to 5.43 ppm. Furthermore, signals for the presence of the tosyl moiety of aminocellulose are evident at δ 7.42 and 7.78 ppm for the aromatic protons and δ 2.28 ppm for the corresponding methyl protons. The solid state ^{13}C -NMR spectrum (**Figure 3.13**) further confirms the structure of aminocellulose. A signal for the aldehyde of C-6 oxidised C-6 tosyl cellulose (**2.3**), C-6, is evident at δ 208.76 ppm. The presence of a tosylated subunit is evident at δ 144.87 ppm, assigned to the aromatic carbons C-8' and C-9', and the methylene carbon C-11' at δ 20.38 ppm of the tosyl moiety; a signal for the C-6' occurs at δ 60.17 ppm. Signals for the backbone of cellulose are present in the region δ 73.59 to 129.04 ppm; and most notably the signal for the $\underline{\text{C}}\text{-NH}_2$ -group, assigned C-6'', occurs at δ 50.03 ppm.

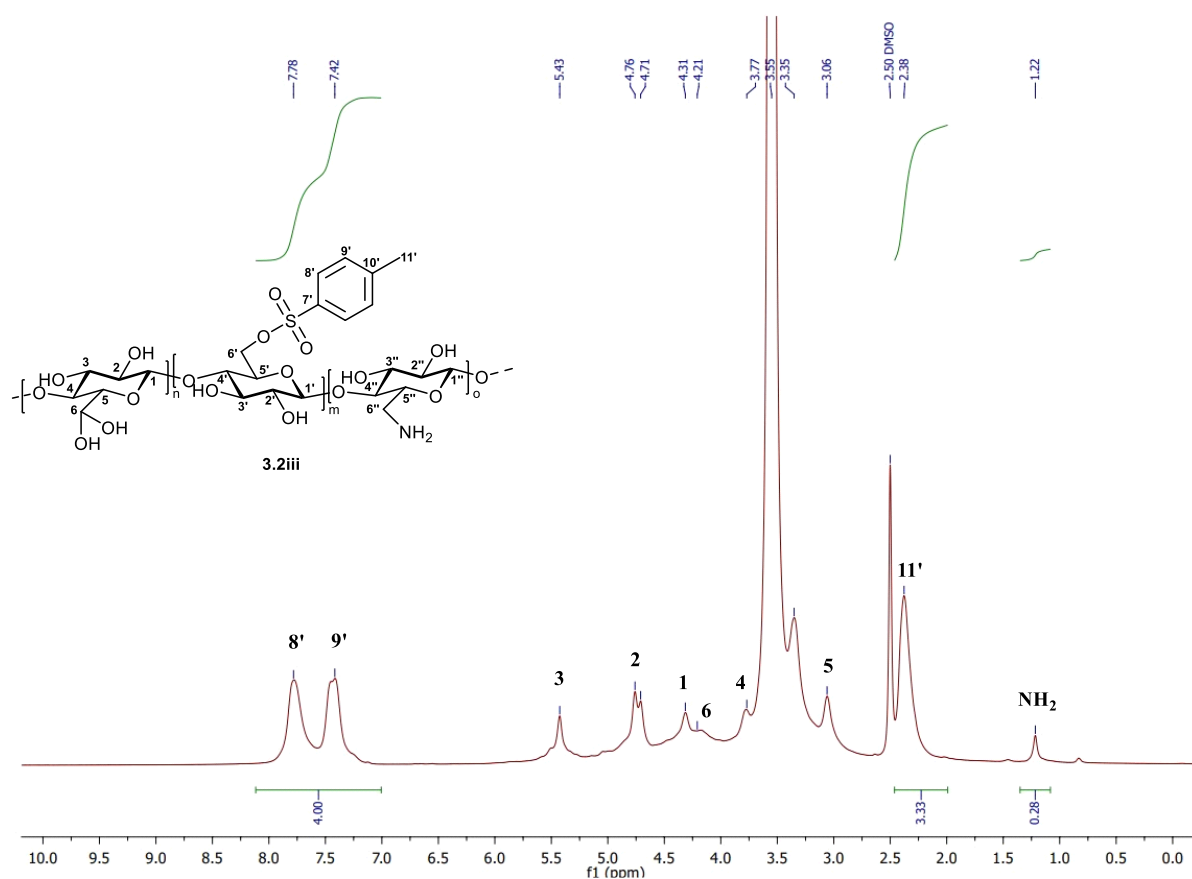


Figure 3.12. ^1H NMR spectrum of aminocellulose (**3.2iii**) in DMSO-d_6 .

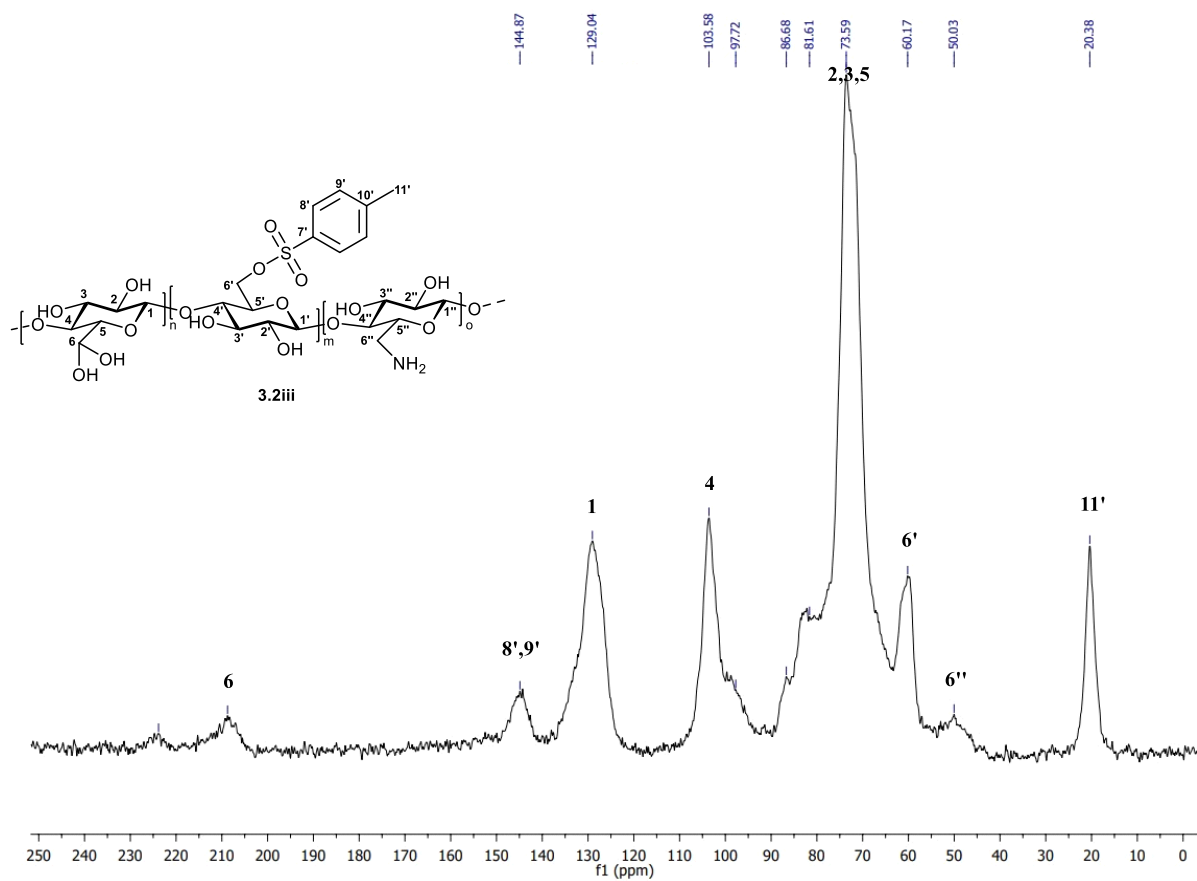


Figure 3.13. Solid state ^{13}C NMR spectrum of aminocellulose (3.2iii).

The PXRD spectrum (**Figure 3.14**) shows that aminocellulose is highly amorphous as evident by the single broad peak with a 2θ of 20.28° . There was no significant change in crystallinity from the C-6 selectively oxidised tosyl cellulose precursor to aminocellulose.

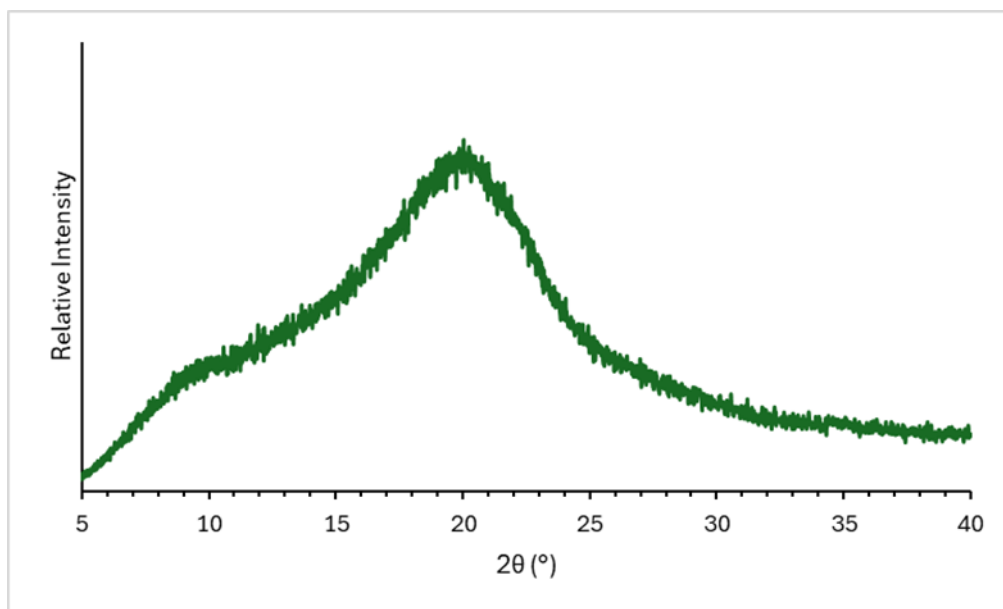


Figure 3.14. PXRD spectrum of aminocellulose (AMINO CELL) (3.2iii).

The thermal stability of aminocellulose (**3.2iii**) was evaluated using TGA and DSC. The thermogravimetric curves shown in **Figure 3.15** depicts two main degradation processes of aminocellulose: the first from 0 to 192°C (9 % mass loss) which is attributed to the loss of free water from the polymer, and the second from 195 to 500°C (60 % mass loss) which is due to depolymerisation or pyrolysis of the polymer. The DSC thermogram shows an endothermic peak at 62°C which suggests that the polymer is thermally less stable than C-6 oxidised C-6 tosyl cellulose (**2.3**) and degrades at a lower temperature.

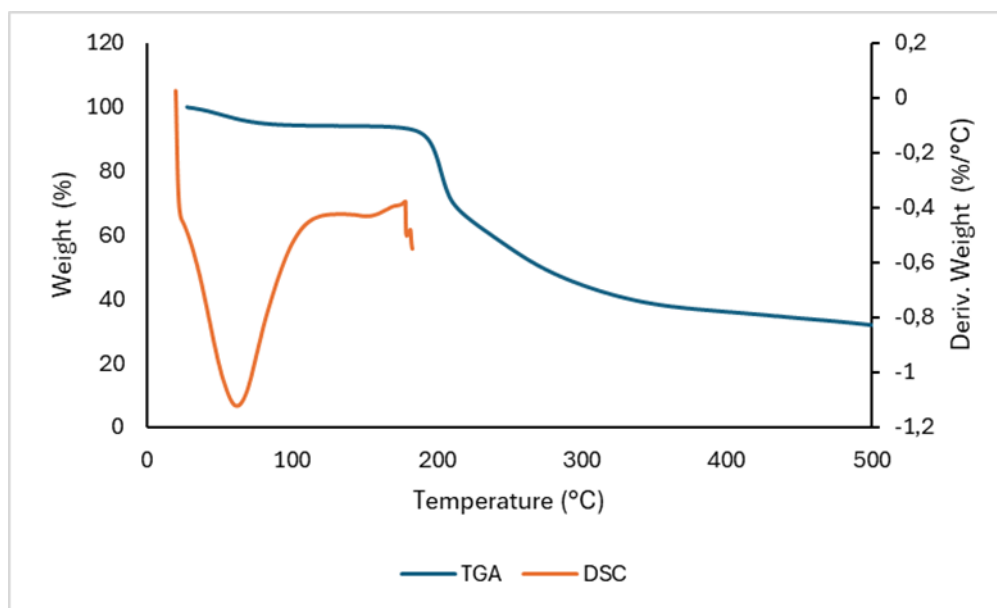


Figure 3.15. The TGA and DSC curves of aminocellulose (3.2iii).

3.3 Summary of the reductive amination of cellulose derivatives

The use of pic-BH_3 as a reducing agent was unsuccessful and did not produce aminated biopolymer as evident by a negative Kaiser ninhydrin test result. On the other hand, when NaBH_4 was used as a reductant, the biopolymers tested positive for the presence of primary amines as indicated by the dark blue colour change of the Kaiser ninhydrin test. However, the aminated celluloses obtained were insoluble in aqueous and organic solvents which limited their characterisation by liquid state NMR. Lastly, the use of NaH_2PO_2 proved successful in the reductive amination of DAC and C-6 oxidised C-6 tosyl cellulose (2.3). A positive dark blue colour change was observed for the presence of primary amines *via* the Kaiser ninhydrin test and a DS of 0.31 and 0.022 for diamino and aminocellulose, respectively, was obtained. Furthermore, except for the when the reductants pic-BH_3 and NaBH_4 were used, the aminated biopolymers produced were soluble in DMSO and characterised using NMR spectroscopy, IR spectroscopy, elemental analysis, PXRD, TGA and DSC. The use of NaH_2PO_2 as a reductant has advantages such as being eco-friendly, accessible and economically viable. Furthermore, the 12 Green Chemistry Principles of using less hazardous reagents and solvents were met by using NaH_2PO_2 as a ‘green’ reductant and a mixture of water/ethanol as solvent. This makes it the ideal reductant for large-scale synthesis of aminated celluloses from oxidised celluloses.

3.4 Applications of aminated biopolymers

Aqueous solubility is essential for most applications of cellulose, most notably biomedical applications; hence the amination of cellulose was intended to enhance its solubility in water. The aminated celluloses synthesised, namely, diaminocellulose and aminocellulose were not water soluble and therefore were dissolved in DMSO with subsequent dilution in water. In this section, the cytotoxicity of aminated celluloses against brain cancer cell lines was investigated.

3.4.1 Cytotoxicity studies of aminated celluloses

The cytotoxicity of aminated cellulose derivatives is an understudied area of research. The cytotoxicity of these materials must be evaluated as an initial step for further applications in the biomedical field. Finger *et al.* reported the effect of different degrees of substitution (DS) of 6-deoxy-6-aminoethyleneaminocellulose *via* tosylation on biocompatibility. They found that the lowest DS of 0.3 was most biocompatible with immortalised human keratinocyte (HaCaT) cells.²³ Nazir *et al.* explored the cytotoxicity of the aminated microcrystalline cellulose (MCC) derivatives, 6-deoxy-6-hydrazide cellulose (Cell Hyd), 6-deoxy-6-diethylamide cellulose (Cell DEA) and 6-deoxy-6-diethyltriamine cellulose (Cell DETA) (**Figure 3.16**) against normal fibroblasts, melanoma and breast cancer cell lines using the PrestoBlue cell viability and live/dead imaging assays. Analysis of the resultant 50% inhibitory concentration (IC₅₀) values showed that MCC was non-cytotoxic, while its derivatives were non-cytotoxic up to 200 µg/mL in non-malignant NIH3T3 cells, which proposes its safe application in a clinical setting. It was found that Cell Hyd, Cell DEA and Cell DETA displayed the greatest cytotoxic effect in mouse skin melanoma (B16F10), followed by human breast adenocarcinoma (MCF-7). The authors suggested that aminated cellulose derivatives have potential for applications of tissue engineering and cancer inhibition studies.²⁴

The literature reports the bioactivity of 6-deoxy-6-aminoalkylaminocelluloses but there has been no reported research on the bioactivity of 6-deoxy-6-aminocellulose. This motivated the further investigation of the cytotoxicity of aminated cellulose on cell lines for use in biomedical applications. Glioblastoma multiforme (GBM) is the most commonly occurring form of brain cancer and is also the most aggressive and lethal with less than 1 % of patients living longer than ten years.^{25, 26} The human malignant glioblastoma cell lines U251 and U87 were used for cytotoxicity evaluation of aminated celluloses with the aim of conjugation of drugs against brain cancer as post-surgical implants. The cytotoxicity of diamino and aminocellulose against U251 and U87 was evaluated using the MTT (3-(4,5-dimethylthiazolyl-2)-2,5-diphenyltetrazolium bromide) cell viability assay. The aminated celluloses were dissolved in DMSO to make stock solutions of 5 mg/mL, which were further diluted with water to a final concentration of 0.05 mg/mL. Cells were grown for a period of 24 h at a density of 4500 cells (U251) and 5500 cells (U87) per well in sterile 96-well plates and thereafter exposed to 0.05 mg/mL of polymer. A non-treated control of 0 mg/mL polymer in the equivalent amount of DMSO served as a control. The results are shown in **Figures 3.17 and 3.18**. The percentage survival of diaminocellulose (**3.1iii**) and aminocellulose (**3.2iii**) treated cells was found to be 97.4% and 98.4% against the U251 cell lines; and 97.9 % and 97.6 %, against the U87 cell lines, respectively. These results were validated using phase contrast light microscopy, shown in **Figures 3.19 and 3.20**. These images depict no significant cell death relative to the DMSO control. Therefore, it can be concluded that the aminated celluloses do not have any inherent anticancer activity. However, these aminated celluloses may be suitable for drug conjugation and stimuli triggered delivery. It is of note that the concentration of polymer used was significantly lower than the commonly used 5 mg/mL due to the poor solubility of the biopolymers. This could be a possible reason for the non-cytotoxicity observed. Higher DS of aminocellulose may be more water soluble and comparable in activity as observed with Cell DEA and Cell DETA.²⁴

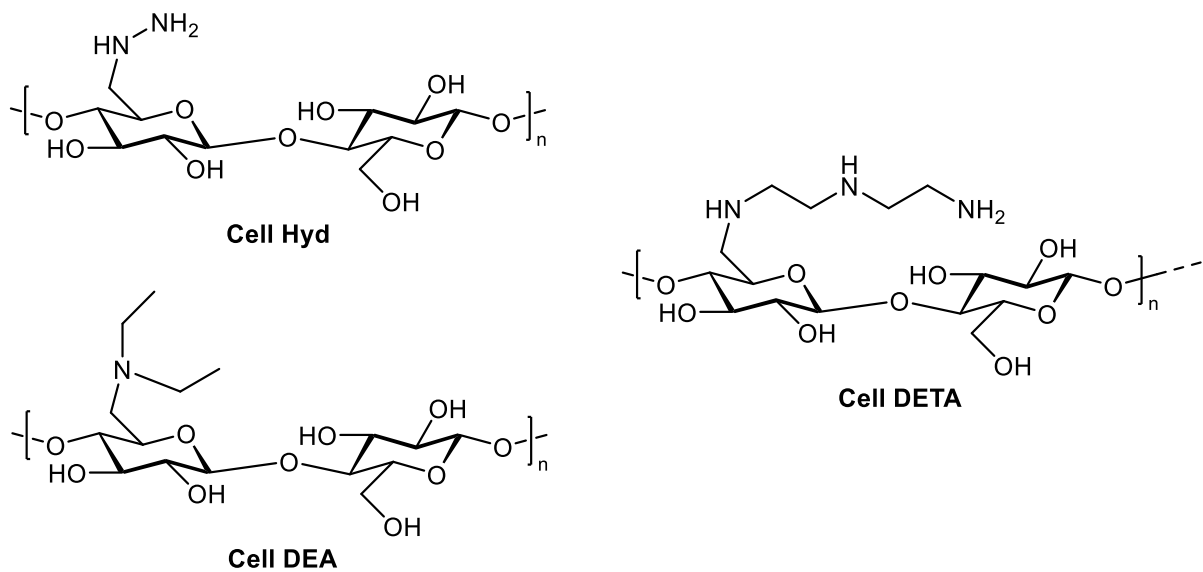


Figure 3.16. Structures of 6-deoxy-6-hydrazide Cellulose (Cell Hyd), 6-deoxy-6-diethylamide cellulose (Cell DEA) and 6-deoxy-6-diethyltriamine cellulose (Cell DETA).²⁴

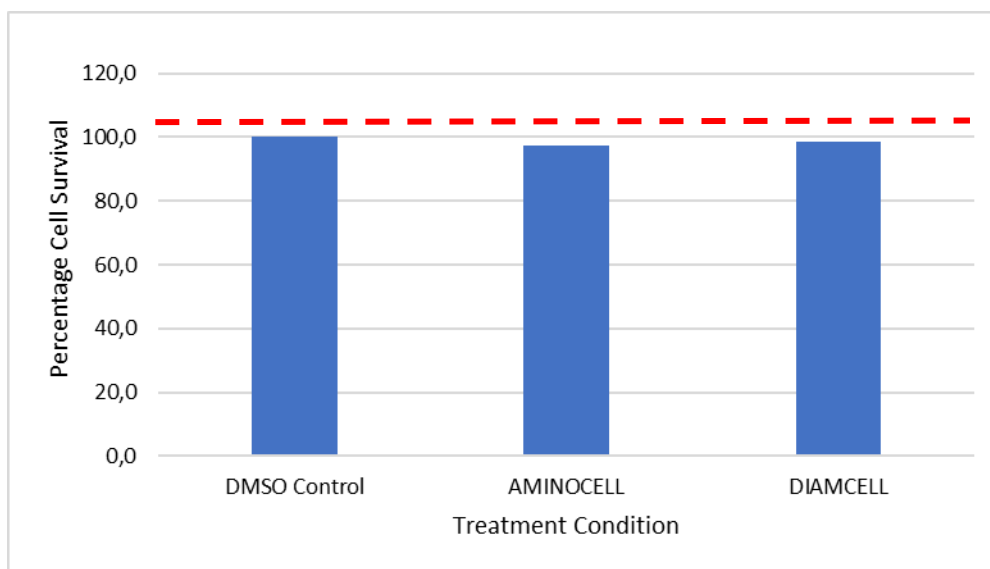


Figure 3.17. Cell culture evaluating the Percentage Cell Survival of aminocellulose and diaminocellulose against U251 cell lines.

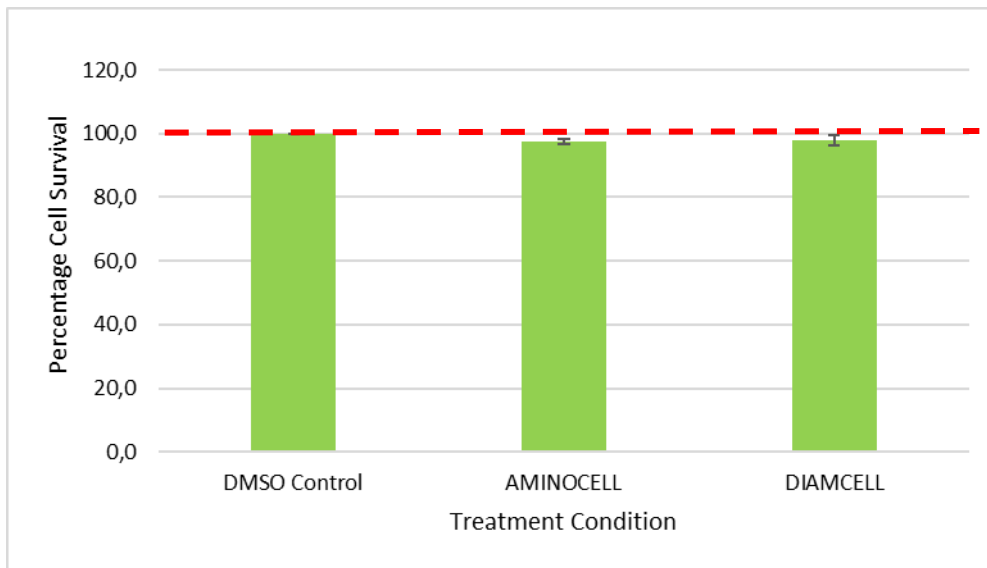


Figure 3.18. Cell culture evaluating the Percentage Cell Survival of aminocellulose and diaminocellulose against U87 cell lines.

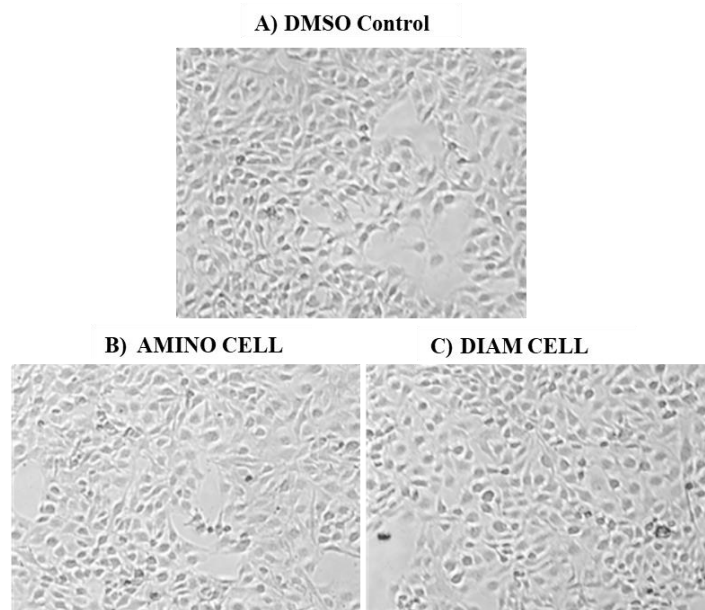


Figure 3.19. Phase contrast light microscopy images of A) DMSO control, B) aminocellulose and C) diaminocellulose after treatment with U251 cell lines.

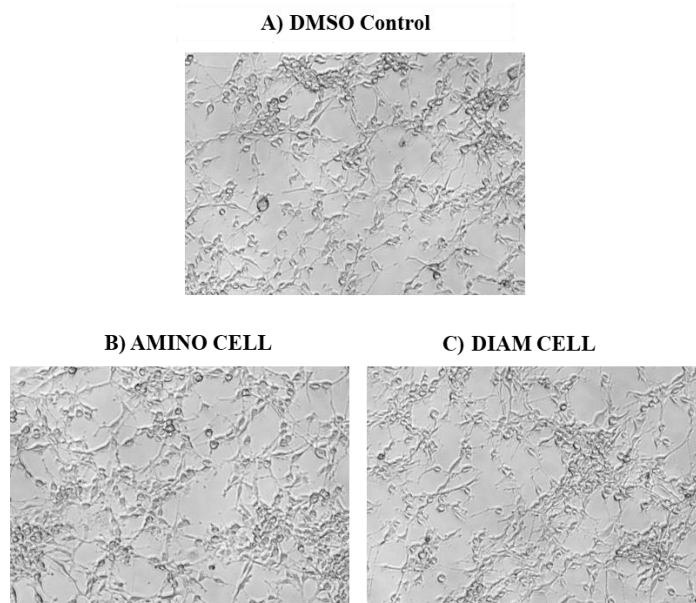


Figure 3.20. Phase contrast light microscopy images of A) DMSO control, B) aminocellulose and C) diaminocellulose after treatment with U87 cell lines.

3.5 Conclusion

This chapter investigated the use of different reductants for the synthesis of diamino and aminocellulose, as summarised in **Section 3.4**. Sodium hypophosphite was found to be the ideal reductant as it produced DMSO-soluble aminated celluloses while being green and cost-effective. The cytotoxicity of aminated celluloses against brain cancer cell lines was investigated. The cytotoxicity studies showed that the aminated celluloses at a relatively low concentration do not have any inherent anticancer activity and however, could be suitable for drug conjugation and delivery.

3.6 References

1. A. Jardine, *Current Research in Green and Sustainable Chemistry*, 2022, **5**, 100309.
2. K. Rahn, M. Diamantoglou, D. Klemm, H. Berghmans and T. Heinze, *Die Angewandte Makromolekulare Chemie: Applied Macromolecular Chemistry and Physics*, 1996, **238**, 143-163.
3. K.-i. Furuhata, K. Koganei, H.-S. Chang, N. Aoki and M. Sakamoto, *Carbohydrate research*, 1992, **230**, 165-177.
4. K.-i. Furuhata, H.-S. Chang, N. Aoki and M. Sakamoto, *Carbohydrate research*, 1992, **230**, 151-164.
5. T. Satoh, H. Kano, M. Nakatani, N. Sakairi, S. Shinkai and T. Nagasaki, *Carbohydrate research*, 2006, **341**, 2406-2413.
6. J. Haskins and A. Weinstein, *The Journal of Organic Chemistry*, 1954, **19**, 67-69.
7. P. Berlin, D. Klemm, A. Jung, H. Liebegott, R. Rieseler and J. Tiller, *Cellulose*, 2003, **10**, 343-367.
8. A. Jardine and S. Sayed, *Pure and Applied Chemistry*, 2018, **90**, 293-304.
9. P. Anastas and N. Eghbali, *Chemical Society Reviews*, 2010, **39**, 301-312.
10. B. Lu, X. Liu, Z. Huang, H. Xu, P. Xu, Y. Wang, H. Zheng, Y. Yin, X. Zhang and R. Zhuo, *Carbohydrate polymers*, 2012, **87**, 1453-1459.
11. S. Tsuchida, R. Takahashi, K. Yabe, N. Hamaue and T. Aoki, *Cellulose*, 2022, **29**, 3025-3033.
12. J. Simon, L. Fliri, J. Sapkota, M. Ristolainen, S. A. Miller, M. Hummel, T. Rosenau and A. Potthast, *Biomacromolecules*, 2022, **24**, 166-177.
13. R. Koshani, J. Zhang, T. G. van de Ven, X. Lu and Y. Wang, *ACS Sustainable Chemistry & Engineering*, 2021, **9**, 10513-10523.
14. T. Hosoya, M. Bacher, A. Potthast, T. Elder and T. Rosenau, *Cellulose*, 2018, **25**, 3797-3814.
15. A. Potthast, S. Schiehser, T. Rosenau and M. Kostic, *Holzforschung*, 2009, **63**, 25-29.
16. L. Münster, J. Vícha, J. Kľofáč, M. Masař, P. Kucharczyk and I. Kuřitka, *Cellulose*, 2017, **24**, 2753-2766.
17. J. Simon, L. Fliri, F. Fröhlich, J. Sapkota, M. Ristolainen, M. Hummel, T. Rosenau and A. Potthast, *Cellulose*, 2023, **30**, 8205-8220.
18. F. Kliuev, A. Kuznetsov, O. I. Afanasyev, S. A. Runikhina, E. Kuchuk, E. Podyacheva, A. A. Tsygankov and D. Chusov, *Organic Letters*, 2022, **24**, 7717-7721.
19. A. Codou, N. Guigo, L. Heux and N. Sbirrazzuoli, *Composites Science and technology*, 2015, **117**, 54-61.
20. A. Varma, V. Chavan, P. Rajmohan and S. Ganapathy, *Polymer degradation and stability*, 1997, **58**, 257-260.
21. T. S. Anirudhan, J. Nima and P. L. Divya, *Applied Surface Science*, 2015, **355**, 64-73.
22. J. A. Sirviö, M. Visanko, O. Laitinen, A. Ämmälä and H. Liimatainen, *Carbohydrate polymers*, 2016, **136**, 581-587.
23. S. Finger, M. Zieger, C. Wiegand, T. Liebert, T. Heinze, P. Elsner and U.-C. Hipler, *Journal of Biosciences and Medicines*, 2017, **6**, 51-62.
24. F. Nazir and M. Iqbal, *Polymers*, 2020, **12**, 2634.
25. Glioblastoma Multiforme (GBM), [https://braintumourresearch.org/pages/types-of-brain-tumours-glioblastoma-multiforme-gbm#:~:text=Glioblastoma%20multiforme%20\(GBM\)%20is%20the,of%20cases%2C%20it%20is%20fatal.](https://braintumourresearch.org/pages/types-of-brain-tumours-glioblastoma-multiforme-gbm#:~:text=Glioblastoma%20multiforme%20(GBM)%20is%20the,of%20cases%2C%20it%20is%20fatal.), (accessed 20 April 2024).

26. World Health Organization,
<https://gco.iarc.who.int/today/en/dataviz/bars?mode=population>, (accessed 24 April, 2024).

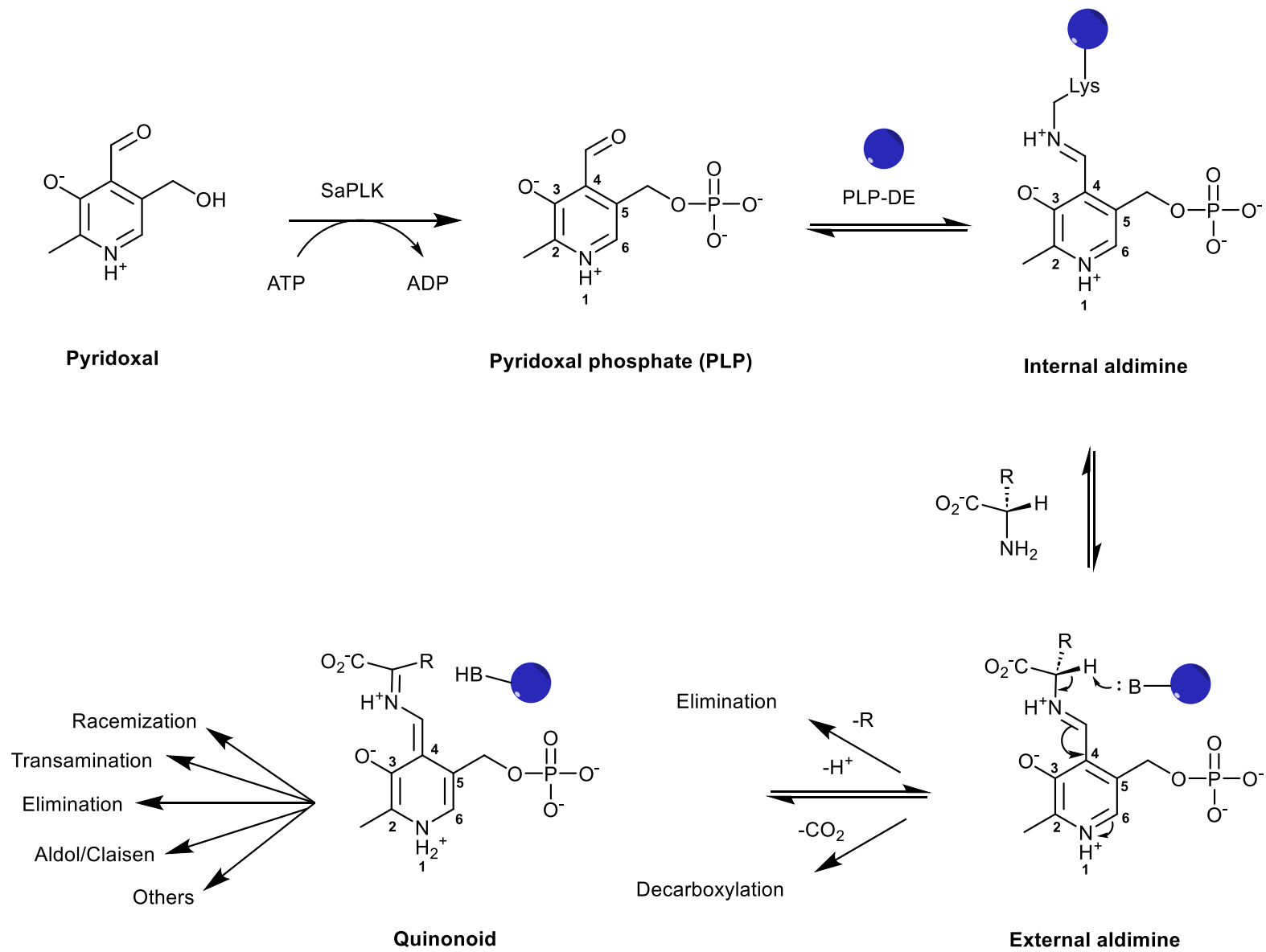
Chapter 4: Immobilisation of Pyridoxal on Aminated Biopolymer Solid Supports for Biomimetic Applications

4.1 Literature Review

Pyridoxal phosphate dependent enzymes

Pyridoxal-5-phosphate (PLP) is the metabolically active form of Vitamin B₆, first discovered by Snell *et al.* in 1942.¹ PLP is a multifaceted enzyme cofactor that catalyses diverse chemical reactions of biological amino acids.^{2,3} Almost 4 % of all enzyme activities utilises PLP as a cofactor.^{4,5} PLP-dependent enzymes (PLP-DEs) account for a family of biocatalysts that are omnipresent and are extensively involved in essential cellular processes such as amino acid, lipid as well as glucose metabolism.⁶ PLP-DEs catalyse a broad variety of chemical reactions such as transaminations, decarboxylations, transaldolations, Claisen condensations, racemisations, α , β , γ -eliminations and substitutions as well as oxidative deaminations in the presence of amino acids.^{4,7} In spite of this great diversity of chemical reactions, PLP-DEs function through common mechanistic principles.^{6,8}

Scheme 4.1 depicts the mechanism of action for PLP-DEs in chemical reactions. Pyridoxal is phosphorylated by cellular pyridoxal kinase (PLK); PLP subsequently binds PLP-DEs at the active-site lysine residues *via* an internal aldimine. The external aldimine forms by means of transamination with substrate amine. This enables diverse chemical reactions *via* select quinoid formation. PLP behaves as an electrophilic catalyst to stabilise negative charge at C _{α} by delocalisation in an extended conjugated system and through the electronic stabilisation effects of the Schiff base and protonated pyridine. PLP has great chemical specificity due to its chemical properties and the surrounding protein matrix interplaying through hydrogen bonding and stereoelectronic effects.⁶



Scheme 4.1. Mechanism of action for Pyridoxal-Dependent Enzymes in chemical reactions.⁶

PLP-DEs are acknowledged as important drug targets in human disease because of its extensive involvement in principle metabolic processes.^{6, 9} An example of PLP-DEs for which clinical drugs have been developed are DOPA decarboxylase (Parkinson's), serine hydroxymethyltransferase (tumours, malaria) and GABA aminotransferase (epilepsy) amongst others.^{6, 10} However, application of PLP-DEs in drug therapy often have side effects of off-target reactivity, which is a common challenge in creating PLP-DEs inhibitors. Research effort focussing on the identification and functional classification are needed to overcome this challenge. Hoegl *et al.* introduced a chemo-proteomic platform for the universal identification and characterisation of PLP-DEs in living cells using functionalised pyridoxal cofactor mimics. These functionalised pyridoxal cofactor mimics were designed to be integrated into cellular pyridoxal uptake mechanisms and metabolic processing to access the entire complement of PLP-DEs in *Staphylococcus aureus*.⁶

PLP can catalyse reactions independently of enzymes. Amino acids may undergo reactions of decarboxylations, transaminations and α,β – substitutions in a non-enzymatic manner in aqueous solutions using PLP and multivalent metal ions as catalysts.¹¹⁻¹⁸ There have been reports of these reactions proceeding without the aid of metal ions, however, at a much slower rate.^{4, 19} An example is the slow formation of pyridoxamine when PLP in the absence of enzymes experiences transamination when heated with amino acids.^{4, 11} A study conducted by Mulay *et al.* demonstrates that the breakdown of cysteine catalysed by PLP occurs independently of enzymes, multivalent metal ions and base to produce H₂S.⁴

Pyridoxal immobilisation

PLP has previously been immobilised onto agarose as a solid support for affinity chromatography of enzymes that utilise PLP as a co-factor. Linkage to the co-factor has been through the aldehyde functional group, but this is disadvantageous for enzyme mimicry as the pyridoxal aldehyde moiety is required for reactivity.²⁰ More recently, C-6 immobilised PLP onto *p*-diazobenzoyl-derivatised SepharoseTM 4B (**Figure 4.1**) was synthesised by using *N*-hydroxysuccinimide (NHS) ester chemistry. This method of C-6 immobilisation of PLP avoids the use of hazardous azide reagents.²¹

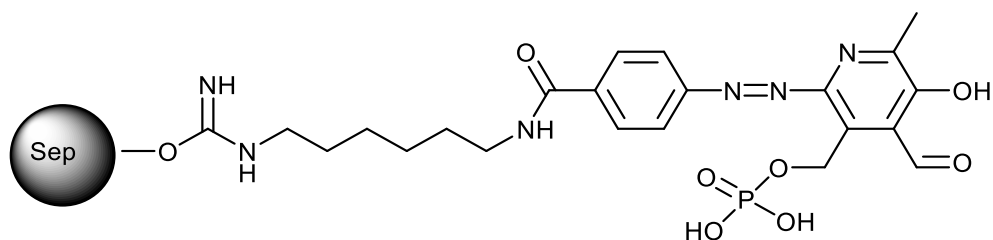


Figure 4.1. C-6 immobilised PLP to *p*-diazobenzoyl derivatised Sepharose™ 4B.²¹

The use of PLP is limited as a single enzyme is specific for a type of reaction, hence PLP cannot be reused in different types of reactions.⁸ The immobilisation of pyridoxal onto solid supports is an attractive strategy to overcome the reusability and recyclability issues of PLP caused by reaction specificity. Ikeda *et al.* demonstrated that the position of immobilisation of PLP is important for it to perform its catalytic activities. They prepared *N*-immobilised (**Figure 4.2A**) and 3-*O*-immobilised pyridoxal analogues (**Figure 4.2B**) by the use of a bromoacetyl derivative of Sepharose™ and evaluated their catalytic activities in the enzyme-independent cleavage reaction of tryptophan.²² The *N*-methyl derivative of pyridoxal exhibits the same catalytic activity as pyridoxal in non-enzymatic vitamin B₆ model reactions whereas the 3-*O*-methyl derivative of pyridoxal shows no activity because the aldehyde moiety of pyridoxal needs to be free and accessible for pyridoxal to behave as an ‘enzyme mimic’.²² This information was used to corroborate the structure of the immobilised pyridoxal products by evaluating the catalytic activities in the non-enzymatic tryptophan cleavage reaction. The *N*-immobilised pyridoxal analogue displayed catalytic activity comparable to free pyridoxal. However, the 3-*O*-immobilised pyridoxal analogue did not show any significant catalytic activity due to the 3-OH group of PLP being blocked. The authors previously synthesised 6-immobilised pyridoxal by coupling a diazotized derivative of Sepharose™ and evaluated the affinities of these analogues for apotryptophanase. The 6-immobilised pyridoxal analogue (**Figure 4.2C**) was observed to be the most useful for the immobilisation of apotryptophanase and the *N*-immobilised pyridoxal analogue was better than the 3-*O*-immobilised analogue. This is due to the 6-immobilised analogue having all the necessary functional groups of PLP free for catalytic activity and binding to apoenzyme whereas the *N*-immobilised analogue has a decreased affinity for apoprotein due to the alkylation at the pyridine nitrogen. The 3-*O*-immobilised analogue has the main PLP groups needed for the binding of apoprotein but the 3-OH group of PLP is blocked and hence cannot partake in catalytic activity.²²

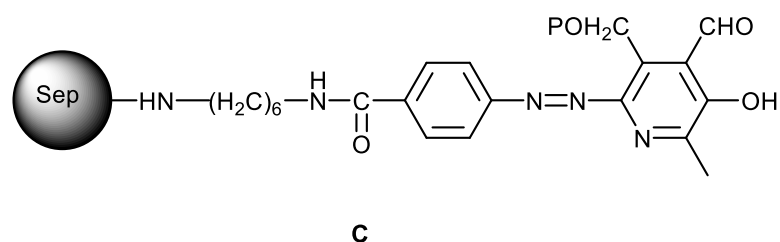
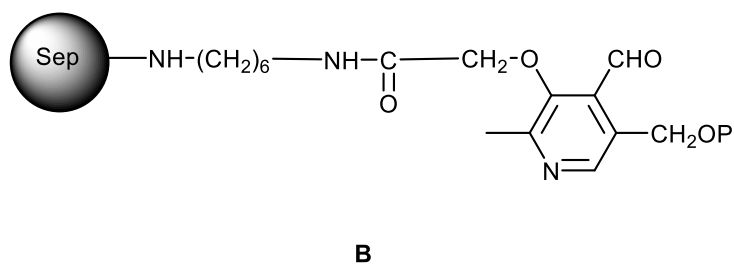
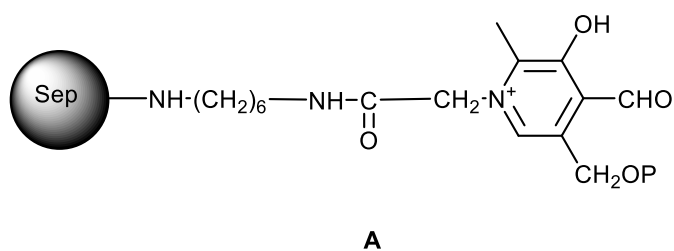
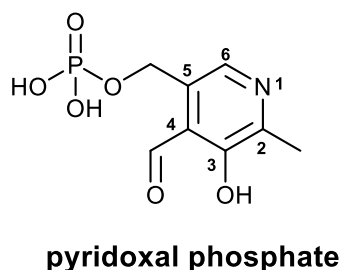


Figure 4.2. Structures of three types of immobilised PLP analogues (Sepharose™-bound PLP analogues). (A) *N*-immobilised Sepharose™-bound PLP; (B) 3-*O*-immobilised Sepharose™-bound PLP; (C) 6-immobilised Sepharose™-bound PLP.²²

A self-sufficient catalyst is a biocatalyst based on co-immobilisation of enzyme and its cofactor. The benefit of using a self-sufficient catalyst is that it is regarded as an *in situ* method to regenerate and reutilise cofactors. There are two approaches for the synthesis of self-sufficient biocatalysts, namely covalent or non-covalent immobilisation.²³

Non-covalent immobilisation of self-sufficient biocatalysts for the synthesis of chiral amines using PLP-dependent transaminases has been investigated by many researchers. Andrade *et al.* immobilised *E.coli* cells containing overexpressed (*R*)-selective ω -transaminase and the cofactor PLP onto methacrylate beads to synthesise chiral amines by asymmetric amination of non-natural ketones.²⁴ The advantages of using this system were that the non-natural ketones were transformed in flow with exceptional enantioselectivity, the production was clean, the enzyme stability high and the mass recovery great.²⁴ Transaminases and PLP were co-

immobilised on agarose microbeads activated with polyethyleneimine based on ion adsorption by Velasco-Lozano *et al.*²⁵ The biocatalyst catalysed the synthesis of *rac*-1-phenylethan-1-amine through (S)-selective deamination and was reused for four cycles.²⁵ There were many disadvantages in these reported non-covalent immobilised catalysts: complex preparation procedures, restricted reusability, high preparation cost, and low industrial scalability potential.²³

Alternative to non-covalent immobilisation, where there are weak ionic interactions between the enzyme/cofactor and the solid support, is covalent immobilisation technology which uses stable and strong binding of enzyme/cofactor to carriers which results in the biocatalyst having long-term stability, the ability to withstand environmental conditions, and great *in situ* cofactor regeneration.²⁶ These advantages of covalent immobilisation all arise due to the covalent bonds which securely stabilise the protein structure, prevent leaching of the protein and cofactor, as well as localise the enzyme and cofactor for efficient catalysis.²⁶ Zhang *et al.* constructed a self-sufficient biocatalyst based on covalent co-immobilisation of transaminase and PLP which was utilised in the biosynthesis of sitagliptin.²⁶ This self-sufficient biocatalyst displayed high activity and stability, and had low operation costs; and synthesised sitagliptin without extra coenzyme addition as well as with high optical purity and great space-time yield.²⁶

Both these methods have drawbacks such as complex preparation methods, expensive materials and environmentally unfriendly processes. The need therefore arises to find efficient yet inexpensive and eco-friendly material to immobilise cofactor/enzyme to form a self-sufficient catalyst.²⁷ Wei *et al.* co-immobilised PLP and L-lysine decarboxylase using chitin as the solid support to form a self-sufficient biocatalyst which was reusable for up to five cycles without decreasing in activity. The DDA of chitin was regulated to 36 % for optimal PLP adsorption and immobilisation. The self-sufficient biocatalyst retained 55 % of its activity for up to five cycles. The preparation of the self-sufficient biocatalyst using chitin as a solid support is shown in **Figure 4.3**.

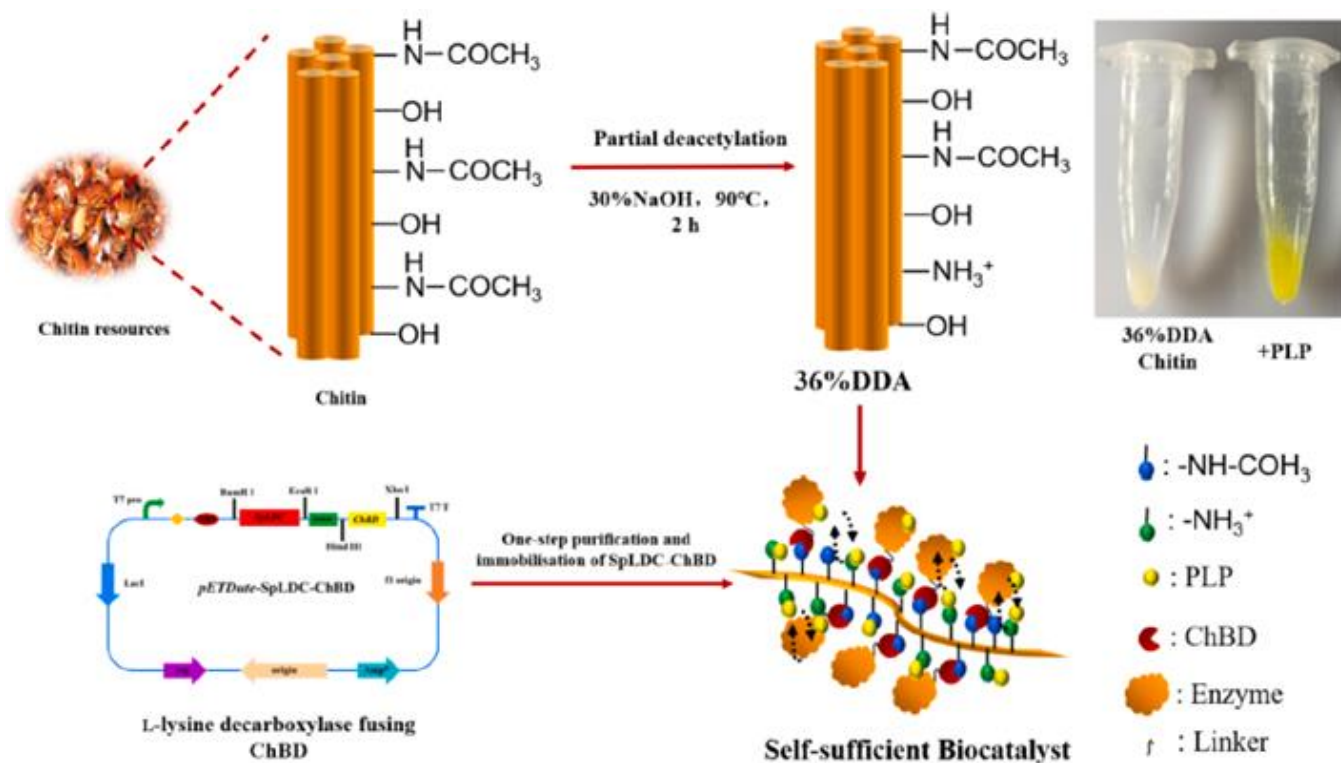


Figure 4.3. Preparation process of self-sufficient biocatalyst.²⁷

The use of chitinous biomass as solid supports for the immobilisation of biocatalysts is an under researched area of study. To the best of our knowledge, there are no reported literature on the immobilisation of PLP on the solid support chitosan. The synthesis of PLP immobilised chitosan biocatalysts stems from the success of the biocatalyst of co-immobilised PLP and L-lysine decarboxylase using chitin as the solid support by Wei *et al.*²⁷ The use of chitosan derivatives as solid supports for non-enzymatic PLP mediated bond cleavage could potentially provide a more environmentally-friendly, cost-effective, recyclable and reusable approach as a biocatalyst with application in PLP mediated deamination of amino acids to α -keto acids.

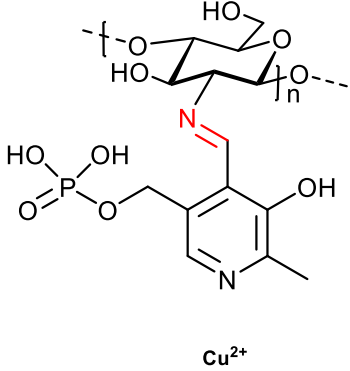
In this chapter, the use of amino-functionalised biopolymers as solid supports for the immobilisation of PLP is explored. A point of interest is whether these immobilised pyridoxal products could behave as an enzyme mimic in the deamination reaction to produce α -keto acids. Moreover, the method of immobilisation, either covalent or ionic bonding between PLP and the biopolymer, and its influence on deamination reactions is of great importance.

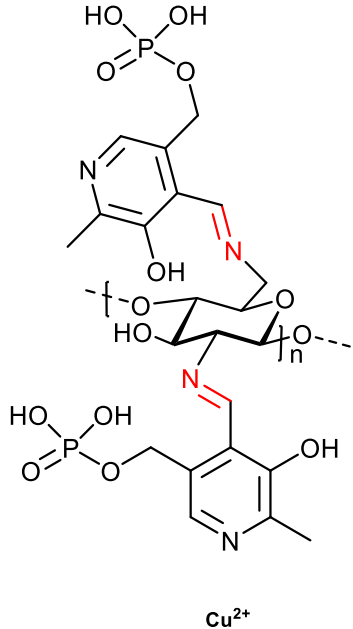
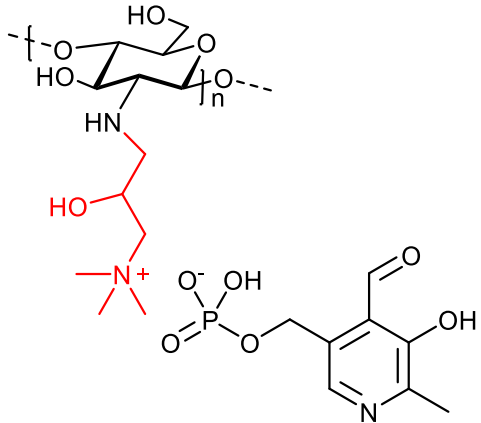
4.2 Results and Discussion

4.2.1 Background on the ionic immobilisation of pyridoxal phosphate

Amino-functionalised biopolymers display enhanced properties of solubility and biocompatibility.²⁸ The improved aqueous solubility of amino-functionalised biopolymers, such as 6-deoxy-6-amino chitosan, permits its use in applications of enzyme immobilisation. Previous reports have synthesised immobilised PLP on 6-deoxy-6-aminochitosan through the covalent formation of a Schiff base, as shown in **Table 4.1**. However, these immobilised biocatalysts lost activity over time due to leaching of pyridoxal, possibly due to the cleavage of the imine bond binding PLP to the biopolymer.²⁹

Table 4.1: Table showing the Structure of Immobilised Products of PLP on Biopolymer by Sayed *et al.* and their respective limitations.²⁹

Structure	Limitations
 <p style="text-align: center;">Cu^{2+} Chitosan – PLP – Cu</p>	<ul style="list-style-type: none">• Yield of 21 % vs 11 % of polymer free reaction.• Aldehyde group of PLP is not available for use in enzyme mimics.

 <p style="text-align: center;">Cu²⁺</p> <p style="text-align: center;">6-Deoxy-6-amino chitosan – PLP Schiff base</p>	<ul style="list-style-type: none"> • Yield of 24 % vs 11 % of polymer free reaction. • Can be recycled and reused twice. • Aldehyde group of PLP is not available for use in enzyme mimics.
 <p style="text-align: center;">Q188-PLP</p>	<ul style="list-style-type: none"> • Yield of 29 % vs 11 % of polymer free reaction.

Herein, alternative methods of immobilisation are explored to overcome this challenge. Firstly, immobilisation *via* ionic bonding was studied as ionic bonds are strong and stable. There are, however, limitations of ionic bond formation such as its dependence on the electronegativity difference between ions influencing bond formation and bond strength.

A review by Schnackerz *et al.* highlights how useful ³¹P-NMR spectroscopy is to understand the microenvironment around the phosphate group of enzyme-bound PLP which is key in understanding its mechanistic principles. PLP-dependent enzymes, e.g. cytosolic aspartate aminotransferase and dialkylglycine decarboxylase, all bind in a similar manner at the 5-phosphate binding site. A series of glycine residues of the respective protein surrounds the

phosphate group of bound PLP; hydrogen bonding between the oxygen atoms of the phosphate group and the backbone atoms of the glycine residues occurs, resulting in the phosphate groups being tightly bound which serves as an anchor of the cofactor along with the Schiff base linkage.³⁰

To demonstrate the general binding of PLP in the enzyme active site, the PLP-binding site of tryptophanase is shown in **Figure 4.4**. The internal Schiff base between PLP and K266, and the 5'-phosphate binding site and the K⁺- binding site are depicted. There are six hydrogen bonds to the 5'-phosphate (orange) donated by enzyme side chains or backbone NHs and two of the hydrogen bonds are donated by R101. The K⁺ ion is coordinated with three of the coordination bonds donated by H₂O molecules, in an octahedral manner. Yellow (subunit A) or green (subunit B) are coded for the side chains; and O is red while N is blue.³⁰

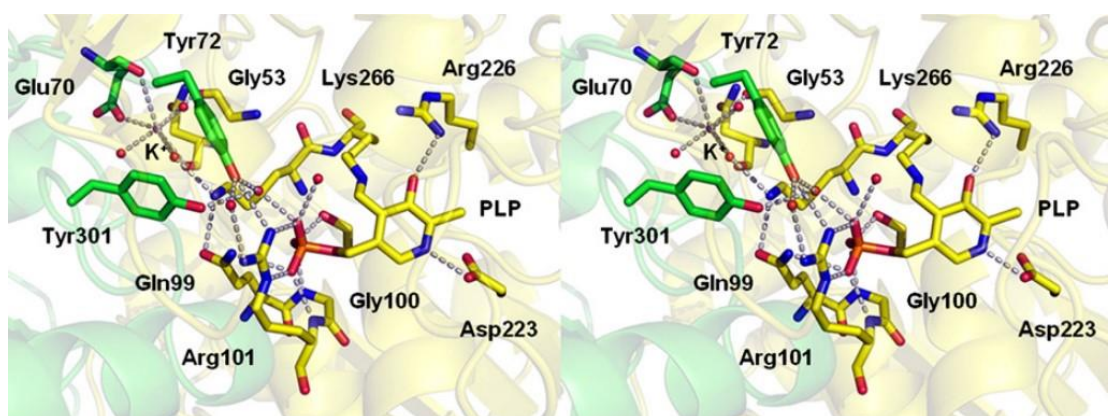


Figure 4.4. Stereoview of the active site of tryptophanase.³⁰

In comparison, the Q188-PLP complex (3-trimethylammonium-2-hydroxypropyl-*N*-chitosan chloride-PLP complex) is anchored into the highly positively charged quaternary ammonium residue complexed to the negatively charged phosphate group of PLP. The aldehyde group of PLP is free to react with the amino acid amine functional group.⁸ The extended linker of Q188-PLP creates a notable distance between the bulky polymer and PLP, hence allows PLP to easily bind to the -NH₂ of the amino acid.

The question arises whether the Q188-PLP complex is well-bound and stable for application of enzyme-independent deamination reactions; and if its activity is comparable to that of covalently bound PLP-dependent enzymes.

4.2.2 Synthesis of an ionic PLP complex

Ionic complex of PLP and 3-trimethylammonium-2-hydroxypropyl-*N*-chitosan

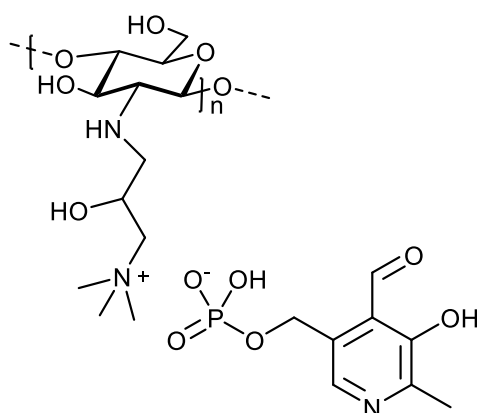
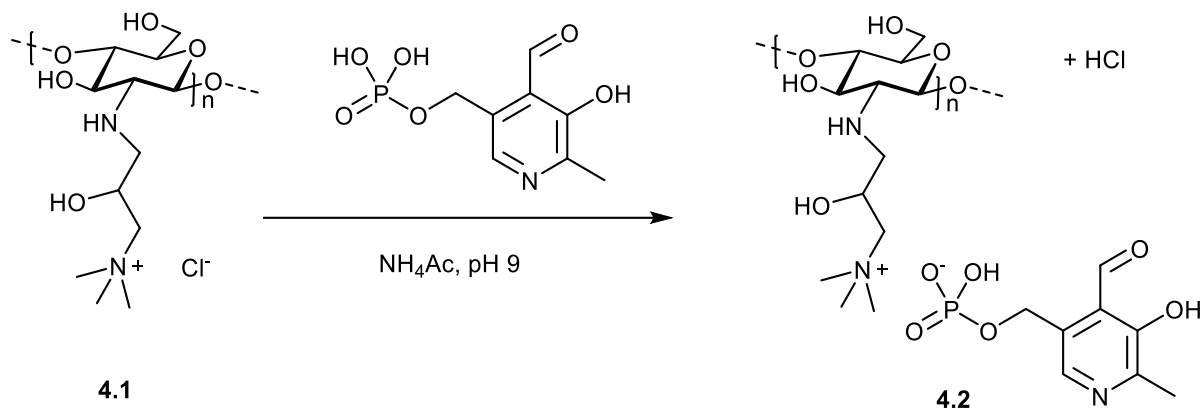


Figure 4.5. Structure of the 3-trimethylammonium-2-hydroxypropyl-*N*-chitosan chloride-PLP complex (**4.2**).

PLP is anchored to enzyme structures by the ionic complexation of its phosphate group.³¹ In this study, a quaternary trimethyl ammonium chitosan derivative was used as an anchor for PLP. The ionic complex was formed *via* ionic bonding whereby the positively charged amine of 3-trimethylammonium-2-hydroxypropyl-*N*-chitosan chloride (Q188) (**4.1**) and the negatively charged phosphate group of PLP interact (**Figure 4.5**).

Quaternary derivatives of chitosan evidently display enhanced properties with an increase in solubility due to the presence of the quarternised nitrogen.³² Therefore, Q188 was used to form an ionic complex with PLP due to its enhanced properties of aqueous solubility as well as its extended linker which allows ease in accessibility of PLP to the site of its amino acid deamination application.³² Q188 (**4.1**) was previously synthesised by Sayed *et al.* by reacting chitosan with glycidyl trimethylammonium chloride.³² Q188 was allowed to stir with excess PLP overnight at 25 °C and subsequently dialysed against water to expel any free PLP. A complex (**4.2**) was formed between PLP and Q188 due to the ionic interaction between the negative phosphate group of PLP and the positive quaternary nitrogen of Q188, with an exchange of the PO_4^- and Cl^- groups as shown in **Scheme 4.2**.



Scheme 4.2. Formation of the complex between 3-trimethylammonium-2-hydroxypropyl-*N*-chitosan (**4.1**) and PLP (Q188-PLP) (**4.2**).

The polymer was recovered as an orange solid with a moderate yield of 52 % and a DS of 1, which was poorly soluble because of the complexation.

The IR spectrum identifies the key functionalities of **Q188-PLP (4.2)** (**Figure 4.6**). There are signals for the C=C – CH₃, P=O, P-OH and P-O-C groups of PLP, as well as the C-H bending of the trimethyl ammonium group of Q188 present. There is a weakening of intensity of the absorption bands for Q188-PLP compared to Q188, which implies complexation to PLP.

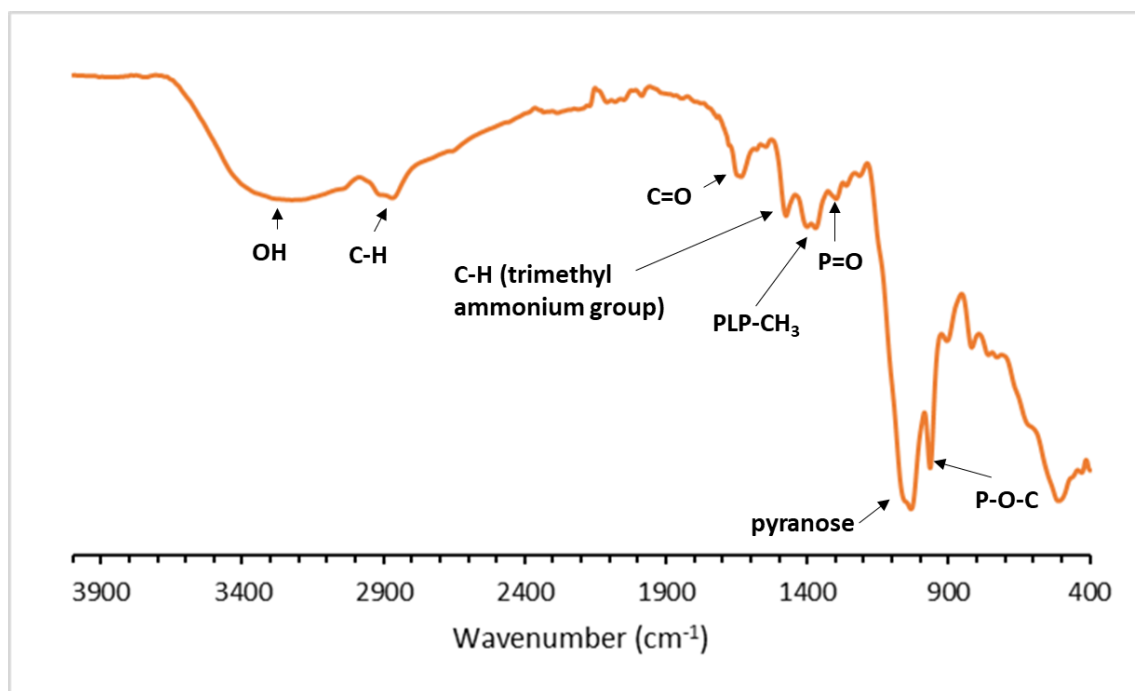


Figure 4.6. IR spectrum of 3-trimethylammonium-2-hydroxypropyl-*N*-chitosan-PLP complex (**Q188-PLP (4.2)**).

A $^1\text{H-NMR}$ spectrum was obtained by lowering the pH of the solution with DCl acid. The $^1\text{H-NMR}$ spectrum shown in **Figure 4.7** confirms the successful synthesis of **4.2** as the signals assigned to the polymer and PLP are all evident. The characteristic polymer signals for Q188, namely, CH-OH , $\text{CH}_2\text{-N}^+$ and $\text{N}^+(\text{CH}_3)_3$, assigned H-8, H-9 and H-10, are present upfield in the spectrum at δ 4.29 ppm, δ 3.53 ppm and δ 3.20 ppm, respectively in agreement with literature.³² The signals assigned to PLP show a slight upfield shift relative to free PLP, where the aldehyde proton H-d occurs at δ 10.10 ppm, the aromatic proton assigned H-b at δ 7.84 ppm, and the CH_2 – group of PLP, H-a, at δ 6.14 ppm. The two overlapping signals at δ 2.38 and 2.26 ppm are due to the residual chitosan NAc and H-c respectively. The ratio of signals H-a: H-8 (1:2) suggests that at least half of the quaternary sites of Q188 complexed with PLP.

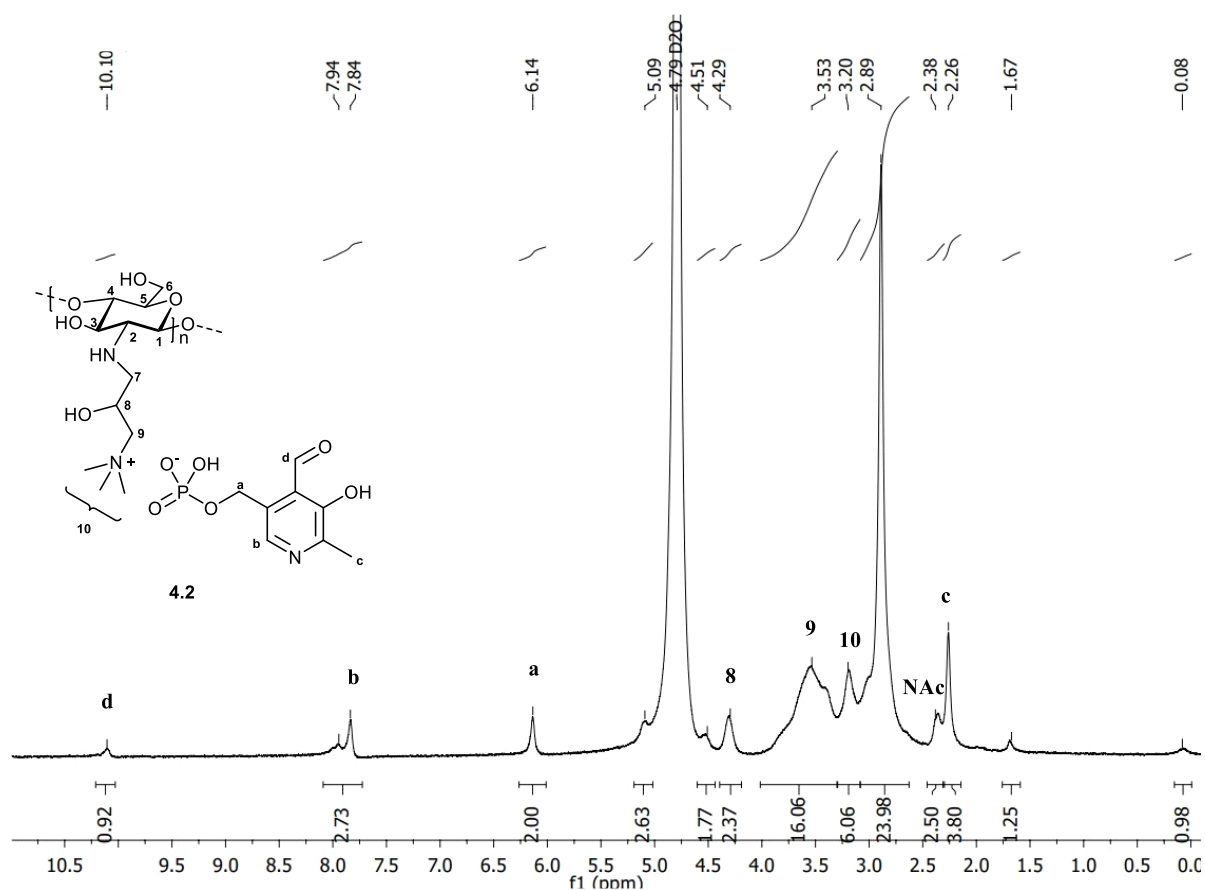


Figure 4.7. $^1\text{H-NMR}$ spectrum of 3-trimethylammonium-2-hydroxypropyl-*N*-chitosan-PLP complex (**4.2**) in 2 % DCl/D₂O.

The ^{31}P NMR spectrum of the polymer (**Figure 4.8**) displays two signals at -0.18 and -0.80 ppm compared to free PLP which displays two signals at -0.61 and -1.39 ppm at the same pH of 1.²⁹ PLP exists in two forms in acidic aqueous medium (**Scheme 4.3**). The upfield shift in the spectrum relative to free PLP indicates that PLP is in a different environment and hence implies complexation with Q188. This is further corroborated by the broad, shouldered signal at -0.80 ppm which is indicative of immobilisation to a solid support.

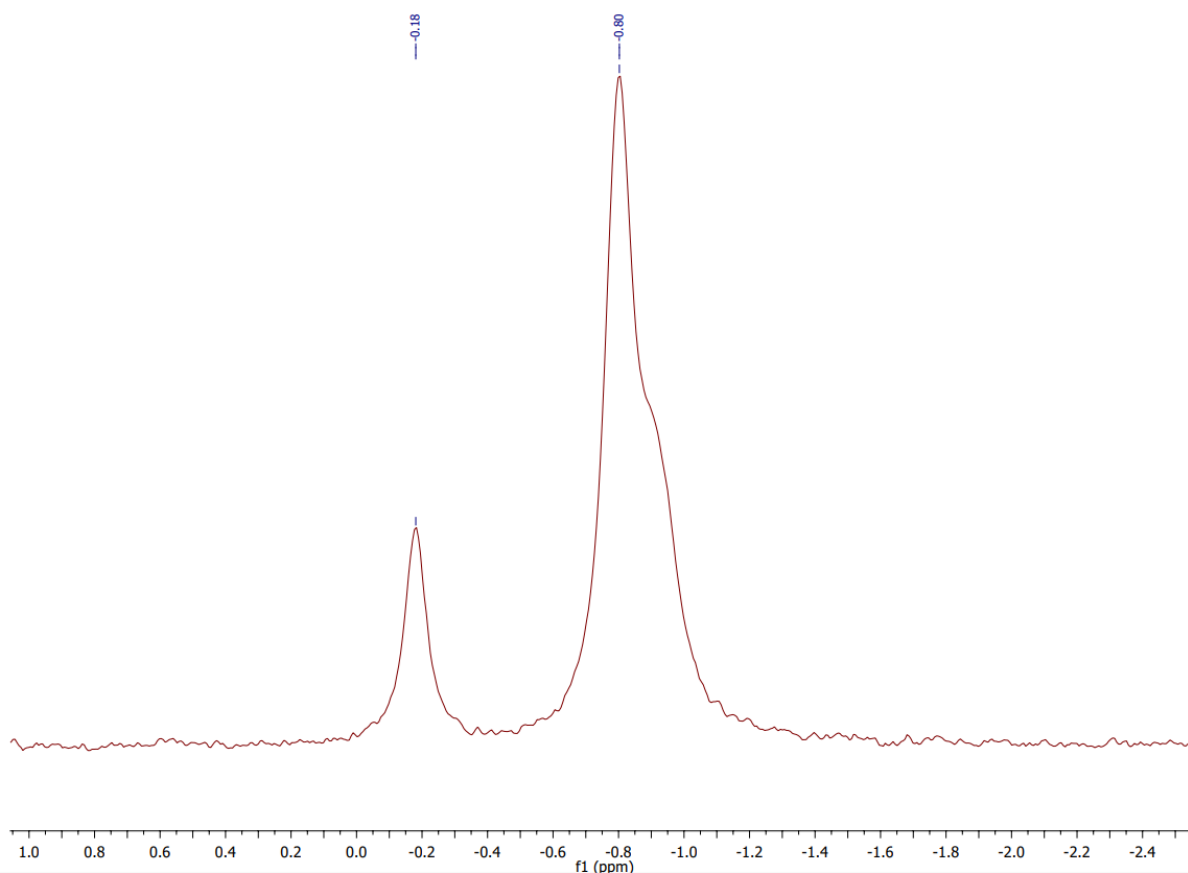
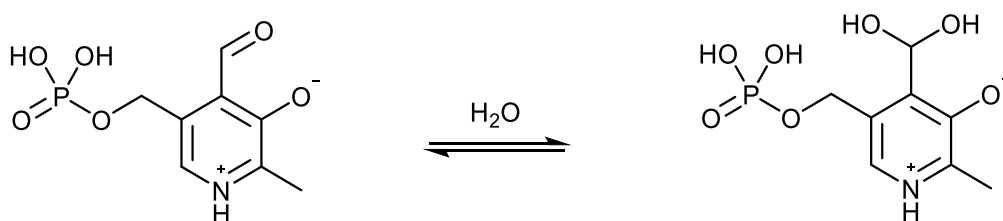


Figure 4.8. ^{31}P -NMR spectrum of 3-trimethylammonium-2-hydroxypropyl-*N*-chitosan-PLP complex (Q188-PLP) in 2 % DCl/D₂O.



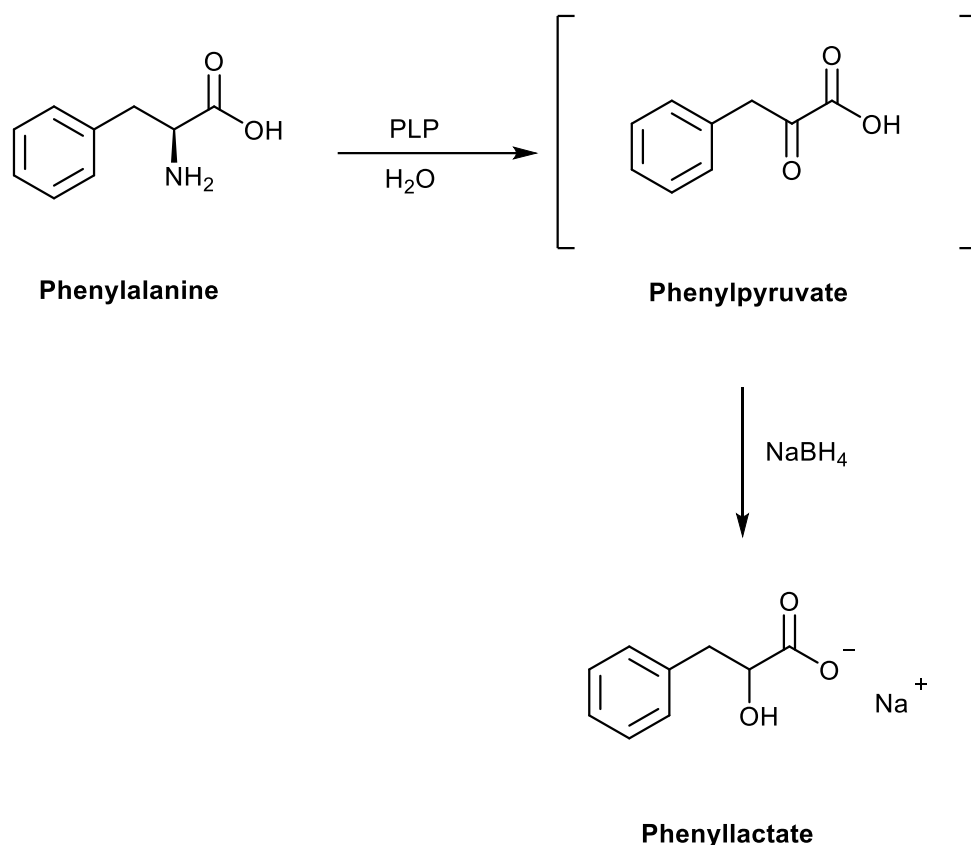
Scheme 4.3. The different forms of PLP in an acidic aqueous environment.

4.2.3 Application of non-enzymatic PLP-mediated conversion of amino acids to α -keto acids

The immobilised pyridoxal products were synthesised with the aim to mimic enzymes in applications such as the deamination of amino acids to α -keto acids. The commercial conversion of phenylalanine to phenylpyruvic acid is a prominent commercial example of deamination reactions (**Scheme 4.4**). Phenylpyruvic acid (PPA) is widely used in the chemical, food and pharmaceutical industries and serves as an advantageous intermediate in the synthesis of D-phenylalanine, which is used in the manufacturing of food additives as well as chiral pharmaceuticals.³³ Phenyllactic acid is the reduced form of PPA and has applications as an antimicrobial, flavour enhancer and food preservative. Aspartame is also derived from PPA and commonly serves as an artificial sweetener.³³ Due to the many applications of PPA and hence its commercial demand, its synthesis is important. Commercially, PPA is usually synthesised using several methods, however, these methods have major setbacks such as the production of many by-products, relatively low yields and causes significant environmental pollution.³³

Alternative routes to produce PPA have been explored, such as enzymatic transformations. Nierop Groot *et al.* synthesised benzaldehyde *via* the conversion of phenylalanine to PPA by an aminotransferase in the cell extract, followed by chemical oxidation of the keto acid to benzaldehyde.³⁴ A study conducted by Hou *et al.* expressed L-amino acid deaminase (L-AAD), a membrane bound gene, from *Proteus mirabilis* in *E.coli* which was used to synthesise PPA.³³ The authors later utilised the engineered *E.coli* in a two-step production process of PPA by means of the growing and resting of cells and a two-stage temperature control strategy. This method was optimised to a large scale of 3 L and a mass conversion rate of 94 % was obtained.³⁵

The production of PPA using a more green, sustainable method with milder reaction conditions and greater efficiency is yearned for, following growing commercial interest. In this study, the conversion of phenylalanine to PPA was investigated using immobilised PLP on biopolymer solid supports.



Scheme 4.4. The conversion of phenylalanine to phenylpyruvate.

Previous unpublished work by Sayed *et al.* found that the ionically immobilised PLP on Q188 in the presence of CuSO₄, successfully converted phenylalanine to phenylpyruvate, with subsequent reduction to phenyllactate. Note that due to the instability of PPA, it was reduced to PLA. The conversion yield was 29 % which is significantly greater than the 11 % of the polymer free reaction, however, a loss of activity occurred over time possibly due to the leaching of PLP from the polymer. Nonetheless, these results looked promising and a further investigation into the kinetics of the deamination reaction was conducted using LCMS. The rates of phenylalanine depletion and phenylpyruvic acid formation was of interest.

Q188-PLP and phenylalanine were allowed to stir in the presence of CuSO₄ in PBS buffer at 25 °C. Aliquots of the reaction mixture was taken at different time intervals over a 24 h period and subjected to LCMS. The peak area against time was plotted to depict phenylalanine depletion as shown in **Figure 4.9**. Depletion of phenylalanine occurred at the fastest rate in the first 200 min and the rate slowly decreased after 200 min until a plateau was reached and no more phenylalanine was present. The rate of product formation was more challenging to observe as phenylpyruvic acid is known to be unstable and was therefore reduced to phenyllactic acid. Standards of known concentration of phenylalanine, phenylpyruvic acid and

phenyllactic acid were evaluated using HPLC following the literature method by Cheng *et al.*³⁶ However, phenyllactic acid was also difficult to observe using HPLC because it is poorly UV active, which is also evident in the HPLC chromatogram reported by Cheng *et al.* where a low absorbance of phenyllactic acid at a concentration of 20 mg/mL was observed.³⁶ Due to these reasons, liquid chromatography was not the most suitable method for the investigation of reaction kinetics for the deamination of phenylalanine to phenylpyruvic acid.

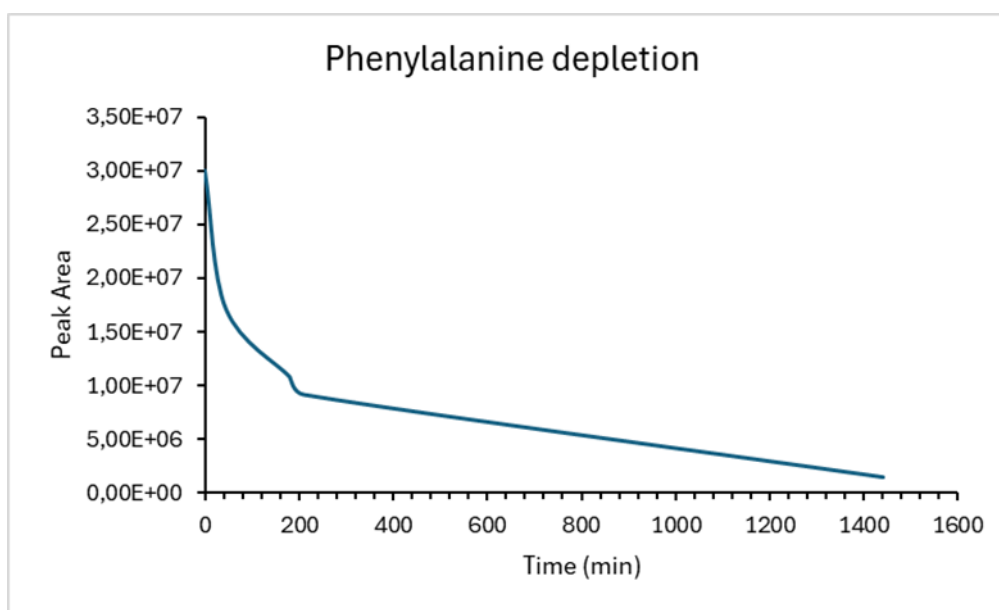


Figure 4.9. Peak area vs time for phenylalanine depletion for the deamination reaction of phenylalanine to phenylpyruvic acid using Q188-PLP as an immobilised catalyst, measured by LCMS.

The loss of activity due to the PLP leaching warranted the synthesis of covalent immobilisation of PLP on biopolymer solid supports.

4.2.4 Background on covalent immobilisation of pyridoxal

Covalent immobilisation of pyridoxal on biopolymer solid supports is advantageous because covalent bonds are stable. Two immobilisation synthetic strategies were explored in this section: direct substitution and esterification. Direct substitution reactions on the biopolymer are well established and are versatile, hence immobilisation of pyridoxal *via* this method using tosyl cellulose was attempted. Tosyl cellulose allows for regioselective substitution at the C-6 position as tosyl is a good leaving group.

4.2.5 Synthesis of immobilised pyridoxal on cellulose *via* direct substitution

Covalent immobilisation of pyridoxal on tosyl cellulose

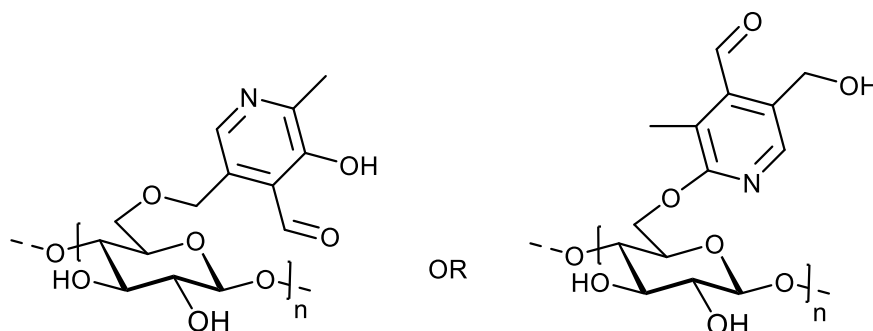
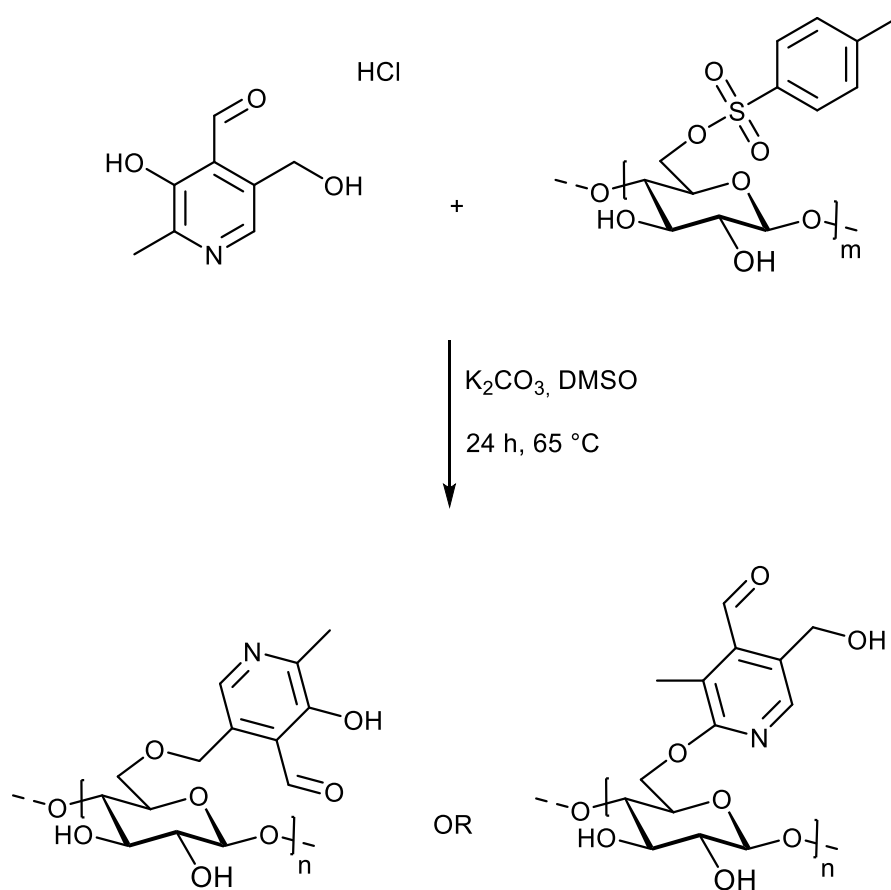


Figure 4.10. Structure of covalently immobilised pyridoxal on tosyl cellulose (4.3).

The synthesis of immobilised pyridoxal on tosyl cellulose (4.3) (**Figure 4.10**) was achieved by a S_N2 reaction between pyridoxal hydrochloride and tosyl cellulose in the presence of K_2CO_3 in DMSO (**Scheme 4.5**). The optimal reaction conditions were at 65 °C for a period of 48 h. The pKa of the 3-OH of pyridoxal is lower than that of the CH_2OH and will therefore be more acidic and be deprotonated first. Therefore, four equivalents of K_2CO_3 were used to fully deprotonate the 3-OH of pyridoxal and the CH_2OH at the 7-position. The product was dialysed against water, lyophilised and obtained as a brown powder with a low mass yield of 28 % and a high degree of substitution of 0.83. Regioselective substitution is most likely to occur at the 5 -position of the pyridoxal ring, possibly due to two reasons: the thermodynamic unfavourability for the nucleophilic attack of a large molecule like tosyl cellulose; and the hydroxymethyl of pyridoxal being less sterically hindered and more easily accessible than the hydroxy at the 4 -position of pyridoxal.³⁷ However, the position at which pyridoxal was substituted was not confirmed.



4.3

Scheme 4.5. Reaction scheme for formation of covalently immobilised pyridoxal on tosyl cellulose (**4.3**).

The IR spectra shown in **Figure 4.11** supports the successful synthesis of covalently immobilised pyridoxal on tosyl cellulose (**IMMOB PL TS CELL**) (**4.3**) as evident by the visible weakening of the tosyl moiety of tosyl cellulose and the appearance of absorption bands for the aldehyde and pyranose groups of pyridoxal at 1608 and 1028 cm^{-1} , respectively.

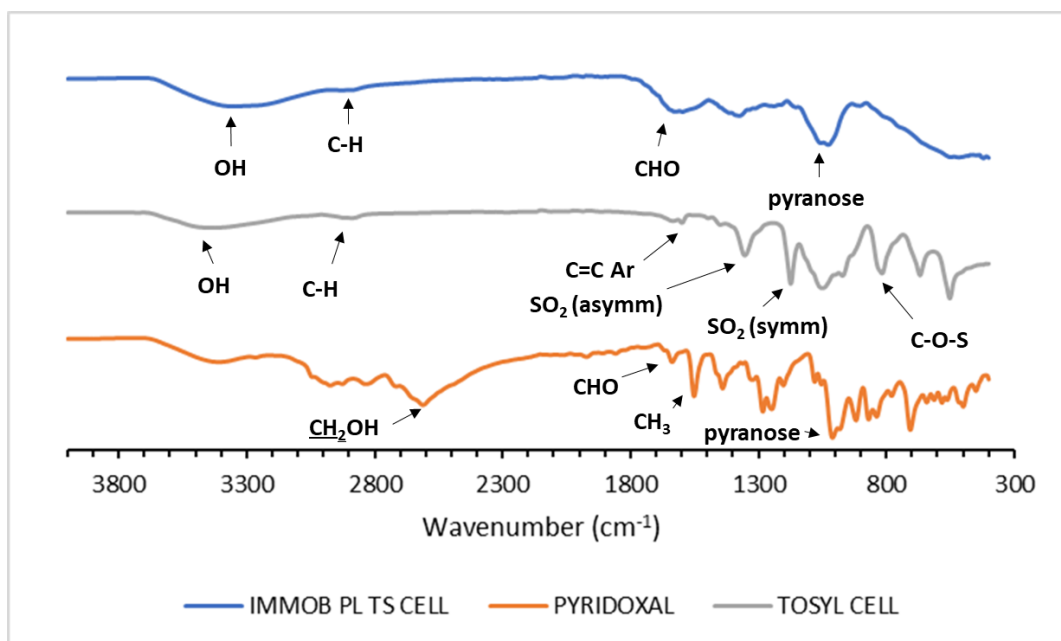
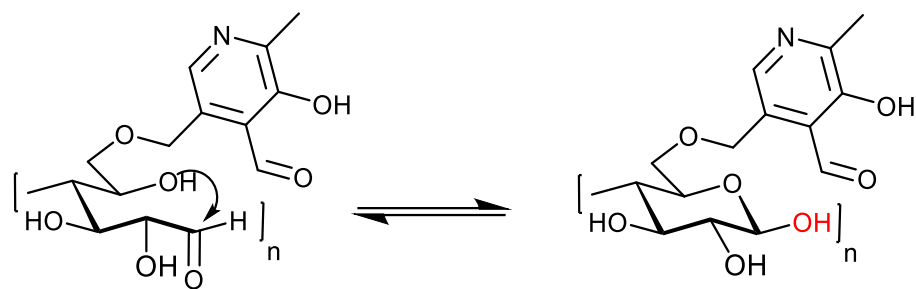


Figure 4.11. FT-IR spectra of covalently immobilised pyridoxal on tosyl cellulose (**IMMOB PL TS CELL**) (**4.3**), tosyl cellulose (**TOSYL CELL**) and pyridoxal hydrochloride.

The $^1\text{H-NMR}$ spectrum of covalently immobilised pyridoxal on tosyl cellulose (**4.3**) (**Figure 4.12**) display the characteristic signals for both pyridoxal and the biopolymer tosyl cellulose. The characteristic signals of pyridoxal are present, namely the aldehyde signal assigned H-13 at δ 8.12 ppm, the singlet for H-12 at δ 6.64 ppm, and the doublet for the CH_2 -group assigned H-7 of pyridoxal, integrating for two protons, at δ 4.93 – 5.08 ppm with a coupling constant of $^3J_{\text{HH}} = 5.0$ Hz. The signal for the methyl protons of pyridoxal, assigned H-14, are present in an overlapping region with the methyl protons of tosyl cellulose and therefore not distinguishable. The broad signals between δ 3.31 – 5.08 ppm are evidence of the presence of the polymer backbone of cellulose. This confirms that pyridoxal has been successfully immobilised onto tosyl cellulose. However, the presence of the phenyl protons of tosyl cellulose at δ 7.52 – 7.84 ppm and the *p*- CH_3 group of tosyl cellulose at δ 2.46 ppm suggest that there are unsubstituted tosyl groups present on the cellulose. Signals for the cellulose backbone are evident between δ 80.60 to 69.12 ppm. When immobilised product **4.3** was synthesised on a larger scale of 1.00 g, it proved to be insoluble in any available NMR solvent due to strong inter-polymer hydrogen bonding from the formation of hemiacetals of the terminal aldehyde moiety of tosyl cellulose (**Scheme 4.6**).



Scheme 4.6. Hemiactal formation of terminal aldehyde moiety of covalently immobilised pyridoxal on tosyl cellulose (**4.3**).

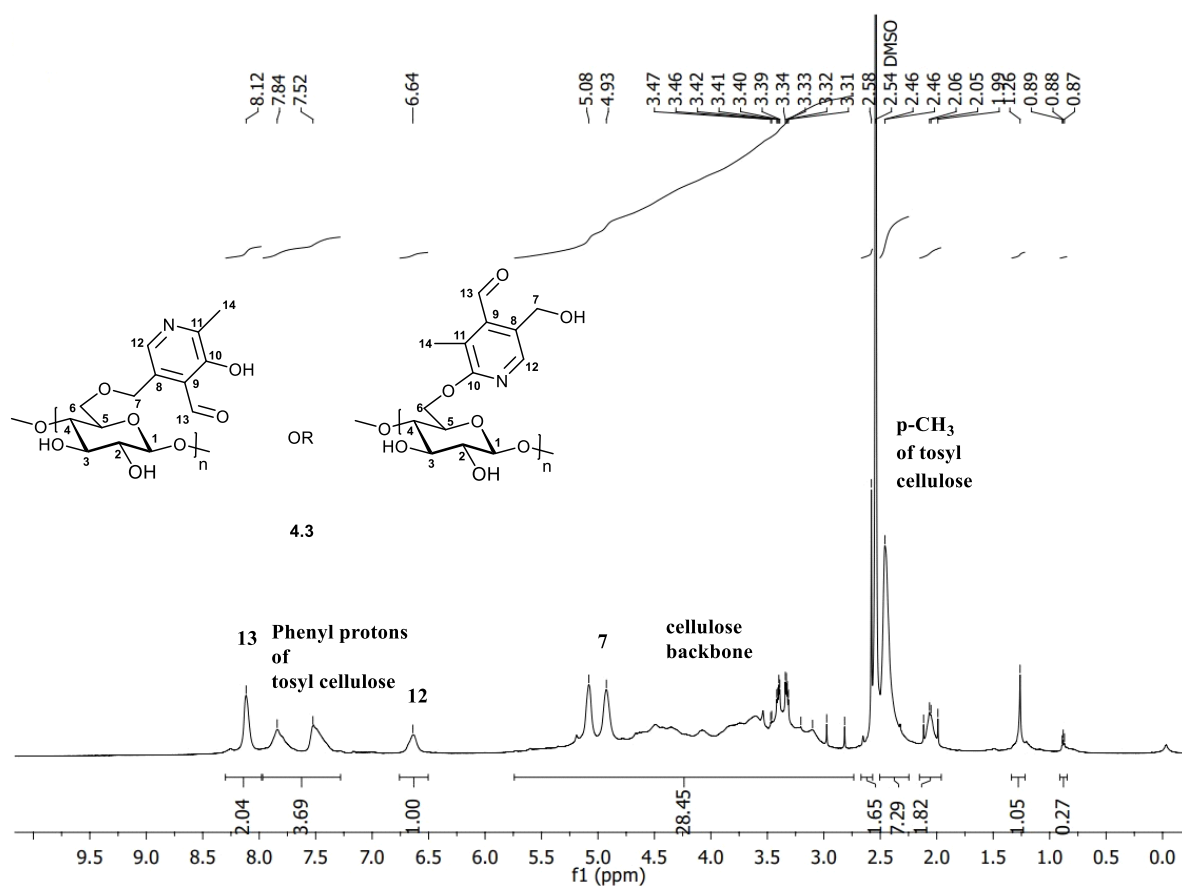


Figure 4.12. ¹H-NMR spectrum of optimised covalently immobilised pyridoxal on tosyl cellulose (**4.3**) at 65 °C and 48 h, with 4 eq. K₂CO₃ in DMSO-d₆.

The covalently immobilised pyridoxal was insoluble in common protic solvents and hence could not be utilised for deamination reactions.

4.2.6 Synthesis of immobilised pyridoxal on carboxy methylchitosan *via* esterification

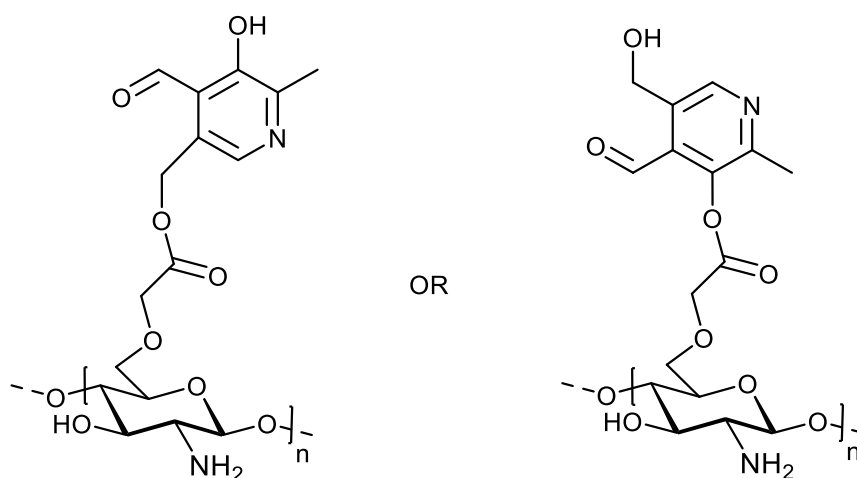
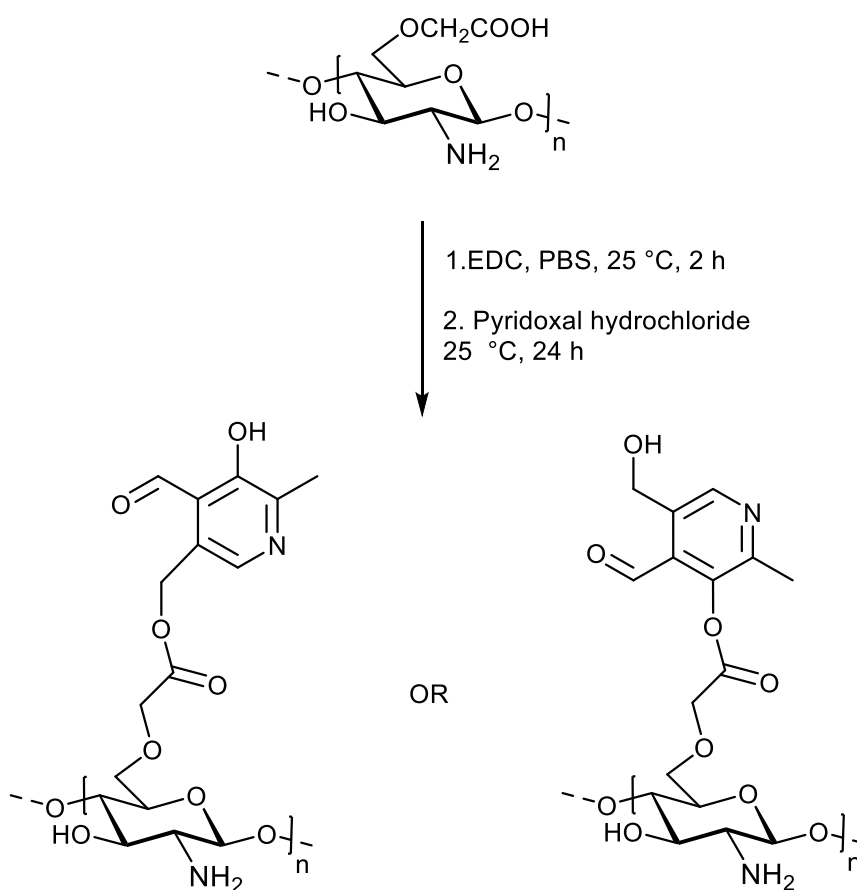


Figure 4.13. Structure of covalently immobilised pyridoxal on carboxymethyl chitosan *via* esterification (4.4).

To overcome the solubility challenges encountered by covalent immobilisation of pyridoxal *via* direct substitution, immobilisation *via* esterification was explored. Cross-linking of biopolymers through the formation of esters is an attractive method for enzyme immobilisation because it improves the rigidity of the biopolymer, making it porous like a sponge wherein pyridoxal can be immobilised. This method can improve stability of the pyridoxal as well as prevent it from leaching.³⁸

Carboxymethyl chitosan (CMC) is greatly soluble in neutral and basic solutions, and also displays improved biodegradability, sensitivity, biocompatibility, as well as moisture-retaining capacity relative to chitosan.³⁹⁻⁴¹ CMC is known to be highly brittle and inflexible, but its porous nature allows for immobilisation of pyridoxal within its pores *via* the formation of ester linkages.³⁹

Pyridoxal was immobilised into CMC *via* esterification to yield compound 4.4 as shown in **Scheme 4.7**. A modified literature method was followed whereby CMC was dissolved in phosphate buffer solution (pH 6) and activated using 1-(3-dimethylaminopropyl)-3-ethylcarbodiimide hydrochloride (EDC). Thereafter, pyridoxal hydrochloride was added to the reaction mixture and allowed to stir at room temperature for a period of 24 h.³⁹ The reaction mixture was dialysed against water for three days to remove any unreacted pyridoxal and dried to obtain orange CMC-pyridoxal sponges.



4.4

Scheme 4.7. Reaction scheme for formation of covalently immobilised pyridoxal on CMC (**4.4**).

Compound **4.4** was insoluble in both aqueous and organic solvents. IR spectroscopy was used to confirm its structure (**Figure 4.14**). Diagnostic absorption bands for CMC are present: the broad signal at 3306 cm^{-1} for the overlapping -OH and -NH stretching vibrations. The characteristic signals for asymmetric and symmetric stretching vibrations of the carboxyl group at 1578 and 1408 cm^{-1} , respectively, as well as signal at 1066 cm^{-1} assigned to the COO-C which is indicative of its involvement in intermolecular bonding during crosslinking.³⁹ Absorption signals for pyridoxal are not visible in the spectrum due to the immobilisation of pyridoxal occurring in the pores of the CMC sponge. The immobilisation position of pyridoxal was not certain, hence the possibility of esterification with CMC at either the 3- or 7-position of pyridoxal. The percentage mass yield of immobilised product **4.4** was not determined because of the uncertainty in structure, but the change in colour and texture from a brown powder (CMC) to an orange gel-like solid provided visual evidence to corroborate the IR result that pyridoxal was successfully immobilised on CMC.

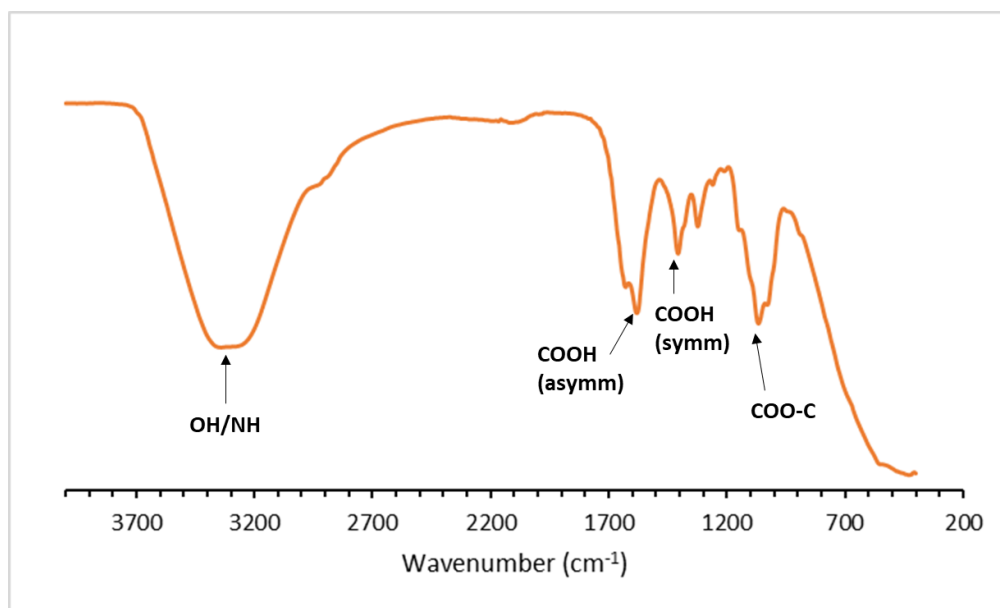


Figure 4.14. FT-IR spectrum of immobilised pyridoxal on carboxy methylchitosan (CMC-PL) 4.4.

Unfortunately, the aqueous insolubility limited the application of the covalently immobilised pyridoxal products. Future studies will focus on synthesising water-soluble immobilised pyridoxal. The plans for future work on this topic are discussed in **Chapter 5**.

4.3 Conclusion

This chapter described the immobilisation of pyridoxal on the aminated biopolymer Q188 to introduce reusability and recyclability of pyridoxal in enzyme-independent deamination of phenylalanine to phenylpyruvate. PLP was successfully immobilised on Q188 *via* ionic bonding and demonstrated the conversion of phenylalanine to phenylpyruvate by means of LCMS. However, the conversion rate decreased over time possibly due to leaching of pyridoxal. Therefore, an alternative method for immobilisation was sought and the immobilisation of pyridoxal *via* covalent bonding, i.e. direct substitution reaction with tosyl cellulose and esterification with CMC. Unfortunately, these covalently immobilised pyridoxal products were insoluble in aqueous and organic solvents and could not be used in the deamination of phenylalanine to phenylpyruvate. Further work requires the investigation and design of water-soluble covalently immobilised pyridoxal products that can be utilised in biomimetic applications.

4.4 References

1. E. E. Snell and P. Pearson, *Proceedings of the Society for Experimental Biology and Medicine*, 1942, **51**, 356-358.
2. M. L. Di Salvo, K. Fesko, R. S. Phillips and R. Contestabile, *Journal*, 2020, **8**, 52.
3. M. L. di Salvo, N. Budisa and R. Contestabile, in *Molecular Engineering and Control*, Martin G. Hicks and Carsten Kettner, 2013, pp. 54-131.
4. P. Mulay, C. Chen and V. Krishna, *Scientific Reports*, 2023, **13**, 312.
5. R. Percudani and A. Peracchi, *BMC bioinformatics*, 2009, **10**, 1-8.
6. A. Hoegl, M. B. Nodwell, V. C. Kirsch, N. C. Bach, M. Pfanzelt, M. Stahl, S. Schneider and S. A. Sieber, *Nature chemistry*, 2018, **10**, 1234-1245.
7. E. R. Hoffarth, K. W. Rothchild and K. S. Ryan, *The FEBS Journal*, 2020, **287**, 1403-1428.
8. M. D. Toney, *Archives of biochemistry and biophysics*, 2005, **433**, 279-287.
9. B. Kappes, I. Tews, A. Binter and P. Macheroux, *Biochimica et Biophysica Acta (BBA)-Proteins and Proteomics*, 2011, **1814**, 1567-1576.
10. A. Amadasi, M. Bertoldi, R. Contestabile, S. Bettati, B. Cellini, M. Luigi di Salvo, C. Borri-Voltattorni, F. Bossa and A. Mozzarelli, *Current medicinal chemistry*, 2007, **14**, 1291-1324.
11. E. E. Snell, *Journal of the American Chemical Society*, 1945, **67**, 194-197.
12. E. E. Snell, in *Vitamins & Hormones*, Elsevier, 1958, vol. 16, pp. 77-125.
13. D. E. Metzler, M. Ikawa and E. E. Snell, *Journal of the American Chemical Society*, 1954, **76**, 648-652.
14. G. Kalyankar and E. E. Snell, *Biochemistry*, 1962, **1**, 594-600.
15. K.-Y. Choi, *Biotechnology and bioprocess engineering*, 2015, **20**, 988-994.
16. J. Yang, P. Minkler, D. Grove, R. Wang, B. Willard, R. Dweik and C. Hine, *Communications biology*, 2019, **2**, 194.
17. A. E. Braunstein, *The enzymes*, 1960, **2**, 113-184.
18. R. F. Zabinski and M. D. Toney, *Journal of the American Chemical Society*, 2001, **123**, 193-198.
19. D. E. Metzler and E. E. Snell, *Journal of the American Chemical Society*, 1952, **74**, 979-983.
20. S.-i. Ikeda, H. Hara, S. Sugimoto and S. Fukui, *FEBS letters*, 1975, **56**, 307-311.
21. K.-H. Lee, M. D. Distefano and B. Seelig, *Results in chemistry*, 2023, **6**, 101044.
22. S.-I. Ikeda, H. Hara and S. Fukui, *Biochimica et Biophysica Acta (BBA)-General Subjects*, 1974, **372**, 400-406.
23. X.-J. Zhang, H.-H. Fan, N. Liu, X.-X. Wang, F. Cheng, Z.-Q. Liu and Y.-G. Zheng, *Enzyme and Microbial Technology*, 2019, **130**, 109362.
24. L. H. Andrade, W. Kroutil and T. F. Jamison, *Organic Letters*, 2014, **16**, 6092-6095.
25. S. Velasco-Lozano, A. I. Benitez-Mateos and F. Lopez-Gallego, *Angew Chemie International Edition* 2017, **56**, 771-775.
26. X. J. Zhang, H. H. Fan, N. Liu, X. X. Wang, F. Cheng, Z. Q. Liu and Y. G. Zheng, *Enzyme Microbiology Technology*, 2019, **130**, 109362.
27. G. Wei, Y. Chen, N. Zhou, Q. Lu, S. Xu, A. Zhang, K. Chen and P. Ouyang, *Chemical Engineering Journal*, 2022, **427**, 132030.
28. S. Sayed, T. Millard and A. Jardine, *Carbohydrate polymers*, 2018, **196**, 187-198.
29. S. Sayed, PhD Thesis, University of Cape Town, 2018.
30. K. D. Schnackerz, B. Andi and P. F. Cook, *Biochimica et Biophysica Acta (BBA)-Proteins and Proteomics*, 2011, **1814**, 1447-1458.

31. J. Liang, Q. Han, Y. Tan, H. Ding and J. Li, *Frontiers in Molecular Biosciences*, 2019, **6**, 4.
32. S. Sayed and A. Jardine, *International journal of molecular sciences*, 2015, **16**, 9064-9077.
33. Y. Hou, G. S. Hossain, J. Li, H.-d. Shin, L. Liu and G. Du, *Applied microbiology and biotechnology*, 2015, **99**, 8391-8402.
34. M. N. Nierop Groot and J. A. de Bont, *Applied and Environmental Microbiology*, 1998, **64**, 3009-3013.
35. Y. Hou, G. S. Hossain, J. Li, H.-d. Shin, L. Liu, G. Du and J. Chen, *Plos one*, 2016, **11**, e0166457.
36. Z. Cheng, Q. Ran, J. Liu, X. Deng, H. Qiu, Z. Jia and X. Su, *Food Analytical Methods*, 2020, **13**, 1673-1680.
37. S. Bai, M. Ren, L. Wang and Y. Sun, *Frontiers of Chemical Engineering in China*, 2008, **2**, 301-307.
38. A. Gerezgiher and T. Szabó, *Crosslinking of Starch Using Citric Acid*, IOP Publishing, 2022.
39. Y. Cheng, Z. Hu, Y. Zhao, Z. Zou, S. Lu, B. Zhang and S. Li, *International Journal of Molecular Sciences*, 2019, **20**, 3890.
40. X.-G. Chen and H.-J. Park, *Carbohydrate Polymers*, 2003, **53**, 355-359.
41. L. Chen, Z. Tian and Y. Du, *Biomaterials*, 2004, **25**, 3725-3732.

Chapter 5: Conclusions and Future Outlook

5.1 Overall summary and conclusions

The main objective of this study was to develop a sustainable method for the synthesis of aminated biopolymers following a two-step oxidation-reductive amination process. The method should yield soluble aminated products, as well as minimal waste and utilise less hazardous reagents.

This was achieved by firstly synthesising oxidised biopolymers: dialdehyde cellulose (DAC) and C-6 selectively oxidised C-6 tosyl cellulose. Dialdehyde cellulose was synthesised following a literature procedure using sodium periodate-mediated oxidation and characterised by IR spectroscopy and elemental analysis. A novel C-6 selective oxidation method was developed for cellulose. Selective oxidation at C-6 partially tosylated cellulose achieved using a green solvent system of NaOH-urea. The tosyl cellulose obtained was soluble in DMSO which allowed for a Swern-like oxidation using TsCl in DMSO in the presence of triethylamine. This was the first report of a C-6 oxidation of a biopolymer utilising a DMSO-TsCl system at ambient temperature. The C-6 selectively oxidised C-6 tosyl cellulose obtained was DMSO-soluble and characterised *via* a $^1\text{H-NMR}$ spectroscopy time study where deuterated DMSO was used to prevent hemiacetal formation and visibly depict the signal for the aldehyde proton, as well as the by-product DMS. A 1D DOSY experiment was conducted to identify the DMS signal which overlapped in the region with signals of the tosyl moiety. Furthermore, a Schiff base test reaction was performed using benzylamine to further confirm the successful C-6 oxidation of tosyl cellulose. This Swern-like oxidation was attempted on chitin and chitosan but was unsuccessful.

The next step was reductive amination of the oxidised celluloses. Three different reductants were investigated using ammonium acetate as the amine source: picoline borane, sodium borohydride and sodium hypophosphite. Reductive amination using picoline borane was performed following literature methods but produced a negative Kaiser ninhydrin test and was therefore deemed unsuccessful; whereas the use of sodium borohydride produced an aminated polymer as evident by a positive Kaiser ninhydrin test, however, the polymer was insoluble. On the other hand, sodium hypophosphite produced DMSO-soluble aminated cellulose in good yield with the highest degree of substitution of the three reductants, as determined by elemental

analysis. To the best of my knowledge, this was the first-time sodium hypophosphite was used as a reductant for the reductive amination of biopolymers.

The synthesised diamino and amino celluloses were DMSO-soluble and were tested for cytotoxicity against brain cancer cell lines. Cytotoxicity studies showed that the aminated celluloses did not display any inherent anticancer activity and would be suitable for drug conjugation and delivery.

The use of aminated biopolymers as a solid support for the immobilisation of pyridoxal 5'-phosphate was explored for application in non-enzymatic deamination of L-phenylalanine to phenylpyruvate. An ionic complex with PLP and Q188 was formed and successfully converted L-phenylalanine to phenylpyruvate, however, showed a decline in activity over time possibly due to the leaching of PLP. Therefore, immobilisation of PLP *via* covalent bonding was explored but the immobilised products synthesised were insoluble in water and could not be used in non-enzymatic deamination reactions.

5.2 Future outlook

There is potential for further improvement of the method for the amination of biopolymers. An alternative bio-derived reagent to *p*-toluenesulfonyl chloride such as *p*-cymenesulfonyl chloride can be used as a source of tosyl for the tosylation and C-6 selective oxidation reactions. More sustainable solvents can be used, and solvents should be recycled to minimise waste production.

Priority lies in the further investigation on the C-6 selective oxidation of chitosan is needed. A new strategy for the protection of the C-2 amino group of chitosan should be explored e.g. Trimethyl chitosan chloride (TMC).

The bioactivity of aminated cellulose with higher DS can be further explored in applications of antimicrobial and antifungal studies.

The use of aminated biopolymers as a solid support for PLP immobilisation can be further explored to include polymers linked *via* click chemistry (**Figure 5.1**) to yield soluble, covalently immobilised PLP.

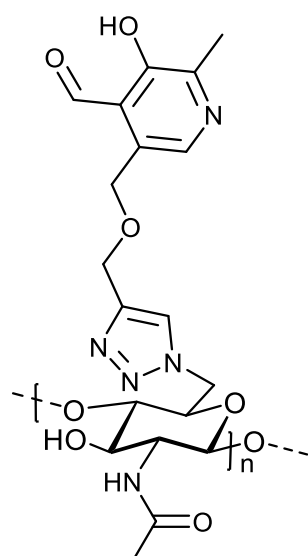
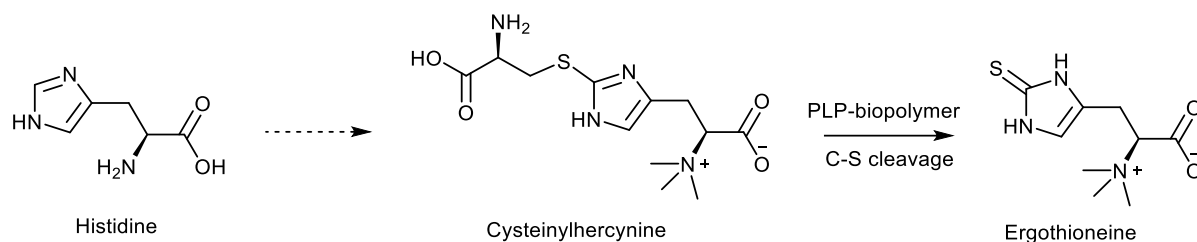


Figure 5.1. PLP immobilised on chitin *via* click chemistry.

Thereafter, the applications of the immobilised product can be investigated in conversion of amino acids to α -keto acids. The covalent link would possibly overcome this issue of PLP leaching under reaction conditions. Furthermore, immobilised products could be used in applications of non-enzymatic carbon-sulfur bond cleavage of cysteine in the synthesis of ergothioneine (**Scheme 5.1**).¹



Scheme 5.1. Synthesis of ergothioneine from histidine.¹

5.3 References

1. P. L. Khonde and A. Jardine, *Organic & biomolecular chemistry*, 2015, **13**, 1415-1419.

Chapter 6: Experimental Procedures

6.1 General procedures

All reagents and solvents were purchased from Merck, Kimix and Sigma-Aldrich and used without further purification unless stated otherwise. Distilled or ultrapure Milli-Q water was used in all reactions.

Avicel® PH-101 and chitin was purchased from Sigma-Aldrich and used without further purification. Chitin was extracted from shrimp shells. Chitosan (DDA > 90%) extracted from crabs was used directly; and was purchased from AK Scientific. Purification of biopolymers by ultra-filtration was performed using a dialysis bag where indicated, with a cut-off molecular weight of 10 kDa.

Nuclear Magnetic Resonance (NMR) spectra were either recorded on Varian Mercury XR300 MHz (^1H at 300.08 MHz at ^{13}C (^1H): 75.46 MHz) or Bruker Ascend 600 spectrometer (^1H at 600.10 MHz, $^{13}\text{C}\{^1\text{H}\}$ at 150.60 MHz) at ambient temperature. Solid-state ^{13}C NMR was recorded on an Avance III 400 NMR spectrometer with a ^{13}C frequency of 400.13 MHz. Chemical shifts for ^1H and $^{13}\text{C}\{^1\text{H}\}$ NMR were all reported using tetramethylsilane (TMS) as an internal standard. Chemical shifts and J -couplings were reported in parts per million (ppm) and Hertz (Hz), respectively. NMR spectra were recorded using either deuterated dimethylsulfoxide (DMSO- d_6) or deuterium oxide (D_2O).

Reactions that were performed at room temperature refer to an average temperature of 25 °C.

Infrared (IR) spectroscopy was measured on a Perkin-Elmer Spectrum One FT-IR Spectrometer using Attenuated Total Reflectance (ATR) with bond vibrations measured in reciprocal centimeters (cm^{-1}).

Elemental Analysis for C, H, N and S were carried out on a Perkin Elmer Series II C, H, N, S analyser.

Ultraviolet-visible (UV-Vis) spectroscopic analyses were performed on a Varian Cary 50 UV-Visible spectrophotometer using 1 cm path length quartz cell cuvettes.

LC-MS analyses were performed using a UPLC Agilent G7117A 1290 DAD FS and a MS Agilent 6150 single quadrupole mass spectrometer equipped with a jet stream ion source. The

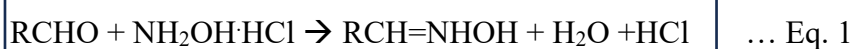
method parameters were as follows: column temperature of 50 °C; injection volume of 1 µL; flow rate of 1.2 mL/min; solvent system: (A) 0.1 % formic acid in water and (B) 0.1 % formic acid in acetonitrile with ratio 95:5. The column used was Kinetex column 1.7µm EVO C18 100Å, 50 x 2.1mm.

Powder X-ray diffraction (PXRD) patterns were recorded on a Bruker D2 Phaser desktop powder diffractometer (Billerica, Massachusetts, USA) using a CuKα₁ radiation source (λ = 1.5406 Å) with X-ray generator settings at 30 kV and 10 mA.

Thermogravimetric analysis (TGA) thermograms were recorded on a TA-Q500 instrument (New Castle, Delaware, U.S.A) and analysed using TA universal analysis 2000 software and Differential scanning calorimetry (DSC) thermograms were recorded on a TA Discovery DSC 25 instrument (New Castle, Delaware, U.S.A) and analysed using TRIOS software.

Determination of Degree of Oxidation (DO)

The degree of oxidation (DO) of oxidised biopolymers was measured by the procedure followed by Koshani et al.¹ A known amount of sample (~30 mg) was suspended in DI water (10 mL) with pH adjusted to 3.5 by the addition of 0.1 M HCl solution. NH₂OH·HCl (5 wt%) was added in excess to the suspension (10 mL) and allowed to stir overnight at 25 °C. The titrator, a 0.1 M solution of NaOH, was used to compensate for the decrease in pH due to the release of HCl after oxime formation. This procedure was repeated until a constant pH of 3.5 was reached, thus indicating the complete conversion of the aldehyde/dialdehyde groups to oxime compounds.



The degree of oxidation was calculate using the following equation:

$$\boxed{\text{DO (mmolg}^{-1}\text{)} = (\text{V (NaOH)} \times \text{N (NaOH)}) / \text{W}} \quad \dots \text{Eq. 2}$$

where V(NaOH) is the volume of the consumed NaOH, N(NaOH) is the normality of the NaOH, and W is the weight of DAC that were used for titration.

Titration were done in **triplicate**. The **average titre** was used for calculations.

Kaiser ninhydrin test

A modified literature method of the Kaiser Ninhydrin test was used to test for the presence of primary amines on polymers *via* a blue-purple colour change.² Firstly, three Kaiser test solutions were prepared:

Reagent A:

KCN (16.5 g) was dissolved in distilled water (25 mL) and then 0.5 mL of this solution was diluted with pyridine (24.5 mL).

Reagent B:

Ninhydrin (1.00 g) was dissolved in *n*-butanol (20 mL).

Reagent C:

Phenol (5.00 g) was dissolved in *n*-butanol.

Secondly, 10 mg of biopolymer was weighed into a test tube and 2 to 3 drops of each reagent was added. The solution was heated at 110 °C for 5 min. The following commercial standards were used for reference:

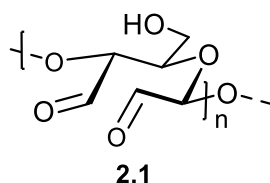
Table 6.1. Kaiser ninhydrin test results on commercial standards.

Biopolymer	Colour	Result
starch	colourless	negative
chitosan	colourless or faint blue colour	negative or similar to chitosan

6.2 Experimental

6.2.1 Synthesis of cellulose and chitosan polymer modifications

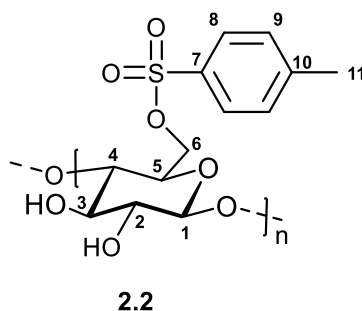
Dialdehyde cellulose (2.1)³



Cellulose (5.00 g) was allowed to stir in distilled water (250 mL) followed by the addition of sodium periodate (8.25 g). The reaction mixture was allowed to stir in the dark at 25 °C for 72 h. The reaction mixture was centrifuged, and the resulting pellet was washed with distilled water (20 mL) several times, as well as dialysed against distilled water followed by lyophilisation to yield the product as a white solid. (3.68 g, 75 %).

FT-IR (ATR) ν (cm⁻¹): 3334 (O-H), 1628 (adsorbed water), 880 (hemiacetals). **Elemental analysis** (%): C, 39.20; H, 6.29; N, 0.04. DO= 9.20 mmol.g⁻¹.

Tosyl cellulose (2.2)⁴

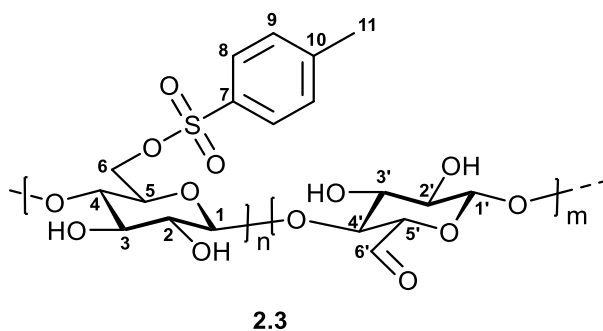


A mixture of NaOH (17.5 g), urea (30.0 g) and distilled water (200 mL) were allowed to stir until a clear solution was obtained. Cellulose (10.0 g) was added whilst stirring. The reaction mixture was stored in the refrigerator for 1 h and cooled to -20 °C. The pre-cooled mixture was subsequently allowed to stir at 25 °C to obtain a transparent cellulose solution. *p*-toluenesulfonyl chloride (72.0 g) and SLS (20.0 g in 40 mL H₂O) were added to the cellulose solution. A white emulsion occurred after stirring for 15 min. The reaction mixture was allowed to stir vigorously at 25 °C for 5 h and the polymer was precipitated by the addition of ethanol

(200 mL). The product was separated by centrifugation, washed with ethanol (20 mL) followed by distilled water (20 mL), and dried by lyophilisation to yield a white powder. (27.20 g, 72 %).

¹H NMR (600 MHz, DMSO-*d*₆) δ(ppm): 7.78 – 7.10 (H-8 & H-9), 4.33 (H-1), 4.07 – 4.06 (H-6), 3.80 – 3.31 (H-3, H-4, H-5), 3.07 (H-2), 2.42 (H-11). **¹³C NMR (600 MHz, DMSO-*d*₆)** δ(ppm): 137.56 (C-7), 132.73 – 125.46 (C-8, C-9, C-10), 102.44 (C-1), 80.25 (C-4), 74.42 (C-3_{TOS}/C-2_{TOS}), 72.97 – 72.43 (C-5, C-3, C-2), 67.31 (C-6_{TOS}), 60.28 (C-6_{OH} UNSUBSTITUTED), 21.02 (C-11). **FT-IR (ATR)** ν (cm⁻¹): 1562 (C=C_{AROMATIC}), 1354 (ASO₂), 1174 (S_{SO}2), 812 (S-O-C). **Elemental analysis (%)**: C 36.01; H 4.44; N 1.53; S 7.48. **DS_{TOS}**: 0.59.

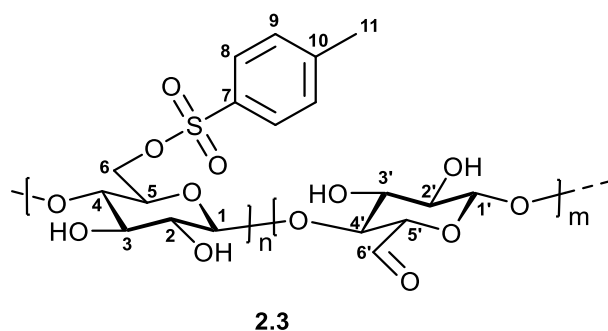
C-6 Oxidised C-6 tosyl cellulose (2.3)



Tosyl cellulose (**2.2**) (20.0 g) was allowed to stir in DMSO (250 mL) until dissolved. Et₃N (69.2 mL) and a solution of *p*-toluenesulfonyl chloride (47.6 g) in DMSO (100 mL) was added to the reaction mixture and allowed to stir overnight at 25 °C. The mixture was poured into ice water (1 L) and the precipitate washed with water (200 mL x 2) and EtOH (200 mL x 2). The product was lyophilised to yield a crystalline solid. (9.10 g, 81%).

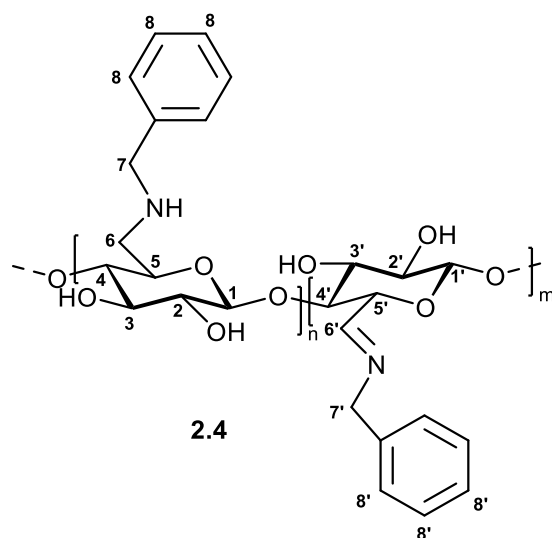
¹H NMR (600 MHz, DMSO-*d*₆) δ(ppm): 9.07 (H-6'), 7.78 – 7.46 (H-8 & H-9), 7.13 – 7.10 (H-Tos), 5.40 (H-3), 4.69 (H-2), 4.07 – 4.04 (H-1), 3.80 (H-6), 3.68 (H-4), 3.48 (H-5), 0.85 (H-11). **FT-IR (ATR)** ν (cm⁻¹): 1598 (C=C_{AROMATIC}), 1354 (ASO₂), 1174 (S_{SO}2), 816 (S-O-C). **Elemental analysis (%)**: C 40.33; H 7.33; N 1.10; S 15.05. **DO** = 1.63 mmol.g⁻¹.

C-6 Oxidised C-6 tosyl cellulose (2.3)- NMR experiment



Tosyl cellulose (**2.2**) (0.050 g) was allowed to stir in DMSO- d_6 (0.5 mL) until dissolved. Et₃N (0.173 mL) was added to the reaction mixture and stirred. A solution of *p*-toluenesulfonyl chloride (0.119 g) in DMSO- d_6 (0.25 mL) was added to the mixture and the reaction progress was monitored by ¹H-NMR spectroscopy at t(0), t(15 min), t(1 h), and t(24 h). **¹H NMR (300 MHz, DMSO)** δ(ppm): 9.99 (C-6'), 7.53 - 7.12 (H-8 & H-9), 3.06 – 2.28 (cellulose backbone/H-11/DMS).

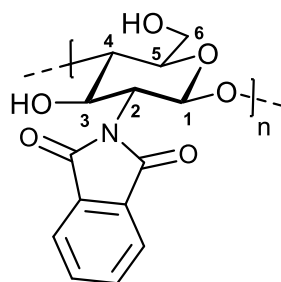
Schiff base of mixed C-6 oxidised C-6 tosyl cellulose (2.4)- test for confirmation of aldehyde group and concomitant tosyl substitution



C-6 Oxidised C-6 tosyl cellulose (**2.3**) (0.250 g) and benzylamine (0.612 mL) were suspended in DMSO (2.5 mL) and heated at 120°C for 4.5 h. The colourless reaction mixture turned orange and once distilled water (5 mL) was added, a precipitate formed. The product was isolated by centrifugation, washed with ethanol (20 mL) and lyophilised to yield the imine product **2.4** as a yellow powder. (0.247 g, 80 %).

¹H NMR (600 MHz, DMSO-d₆) δ(ppm): 8.50 (H-6'), 7.78 (H-8 & H-8'), 5.39 (H-1), 4.68 (H-6), 4.35 – 3.60 (H-3, H-4, H-5), 3.08 (H-2). **FT-IR (ATR)** ν (cm⁻¹): 1643 (C=N). **Elemental analysis (%)**: C 66.85; H 6.80; N 5.16, S 2.24. Ratio N:S 2.30.

N-phthaloyl chitosan (2.5)⁵

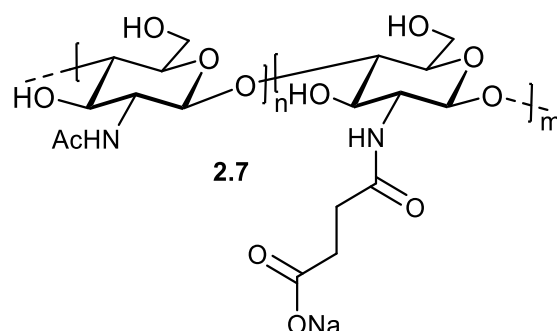


2.5

Chitosan (1.18 g) and phthalic anhydride (2.75 g) was refluxed in 10 % AcOH/H₂O solution (50 mL) at 120 °C for 24 h. The reaction mixture was allowed to cool to room temperature (~ 25 °C). Thereafter, the precipitate was collected by centrifugation and subsequently washed with water (50 mL) and ethanol (50 mL). Unreacted phthalic anhydride was dissolved by allowing the solid to stir in acetone (50 mL). The product was dialysed against water and dried to yield a brown solid. (0.393 g, 19 %).

¹H NMR (300 MHz, DMSO-d₆) δ(ppm): δ 8. – 7.43 (Phth-H), 5.47 – 4.09 (H-1, H-3 – H-6), 2.08 (s, acetylated units).

***N*-succinyl chitosan (2.7)⁶**

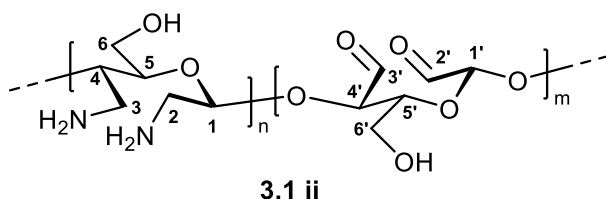


Chitosan (2.50 g) was suspended in DMSO (50 mL) and succinic anhydride (2.5 g) was added. The reaction mixture was allowed to stir for 24 h at 60 °C. The reaction mixture was allowed to cool to room temperature (~25 °C) and the solid was collected by centrifugation. Distilled water (200 mL) (pH 10-11, adjusted with 5% (w/v) NaOH solution), was added to the solid to form a pale-yellow solution. The crude product was precipitated by adding acetone (60 mL) and washed thrice with 75% EtOH and acetone. The wet acylation product was washed with acetone (30 mL) and dried *in vacuo*. (3.46 g, 100 %)

FT-IR (ATR) ν (cm⁻¹): 3272 (O-H & N-H), 2916 (C-H aliphatic), 1384 (COO⁻), 1638 (Amide I), 1540 (Amide II).

Diamino cellulose (3.1ii)¹

Using NaBH₄ as reductant



DAC (0.500 g 10 mmol g⁻¹ aldehyde groups), NH₄Ac (1.16 g, 3 mol per mol -CHO), and NH₄OH (1.75 g, 10 mol per mol -CHO = 100 mmol g⁻¹) were dispersed in 200 mL EtOH, and the resulting slurry was allowed to stir at 80 °C under reflux conditions for 18 h. The reaction mixture was subsequently cooled in an ice bath and NaBH₄ (0.760 g, 4 times excess i.e. 40 mmol g⁻¹) was gradually added followed by stirring for an additional 1 h. The amount of NaBH₄ was calculated based on 1:0.5 M ratio of the anhydroglucose units (~6.17 mmol g⁻¹): NaBH₄. The resulting aminated product was washed 5 times with DI water (20 mL). The mol

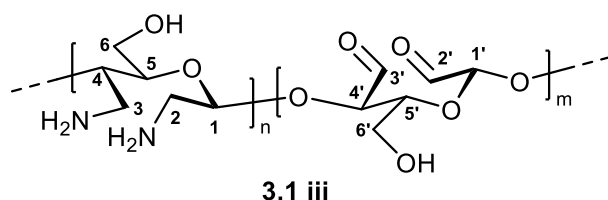
equivalents of reagents used was based on the assumption that all the aldehydes would be converted to amine groups. The product was dialysed against distilled water for 24 h and lyophilised to yield a brown solid. (0.171 g, 34%).

FT-IR (ATR) ν (cm^{-1}): 3273 (N-H & O-H), 2919 (symmetric stretch C-H), 1634 (C-N).

Elemental analysis (%): C 45.29; H 6.26; N 14.83. **DS**: 0.86. **Kaiser test**: positive vs starch.

Diamino cellulose (3.1iii)⁷

Using NaH_2PO_2 as reductant

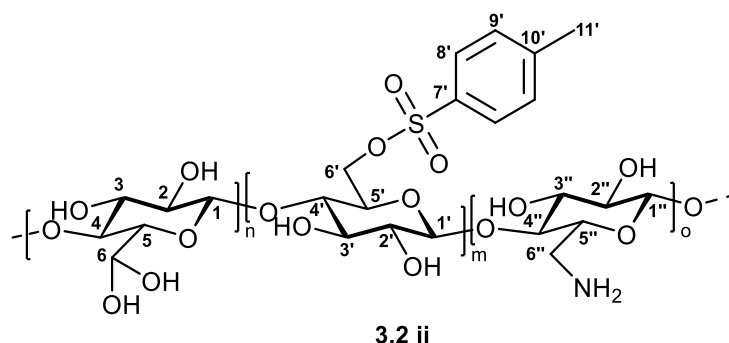


$\text{NaH}_2\text{PO}_2 \cdot \text{H}_2\text{O}$ (0.5 eq., 1.25 g) was allowed to stir in DI water (10 mL) until dissolved. DAC (1 eq., 2.50 g) and NH_4Ac (1.25 eq., 3.13 g) in EtOH (50 mL) was added and allowed to stir at 40°C for 19 h. The reaction mixture was dialysed against water and lyophilised to yield a brown powder. (0.840 g, 33%).

^{13}C CP/MAS NMR (400 MHz) δ (ppm): 103.63 (C-1'), 97.75 (C-1), 87.74 (C-4'), 82.84 (C-4), 73.78 – 64.15 (C-2, C-3, C-5 and C-2', C-3', C-5'), 64.15 (C-6'), 59.92 (C-6). **FT-IR** (ATR) ν (cm^{-1}): 3300 (O-H), 2900 (symmetric stretch C-H), 1632 (C-N). **Elemental analysis** (%): C 34.53; H 4.71; N 5.27. **DS**: 0.31. **Kaiser test**: positive vs starch.

Amino cellulose (3.2ii)¹

Using NaBH_4 as reductant



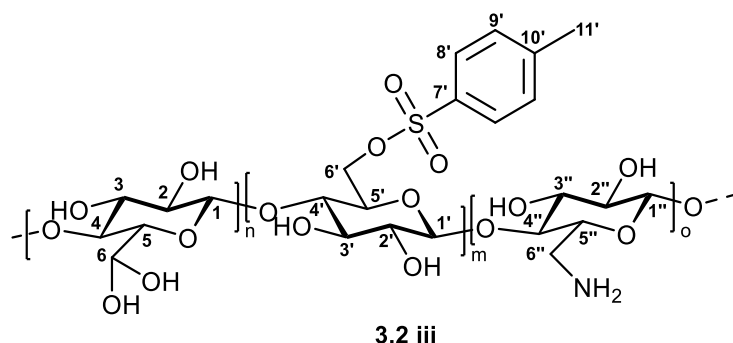
Oxidised cellulose **2.3** (0.500 g, 2 mmol g⁻¹ aldehyde groups), 0.230 g NH₄Ac (3 mol per mol -CHO), 0.350 g of NH₄OH (10 mol per mol -CHO = 100 mmol g⁻¹) were dispersed in 100 mL EtOH, and the slurry was stirred at 80 °C under reflux conditions for 18 h. The reaction mixture was subsequently cooled in an ice bath and 0.15 g of NaBH₄ (4 X excess i.e. 40 mmol g⁻¹) was gradually added followed by stirring for an additional 1 h. The amount of NaBH₄ was calculated based on 1:0.5 M ratio of the anhydroglucose units (~6.17 mmolg⁻¹): NaBH₄. The resultant aminated product was washed thoroughly 5 times with DI water (20 mL). The mol equivalents of reagents used assumed that all the aldehydes would be converted to amine groups. The product was dialysed against water for 24 h and lyophilised to yield a white solid. (0.158 g, 20 %*).

FT-IR (ATR) ν (cm⁻¹): 3396 (N-H & O-H), 2918 (C-H aliphatic), 1624, 1596 (C-N). **Elemental analysis** (%): C 44.90; H 6.00; N 0.26; S 6.70. **DS**: 0.030. **Kaiser test**: positive vs starch.

Note: * percentage mass yield was calculated based on the conversion of tosyl cellulose to aminocellulose because C-6 oxidised C-6 tosyl cellulose was not dialysed and may contain excess starting materials and other impurities.

Amino cellulose (3.2iii) Method 3⁷

Using NaH_2PO_2 as reductant



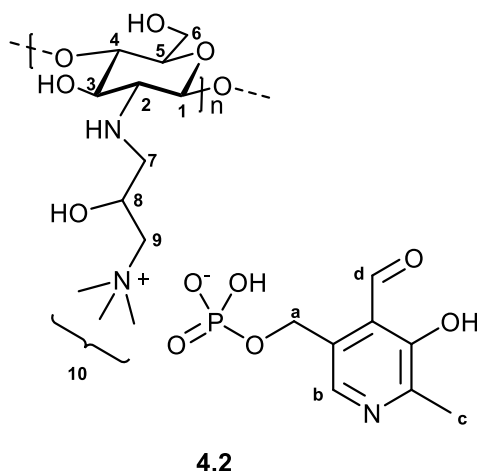
$\text{NaH}_2\text{PO}_2 \cdot \text{H}_2\text{O}$ (0.5 eq., 1.25 g) was allowed to stir in DI water (10 mL) until dissolved. Oxidised cellulose **2.3** (2.50 g, 1 eq.) and NH_4Ac (3.13 g, 1.25 eq.) in EtOH (50 mL) was added and allowed to stir at 40°C for 19 h. The reaction mixture was placed in a dialysis bag and dialysed against water followed by lyophilised to yield a white solid. (1.33 g, 34 %*).

¹H NMR (600 MHz, DMSO-*d*₆) δ (ppm): 7.78 – 7.42 (H-8', H-9'), 5.43 (H-3), 4.76 – 4.71 (H-2), 4.31 (H-1), 4.21 (H-6), 3.77 (H-4), 3.06 (H-5), 2.38 (H-11'), 1.22 (NH_2). **¹³C CP MAS NMR (400 MHz)** δ (ppm): 208.76 (C-6), 144.87 (C-8', C-9'), 129.04 (C-1), 103.58 – 97.72 (C-4), 86.68 – 73.59 (C-2, C-3, C-5), 60.17 (C-6'), 50.03 (C-6''), 20.38 (C-11'). **FT-IR (ATR)** ν (cm^{-1}): 3371 (N-H & O-H), 2876 (C-H aliphatic), 1648, 1596 (N-H₂). **Elemental analysis (%)**: C 39.65; H 5.13; N 0.19; S 6.19. **DS**: 0.022. **Kaiser test**: positive vs starch.

Note: *percentage mass yield was calculated based on the conversion of tosyl cellulose to aminocellulose because C-6 oxidised C-6 tosyl cellulose was not dialysed and may contain excess starting materials and other impurities.

6.2.2 Synthesis of immobilised pyridoxal on biopolymer solid supports

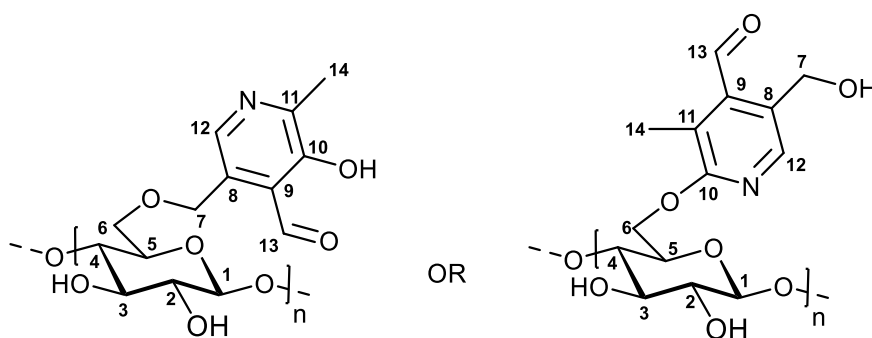
Q188-PLP complex (4.2)



3-Trimethylammonium-2-hydroxypropyl-*N*-chitosan chloride (Q188) (**4.1**) (1.10 g) (synthesised by a previous student following the literature methods reported by Sayed *et al.*⁸), was allowed to stir in ammonium acetate buffer (0.07 mM, 33 mL, pH 9) followed by the addition of PLP (0.503 g). The reaction mixture was allowed to stir overnight at 25 °C. The resulting solid was isolated by centrifugation and dialysed against water. The dialysis buffer was changed regularly until no visible release of unbound PLP (yellow colour) was observed. The solution was centrifuged and dried, yielding an orange solid. (0.841 g).

¹H NMR (300 MHz, 2% DCI/D₂O) δ (ppm): 10.10 (H-d), 7.94 – 7.84 (H-b), 6.14 (H-a), 4.29 (H-8), 3.53 (H-9), 3.20 (H-10), 2.38 (NAc), 2.26 (H-c). **³¹P NMR (81 MHz, 2% DCI/D₂O) δ (ppm):** -0.18, -0.80. **FT-IR (ATR) ν (cm⁻¹):** 3228 (O-H), 2870 (C-H), 1636 (C=O), 1476 (C-H trimethyl ammonium group), 1370 (PLP-CH₃), 1296 (P=O), 1030 (pyranose), 966 (P-O-C). **Elemental Analysis (%):** C, 37.88; H, 6.95; N, 7.29. Degree of complexation: ~50%

Immobilised pyridoxal on tosyl cellulose (4.3)

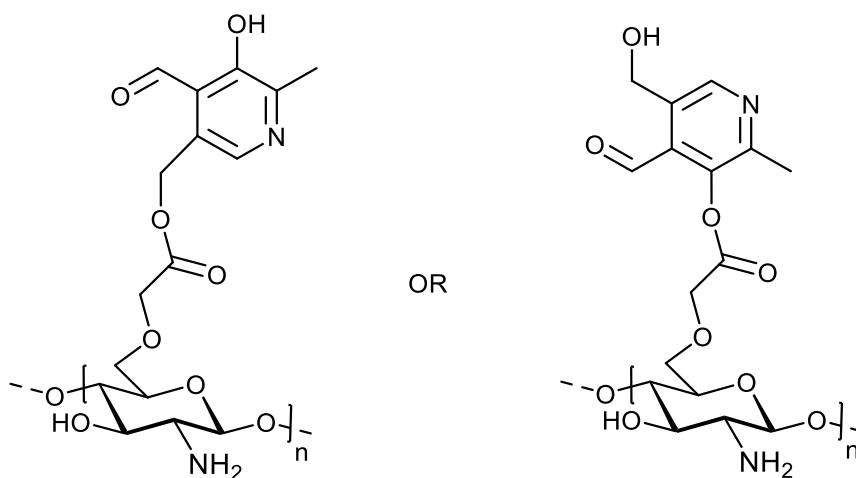


4.3

Pyridoxal hydrochloride was (1.20 g) was dissolved in DMSO (10 mL). K_2CO_3 (3.20 g) was added, and the mixture allowed to stir for 15 min. Subsequently, tosyl cellulose (1.20 g) was added and the reaction mixture allowed to stir at 65 °C for 48 h. The resulting heterogeneous reaction mixture was centrifuged and the solid isolated and dialysed against water, changing the dialysis buffer regularly until no visible release of unbound pyridoxal (yellow colour) was observed. The product was lyophilised to yield a brown powder. (0.563 g, 28 %).

1H NMR (600 MHz, DMSO- d_6) δ (ppm): 8.12 (H-13), 7.84 – 7.52 (phenyl protons of tosyl cellulose), 6.64 (H-12), 5.08 – 4.93 (H-7), 3.47 – 3.31 (cellulose backbone), 2.46 (*p*-CH₃ of tosyl cellulose). **^{13}C NMR (600 MHz, DMSO- d_6) δ (ppm):** 149.80 (C-11), 136.72 – 136.52 (C-10), 131.24 (C-8), 128.64 (C-9), 105.16 (C-12), 80.60 – 69.12 (C-1 to C-6), 61.14 – 60.74 (C-7). **FT-IR (ATR) ν (cm⁻¹):** 3290 (O-H), 2882 (C-H), 1600 (CHO), 1022 (pyranose). **Elemental Analysis (%):** C, 38.00; H, 4.35; N, 3.87; S, 1.32. Degree of complexation: 83 %.

Immobilisation of pyridoxal on carboxy methylchitosan (4.4)



Carboxymethyl chitosan (1.00 g) was dissolved in PBS buffer (pH 6.00, 0.2 mol L⁻¹) and activated at 25 °C for 2 h after the addition of 0.150 g of EDC. Pyridoxal hydrochloride (0.500 g) was dissolved in PBS and added to the reaction mixture. The reaction mixture was allowed to stir at 25 °C for 24 h. (3.26 g).

FT-IR (ATR) ν (cm⁻¹): 3306 (O-H & N-H), 1578 (COOH asymmetric stretch), 1408 (COOH symmetric stretch), 1066 (COO-C). **Elemental Analysis (%):** C, 21.22; H, 3.84; N, 3.38.

6.2.3 Cytotoxicity studies of aminated celluloses

Cell lines and culture conditions

The human malignant glioblastoma cell lines U251 (glioblastoma multiforme, World Health Organization grade IV) were grown in a monolayer using GlutaMAX™ Dulbecco's Modified Eagles Medium (DMEM) supplemented with 10 % foetal bovine serum (FBS, Gibco, Life Technologies Corporation, Paisley, UK) and 1 % 100 U/mL penicillin and 100 µg/mL of streptomycin (Lonza Group Ltd., Verviers, Belgium).

Cell viability assays

The quantity of polymer required to make a stock solution of 5 mg/mL was weighed and dissolved in appropriate volumes of DMSO. The U251 and U87 cells were grown overnight at a density of 4000 cells per well in sterile 96-well plates and thereafter exposed to 0.05 mg/mL of polymer. The 0 mg/mL served as vehicle control (equivalent amount of DMSO) and after treatment, cell viability was assessed with the MTT assay kit (Roche, USA) according to manufacturer's instructions and reading absorbance at 570 nm. Cell viability was calculated relative to control and was obtained using the GraphPad Prism 6 software (GraphPad software Inc., San Diego, CA, USA).

6.2.4 Non-enzymatic PLP – mediated conversion of amino acids to α -keto acids^{10, 11}

The non-enzymatic deamination of phenylalanine to phenylpyruvic acid was monitored over a period of 24 h using LCMS (*the conditions are mentioned under general procedures*) to observe the reaction kinetics. Q188-PLP (4.2) was allowed to stir in PBS buffer, followed by the addition of CuSO₄ and L-phenylalanine. The reaction mixture was allowed to stir for 24 h at 25 °C and aliquots (0.5 mL) of the reaction mixture were drawn at times t(0), t(45), t(180), t(210) and t(1440) where time was measured in minutes. Two additional reactions were set up as controls: Q188 no polymer where no immobilised polymer was present and Q188 no substrate where no phenylalanine was present. **Table 6.3** shows the components of each reaction mixture.

Table 6.2. Reaction table of components for non-enzymatic deamination reactions using Q188-PLP and controls Q188 no polymer and Q188 no substrate.

	Q188 no polymer	Q188 no substrate	Q188 ALL
Polymer-PLP (g)	-	0.0580	0.0582
Polymer (g)	0.0569	-	-
CuSO ₄ (g)	0.0146	0.0144	0.0149
Phenylalanine (g)	0.0151	-	0.0143
PBS (mL)	10	10	10
PLP	-	-	-

6.3 References

1. R. Koshani, J. Zhang, T. G. van de Ven, X. Lu and Y. Wang, *ACS Sustainable Chemistry & Engineering*, 2021, **9**, 10513-10523.
2. G. Jarre, S. Heyer, E. Memmel, T. Meinhardt and A. Krueger, *Beilstein journal of organic chemistry*, 2014, **10**, 2729-2737.
3. J. Simon, L. Fliri, F. Drexler, M. Bacher, J. Sapkota, M. Ristolainen, M. Hummel, A. Potthast and T. Rosenau, *Carbohydrate Polymers*, 2023, **310**, 120691.
4. S. Schmidt, T. Liebert and T. Heinze, *Green Chemistry*, 2014, **16**, 1941-1946.
5. S. Sayed, T. Millard and A. Jardine, *Carbohydrate polymers*, 2018, **196**, 187-198.
6. A. Li, Q. Xue, Y. Ye, P. Gong, M. Deng and B. Jiang, *Molecules*, 2020, **25**, 4698.
7. F. Kliuev, A. Kuznetsov, O. I. Afanasyev, S. A. Runikhina, E. Kuchuk, E. Podyacheva, A. A. Tsygankov and D. Chusov, *Organic Letters*, 2022, **24**, 7717-7721.
8. S. Sayed and A. Jardine, *International journal of molecular sciences*, 2015, **16**, 9064-9077.
9. S. Y. Wang and H. Gao, *LWT-Food Science and Technology*, 2013, **52**, 71-79.
10. K.-Y. Choi, *Biotechnology and bioprocess engineering*, 2015, **20**, 988-994.
11. C. N. Sarkissian, C. R. Scriver and O. A. Mamer, *Analytical Biochemistry*, 2000, **280**, 242-249.

Appendix

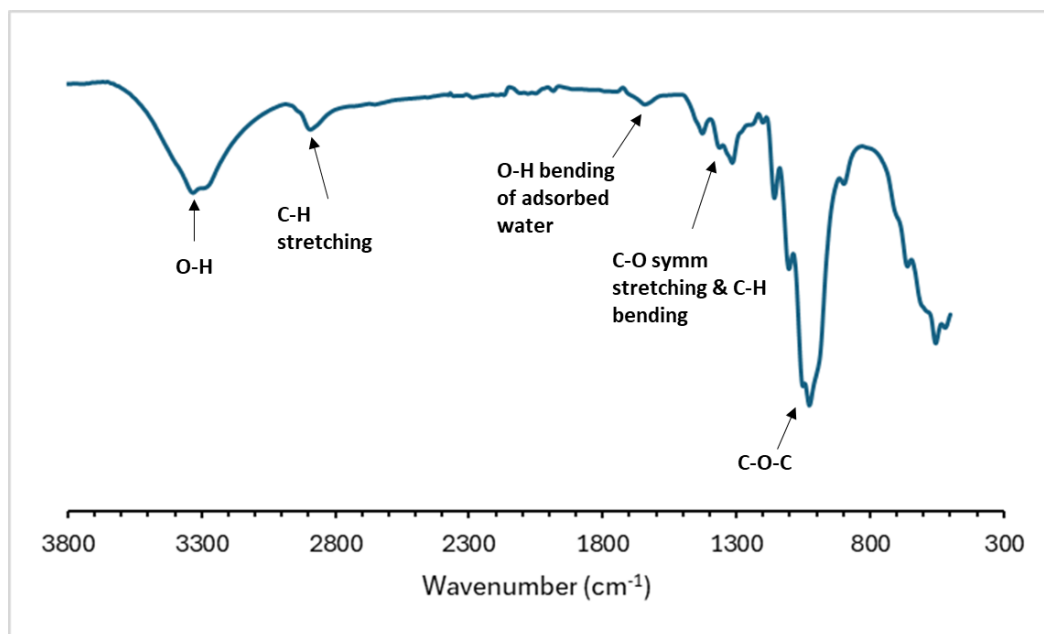


Figure S1. IR spectrum of cellulose.

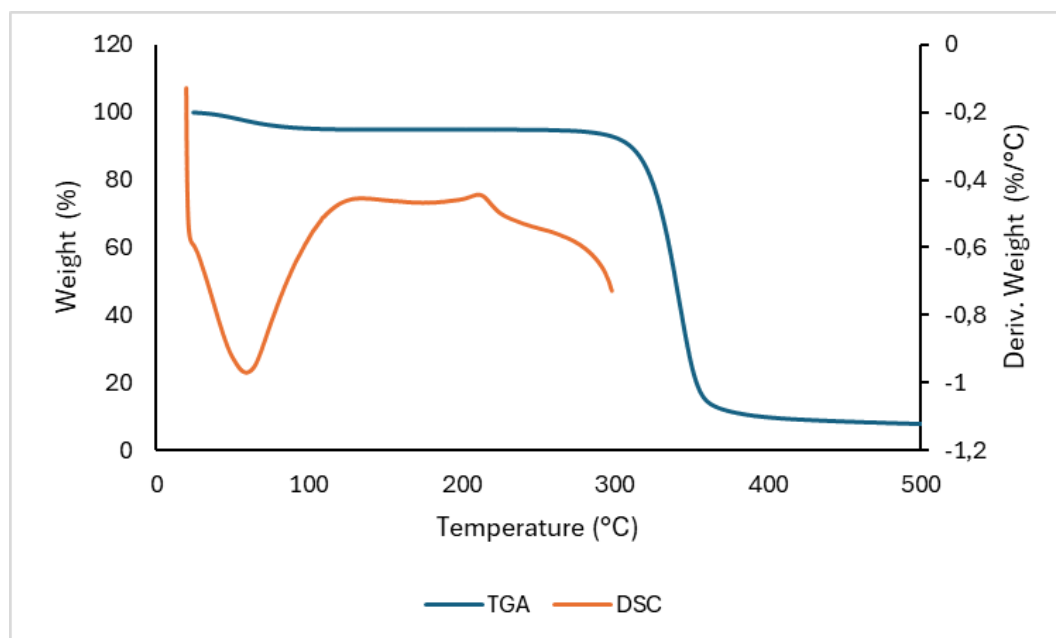


Figure S2. The TGA and DSC curves of cellulose.

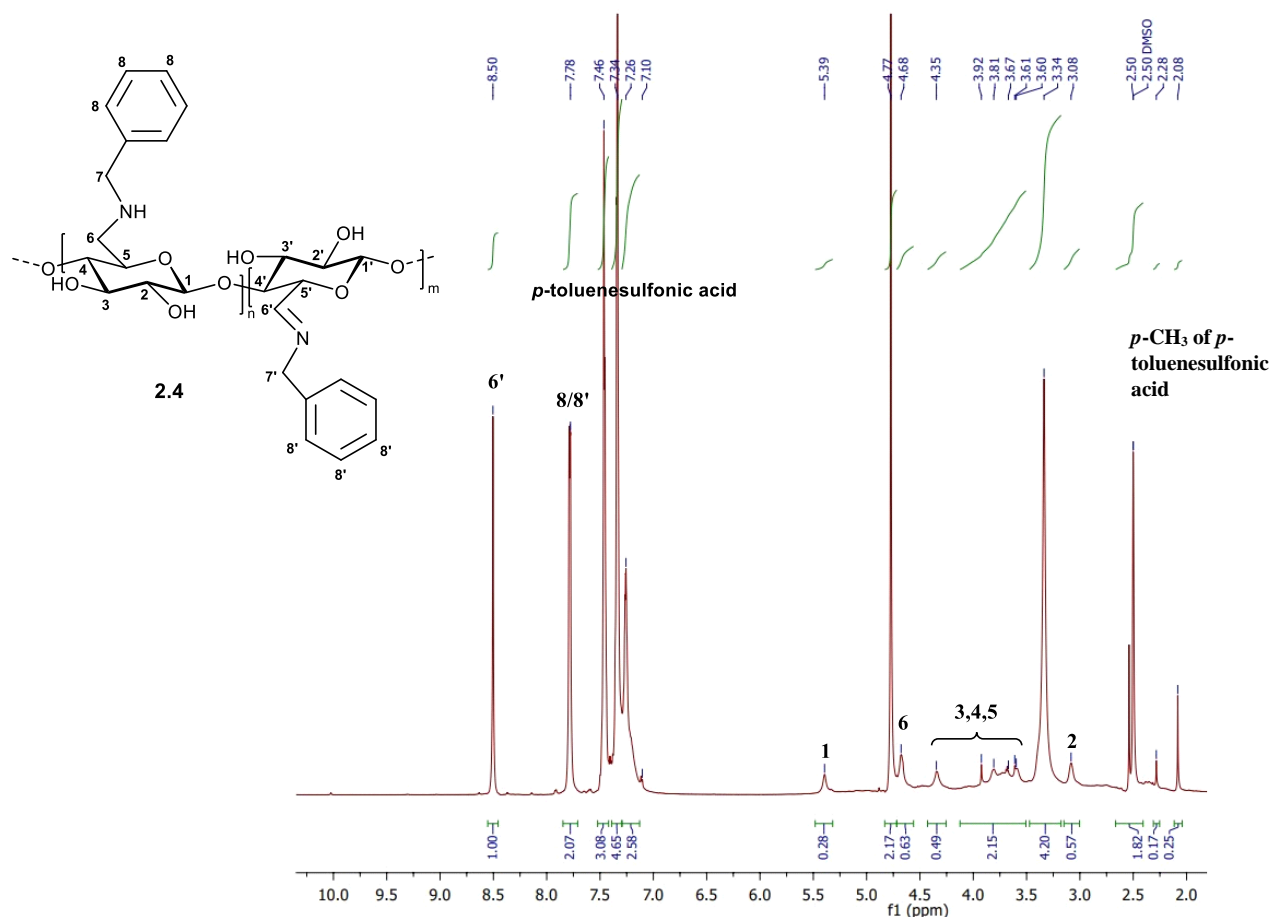


Figure S3. ^1H NMR spectrum of Schiff Base product (**2.4**) in DMSO-d_6 .

Table S1. Peak area vs time for phenylalanine depletion for the deamination reaction of phenylalanine to phenylpyruvic acid using Q188-PLP as an immobilised catalyst, measured by LCMS.

Time (min)	Peak Area
0	3.00E+07
45	1.71E+07
180	1.08E+07
210	9.14E+06
1440	1.45E+06

Note $t_{1/2}$ (min) = 122 min

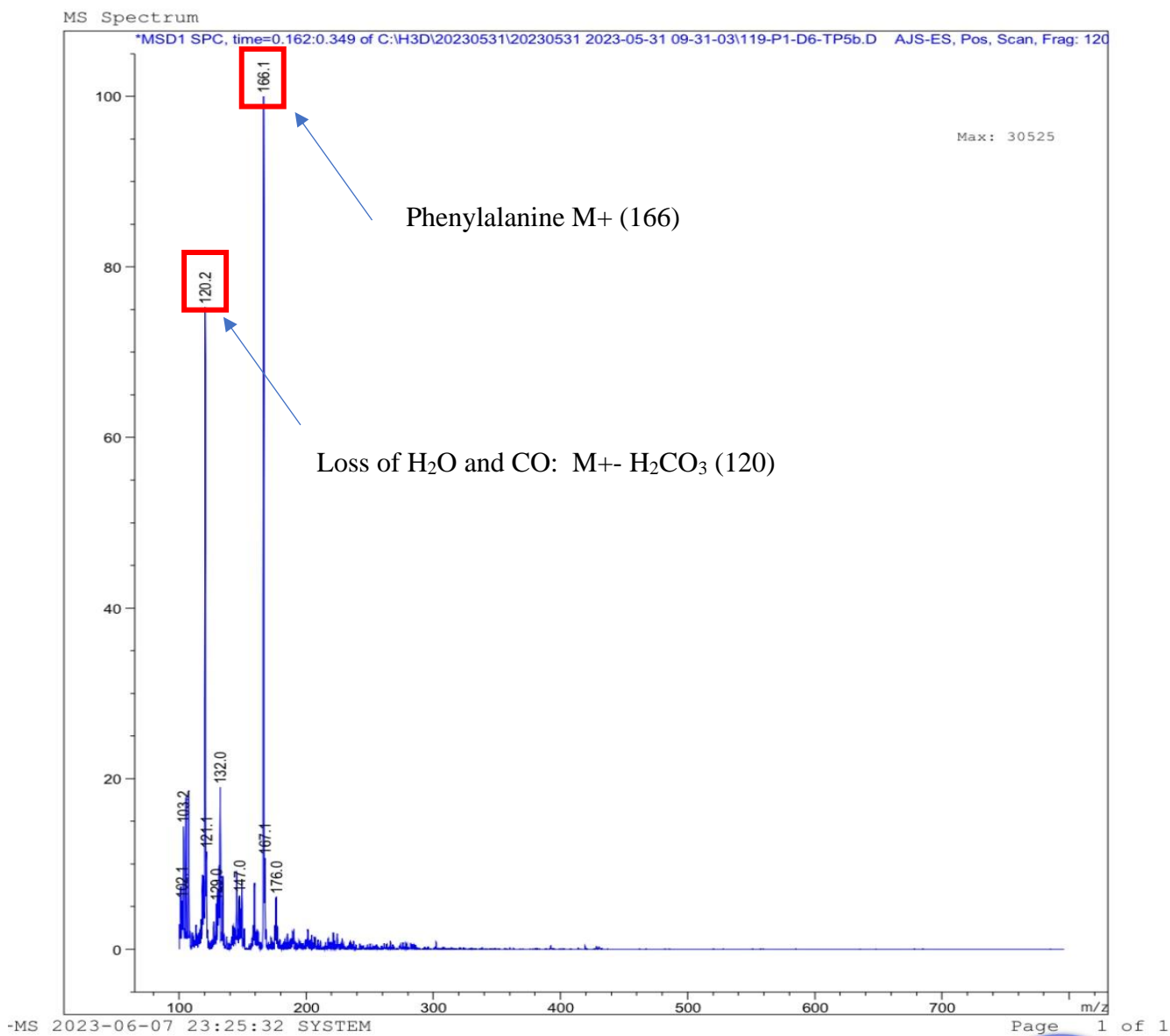


Figure S4. Mass spectrum from LCMS study of Q188-PLP catalysed conversion of phenylalanine to phenylpyruvic acid (at t= 45 min).